

HEAVY-LIGHT MESONS IN A QCD POTENTIAL MODEL



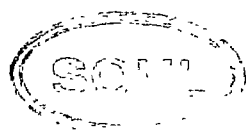
Thesis submitted to the Gauhati University
in partial fulfillment of the requirement for
the award of the degree of

Doctor of Philosophy

in

Physics

under the **Faculty of Science**



By
Krishna Kingkar Pathak
2013

Gauhati University

Gopinath Bardoloi Nagar
Guwahati-781014, Assam, India

Dr. D. K. Choudhury
Professor
Department of Physics



Phone: 91-361-2570531 (O)
+91-9707012976 (Mobile)
Fax: 91-361-2570133
Email: dkc_phys@yahoo.co.in

Certificate

This is to certify that Krishna Kingkar Pathak has worked under my supervision for the thesis entitled "Heavy-Light Mesons in a QCD Potential Model" which is being submitted to the Gauhati university for the degree of Doctor of Philosophy in the faculty of science.

The thesis is his own work. He has fulfilled all the requirements under the Ph.D regulations of Gauhati University and to the best of my Knowledge, the thesis or part thereof has not been submitted to any other University for any degree or diploma.

Date: 14.6.2014

Guwahati-14


(Dilip Kumar Choudhury)
Ph.D Supervisor

Professor
Department of Physics
Gauhati University

Declaration

I hereby declare that I have done the work enclosed in this thesis entitled ***“Heavy-Light Mesons in a QCD Potential Model”*** under the supervision of Prof. D. K. Choudhury, Department of Physics, Gauhati University. The work is original and the results quoted from other workers have been properly referred to in the thesis. Neither this work nor any part therof has been submitted to any other university for any degree or diploma or other similar titles.

Date:


(Krishna Kingkar Pathak)

Guwahati-14

Contents

1	Introduction	1
1.1	The Standard Model of Particle Physics	1
1.1.1	The Particles that Constitute Matter: Quarks and Leptons	2
1.1.2	The Hadrons	4
1.1.3	Role of CKM in the Standard Model	6
1.2	Weak decay of Mesons	10
1.2.1	Leptonic and Semileptonic decay of mesons	10
1.2.2	Status of decay constant f_p in leptonic decay	14
1.2.3	CP violation in meson decays	15
1.2.4	Non-leptonic decay of mesons	16
1.3	Quantum Chromodynamics(QCD)	17
1.3.1	Perturbative and Non perturbative QCD	18
1.3.2	Effective Field Theory(EFT) and Non-relativistic QCD (NRQCD) .	20
1.4	QCD Potential	23
1.5	The Work of this Thesis	30
2	Open Flavour Charmed Mesons in a QCD Potential model	33
2.1	Introduction	33
2.2	Formalism	34
2.2.1	The QCD Potential Model	34

2.2.2	Wave function in the model	35
2.2.3	The short distance scale and the wave function at the origin	37
2.3	Calculation and results	39
2.3.1	Masses and decay constants of open flavoured charm mesons	39
2.3.2	Leptonic decay rate and Branching ratio of D and D_s mesons	41
2.3.3	Weak decay of B_c^+ meson	43
2.4	Conclusion	44
3	Oscillation frequency of B and \bar{B} mesons in the QCD potential model	46
3.1	Introduction	46
3.2	Formalism	47
3.2.1	Mixing of B_d and B_s mesons	47
3.2.2	Allowed range of strong running coupling constant α_s in the model	50
3.2.3	Strong running coupling constant α_s in \overline{MS} scheme	53
3.2.4	An alternate to \overline{MS} scheme	54
3.3	Calculation and results	55
3.3.1	Masses and Decay constants of B mesons	55
3.3.2	Oscillation frequency of $B - \bar{B}$ mesons	56
3.3.3	The results with the mass formula 2.26	57
3.4	Conclusion	58
4	Leptonic decay of B and D mesons in the QCD potential model with relativistic correction	60
4.1	Introduction	60
4.2	Formalism	61
4.2.1	Wave function in the model	61
4.2.2	Masses and Decay constants of D and B mesons	62
4.2.3	Leptonic decay rate and Branching ratio of D, D_s and B mesons . .	64

4.3	Summary and Conclusion	64
5	Isgur Wise function and CKM matrix element V_{cb} in the QCD Potential model	67
5.1	Introduction	67
5.2	Formalism	68
5.2.1	The Isgur-Wise function and Semileptonic decay	68
5.2.2	Isgur-Wise function in the model	70
5.2.3	The strong coupling constant α_s and determination of Λ_{QCD} for semileptonic decay	71
5.3	Results	73
5.3.1	Isgur-Wise function	73
5.3.2	Determination of CKM element V_{cb}	76
5.4	Conclusion	78
6	B_c meson as a heavy-light meson in the QCD potential model	80
6.1	Introduction	80
6.2	Formalism	82
6.2.1	The wavefunctions in the model	82
6.2.2	Wavefunction with Coulombic part as perturbation	83
6.2.3	The strong coupling constant α_s in the Model	84
6.2.4	Form factors and Decay rates of $B_c \rightarrow c\bar{c}(\ell^+\nu_\ell)$ transitions	84
6.3	Results and Discussion	95
7	Summary and Outlook	97
APPENDIX		100
A	Calculation of the wavefunction with linear part as perturbation	101
B	Derivation of Van Royen formula(Eqn.2.24) in chapter 2	108

C Derivation of Eqn. 2.23 from Eqn.4.7	111
D Masses of heavy-light mesons with $\Lambda_{QCD} = 410 \text{ MeV}$	113

List of Figures

1.1	Unitarity triangle from Eqn.1.7	8
1.2	Electric lines between the positive and negative charges in QED.	24
1.3	Flux tube due to chromoelectric lines of force in QCD.	25
1.4	The potential $\frac{4}{3r}\alpha_s$ (coulombic), br (linear) and the potential $\frac{4}{3r}\alpha_s+br$ (Coulomb+linear), plotted against r (in GeV^{-1}) with $b = 0.183\ GeV^2$ and $\alpha_s = 0.4$	29
2.1	The decay diagram for $D_{(s)}^+ \rightarrow l^+\nu_l$	39
3.1	Feynman graphs for $B_{d,s} \bar{B}_{d,s}$ mixing. Quarks are shown as straight lines, while bosons are illustrated by wave-lines.	47
5.1	Feynmann diagram for semileptonic decay of $B \rightarrow D, D^*l\nu$	68
5.2	Variation of I-W function with Y for B meson.	72
5.3	Variation of I-W function with Y for heavy-light mesons with $\Lambda = 200\ MeV$. 75	75
5.4	Variation of I-W function with Y for heavy-light mesons with $\Lambda = 410\ MeV$. 75	75
6.1	Variation of I-W function with Y for different scales of Λ with linear part as perturbation.	87
6.2	Variation of I-W function with Y for different scales of Λ with Coulombic part as perturbation.	88

6.3 Differential decay rates $(1/ V_{cb} ^2)d\Gamma/dq^2$ of $B_c \rightarrow \eta_c e \bar{\nu}$ (in GeV^{-1}) with linear part as perturbation. The red and blue curves correspond to $\Lambda = 382 MeV$ and $430 MeV$ respectively.	90
6.4 Differential decay rates $(1/ V_{cb} ^2)d\Gamma/dq^2$ of $B_c \rightarrow \eta_c e \bar{\nu}$ (in GeV^{-1}) with coulombic part as perturbation. The red and blue curves correspond to $\Lambda = 382 MeV$ and $430 MeV$ respectively.	91
6.5 Differential decay rates $(1/ V_{cb} ^2)d\Gamma/dq^2$ of $B_c \rightarrow J/\psi e \bar{\nu}$ (in GeV^{-1}) with linear part as perturbation. The red and blue curves correspond to $\Lambda = 382 MeV$ and $430 MeV$ respectively.	92
6.6 Differential decay rates $(1/ V_{cb} ^2)d\Gamma/dq^2$ of $B_c \rightarrow J/\psi e \bar{\nu}$ (in GeV^{-1}) with Coulombic part as perturbation. The red and blue curves correspond to $\Lambda = 382 MeV$ and $430 MeV$ respectively.	93

List of Tables

1.1	Masses of the quarks and leptons. The current quark masses and lepton masses are taken from PDG[2]	3
1.2	The pseudoscalar heavy-light mesons and their experimental masses from PDG [2]. B_c meson is included as a heavy-light meson due to its different flavour.	6
1.3	The three types of weak decay and their decay products.	10
2.1	Values of cut-off parameter r_0 for different mesons	39
2.2	The masses of heavy-light mesons in GeV.	40
2.3	The decay constants of heavy-light mesons with and without QCD correction in GeV	41
2.4	The leptonic branching ratio of D and D_s mesons. Values within the bracket represent the branching ratio for f_p with QCD correction.	42
2.5	Decay width(in $10^{-4} eV$) and life time of B_c meson	44
2.6	Masses and decay constants B_d and B_s mesons	45
3.1	Values of Q_0^2 (in GeV^2) for heavy-light mesons above which linear part can be treated as perturbation [118].	51

3.2	Values of Q_0^2 (in GeV^2) for heavy-light mesons with linear part as perturbation and $m_{u/d} = 0.33 \text{ GeV}$, $m_s = 0.483 \text{ GeV}$, $m_c = 1.55 \text{ GeV}$, $m_b = 4.97 \text{ GeV}$	52
3.3	Values of r_0 and M_p for B_d and B_s mesons.	56
3.4	Decay constant and oscillation freq. of B mesons	57
3.5	Values of r_0 and M_p with Eqn.2.26 for B_d and B_s mesons (in unit of GeV) .	58
3.6	Decay constant and oscillation freq. for B_d and B_s mesons	58
4.1	Masses of heavy-light mesons in this work with $m_d = 0.336 \text{ GeV}$, $m_s = 0.465 \text{ GeV}$, $m_c = 1.55 \text{ GeV}$, $m_b = 4.97 \text{ GeV}$ and comparison with experimental data. All values are in units of MeV.	63
4.2	Decay constants of pseudoscalar heavy-light mesons (in MeV) computed in this work and comparison with experimental [188, 192] and theoretical results from (2+1)-flavour asqdat action [193], HPQCD [194], extended chiral quark model (ExChQm) [187], Light cone wavefunction [188], light-front quark model (LQM) [189], field-correlator method (FC) [190], Bethe-Salpeter method (BS) [153, 191], relativistic quark model (RQM) [136], relativistic potential model (RPM) [144]	63
4.3	Leptonic branching ratio of D , D_s and B mesons for three leptonic channels and comparison with experiment and theoretical results.	64
5.1	Slope and curvature of I-W function for B and D mesons.	73
5.2	Comparison of slope and curvature of B mesons with other works.	74
6.1	The slope ρ^2 and curvature C of the I-W function with linear part as perturbation and Coulombic part as perturbation.	86
6.2	Parameters of the form factors for the channel of $B_c \rightarrow \eta_c(J/\psi)$ with $\Lambda = 397 \text{ MeV}$ (from ref.[235]).	87

6.3 Decay width for $B_c \rightarrow c\bar{c}(\ell^+\nu_\ell)$ decay. In the braces “ <i>linear</i> ” means the result with linear part as perturbation and “ <i>coul</i> ” means Coulombic part as perturbation.	93
6.4 Branching ratio for $B_c \rightarrow c\bar{c}(\ell^+\nu_\ell)$ decay. In the braces “ <i>linear</i> ” means the result with linear part as perturbation and “ <i>coul</i> ” means Coulombic part as perturbation.	94
6.5 Variation of I-W function with total wavefunction and parent wavefunction only for $\Lambda = 382 \text{ MeV}$	95
D.1 Masses of heavy-light mesons in this work with $m_d = 0.336 \text{ GeV}$, $m_s = 0.465 \text{ GeV}$, $m_c = 1.55 \text{ GeV}$, $m_b = 4.97 \text{ GeV}$ and comparison with experimental data. All values are in units of MeV.	113

Acknowledgements

First and foremost I express my sincere gratitude and thanks to my supervisor Prof. D. K. Choudhury for his patient guidance, encouragement and invaluable help all throughout my research work. I am most grateful that I have had the opportunity to work with and learn from him and hope that in the future I can show that his teachings have fallen on fertile soil.

I am thankful to the Head of Department of Physics Prof. N. Nimai Singh and all the faculty members for providing me all the facilities in the department as well as their sincere encouragement. I also thank N. S. Bordoloi from Cotton college for her sincere helps with best of her efforts and the colleagues and faculty members of my home institute Arya Vidyapeeth College for their moral and logistic support and constant inspiration to carry out my research work.

All throughout this work, I have obtained tremendous help and encouragement from all my friends and well wishers. I thank them all for their warm friendship and encouragement. I especially thank all the members of the HEP group in Gauhati University Subhankar Roy, Naba Ratna Bhagawati, Akbari Jahan, Samiran Chatterjee, Sanjeeb Kalita, Bhaskar Jyoti Hazarika, Neelakshi and Sabyasachi Roy for helping me in different parts of my research and computational work.

It is difficult to mention all the people who have contributed to my research work and whom I am indebted to. Standing out is Prof. Prasenjit Sen of Jawaharlal Nehru University, India with whom I had a fruitful discussion in the initial stage of my work. I whole-

heartedly thank Prof. P. C. Vinodkumar of Sardar Patel University, India for his valuable counseling and comments on some part of my research work. For some very useful correspondences, I am also grateful to Maxim. Yu. Kholpov from National Research Nuclear University “MEPhI”, Russia, Oleg V. Teryaev from Joint Institute for Nuclear Research, Russia and Seung-il Nam from Korea Institute for Advanced Study (KIAS), Seoul.

I am greatly indebted to my wife Namita for her love and support all throughout. Without my family's unstinting love and encouragement, I would never have had the courage to do this work. I thank my parents, my brother and my two sisters as well as all my in-laws for the love and encouragement they have always bestowed on me. At the last but not the least, I must also thank my little son Pragyan, to whom it was really very difficult to ignore his curiosity without touching my laptop.



(Krishna Kingkar Pathak)

Guwahati-14, India

Chapter 1

Introduction

Particle physics is concerned with the study of the elementary constituents of matter which make up the universe and their interactions. An elementary particle is a particle without any internal structure and is not composed of other particles. Elementary particles can be found in cosmic rays. They can be produced in the laboratory in collisions between high-energy particle beams in accelerators. For this reason Particle Physics is also called High-Energy Physics. Like much of fundamental research, it is impossible to know exactly what benefits might be realized from particle physics. However, it is worth noting that in 1897, the quest to understand the universe led J.J. Thomson [1] to discover electron and this discovery undoubtedly created a history in particle physics.

1.1 The Standard Model of Particle Physics

At present, elementary particle physics is described by the Standard Model(SM) theory, which was developed during the last century. The Standard Model of Particle Physics (SM) is a quantum field theory, which describes the knowledge of the fundamental particles and three of the four fundamental interactions, namely the electromagnetic interaction, the weak interaction and the strong interaction. The fourth interaction, gravity, is not in-

cluded, due to its non-re-normalizable terms in the theoretical description of the interaction. All fundamental particles forming matter in the SM are fermions with spin 1/2, while the interaction fields are mediated by bosons with an integer spin quantum number. The fermions can be divided into two classes, quarks and leptons. Quarks have an additional strong charge, colour and thus can interact through the strong force, while the leptons are colour neutral and not affected by the strong interaction. Both classes consist of 6 particles, divided into three hierachic ordered generations, which differ only by their mass and their flavour quantum number. The first family of the leptons is formed by the electron (e) and the electron-neutrino (ν_e), the second family consists of the muon(μ) and the muon neutrino (ν_μ), and the heaviest generation are the tau lepton(τ) and the τ neutrino ν_τ . The three interactions are introduced into the SM by a $SU(3)_C \times SU(2)_L \times U(1)_Y$ gauge group. Here, C represents the color of the strong interaction and L denotes the fact, that the electroweak force couples only to the left-handed states of the particles. Y represents the weak hyper-charge, which results in the unification of the weak and electromagnetic interaction in the electroweak unified theory given by Glashow, Weinberg and Salam. The interactions are mediated by gauge bosons. The hypercharge acts as the carrier of the electromagnetic force, whereas W^\pm and Z_0 mediate the weak force. The strong interaction is mediated by eight interaction bosons, the gluons.

1.1.1 The Particles that Constitute Matter: Quarks and Leptons

At present, the elementary particles that make up matter are thought to be the quarks and the leptons along with their antiparticles. We consider them to be elementary because, so far, we do not have any indication of other particles inside them. The up (u) quark, charm (c) quark and top (t) quark, all have electric charge $+\frac{2}{3}$ (on a scale where the electron has charge -1), and the down (d), strange (s) and bottom (b) quarks, all have charge $-\frac{1}{3}$. The three leptons all with charge -1 are the electron(e), muon (μ) and tau(τ) leptons and the

three corresponding neutrinos all with charge 0 are ν_e , ν_μ and ν_τ .

$$\begin{aligned}
 \text{Quarks :} \quad & \text{charge } + \frac{2}{3} : \quad \begin{pmatrix} u \\ d \end{pmatrix}, \begin{pmatrix} c \\ s \end{pmatrix}, \begin{pmatrix} t \\ b \end{pmatrix}, \\
 & \text{charge } - \frac{1}{3} : \quad \begin{pmatrix} u \\ d \end{pmatrix}, \begin{pmatrix} c \\ s \end{pmatrix}, \begin{pmatrix} t \\ b \end{pmatrix}, \\
 \text{Leptons :} \quad & \text{charge } 0 : \quad \begin{pmatrix} \nu_e \\ e \end{pmatrix}, \begin{pmatrix} \nu_\mu \\ \mu \end{pmatrix}, \begin{pmatrix} \nu_\tau \\ \tau \end{pmatrix}, \\
 & \text{charge } -1 : \quad \begin{pmatrix} \nu_e \\ e \end{pmatrix}, \begin{pmatrix} \nu_\mu \\ \mu \end{pmatrix}, \begin{pmatrix} \nu_\tau \\ \tau \end{pmatrix}.
 \end{aligned} \tag{1.1}$$

In the following Table(1.1), we tabulate the masses of the fundamental particles- the quarks and leptons. However, for the quarks we list two different masses. The current mass is the mass that appears in the Lagrangian to describe the self-interaction of the quark and is not directly observable. The constituent mass is the effective mass of the quark, when it is bound inside a hadron. The numbers for the constituent quark masses are approximate here because they depend on the hadron model used. The mass parameter is much like a coupling constant in quantum field theory and is technically dependent on the momentum scale and the renormalization scheme and is scale-dependent.

Table 1.1: Masses of the quarks and leptons. The current quark masses and lepton masses are taken from PDG[2]

Quark	Quark Mass		Lepton	Lepton Mass
	Current	Constituent		
u	$2.3^{+0.7}_{-0.5}$ MeV	~ 330 MeV	ν_e	< 5.1 eV (95% CL)
c	1.275 ± 0.025 GeV	~ 1.5 GeV	ν_μ	< 0.16 MeV (90% CL)
t	$173 \pm 0.6 \pm 0.8$ GeV	~ 180 GeV	ν_τ	< 31 MeV (95% CL)
d	$4.8^{+0.7}_{-0.3}$ MeV	~ 330 MeV	e	$0.510998928(11)$ MeV
s	95 ± 5 MeV	~ 500 MeV	μ	$105.6583715(35)$ MeV
b	4.65 ± 0.03 GeV	~ 5 GeV	τ	1776.82 ± 0.16 MeV

The masses of the quarks are generated through a symmetry breaking phase transition of the electro-weak interactions (a transition similar to that of a normal conductor to superconductor in condensed matter physics, in which an effective mass for the photon is

produced) in the standard model. The detailed aspects of the symmetry breaking, such as the existence of Higgs bosons are yet to be confirmed in experiments at high-energy colliders[3] though CMS [4] and ATLAS [5] in LHC have recently updated “a 125 GeV” particle as the Higgs boson.

Quarks are strongly interacting fermions and by convention of quark model, quarks have positive parity whereas antiquarks have negative parity. In addition to their electric charge, each quark has an additional “charge” referred to as colour (but nothing to do with the colours of the everyday world). There are three possible values of a colour charge, plus three anti-colours for the antiquarks. It appears to be a property of nature that coloured objects cannot exist freely by themselves, so quarks are confined inside hadrons in configurations that produce an object without any colour.

1.1.2 The Hadrons

The six quarks and six leptons (plus their antiparticles) may make up matter but only three of them make up the everyday matter around us. We normally do not “see” the quarks and gluons in low-energy experiments. What we usually observe in experimental apparatus are hadrons and nuclei which are bound states of these basic building blocks. It was M. Gell-mann [6] and G. Zweig [7, 8] who in 1964, put forward the quark model according to which the hadrons are composed of a more variety of pointlike objects called quarks.

Baryons and mesons are the two groups to find under the classification of Hadrons. Baryons are made up of three quarks (qqq) and hence an anti-baryon would be made up of three antiquarks. The other known type of structure is the meson, which is made up of a quark and an antiquark, $q\bar{q}$ (so an anti-meson is just a meson). The complicated structure of QCD means that the groups of quarks can be bound together to form a hadron which is possible only for certain configurations which can have no net colour (so they are in a colour singlet state). It also means that the attractive force between coloured objects is huge, so

they are always confined together into colourless objects. This specific property of quark due to which the strong interaction has got its own importance is known as confinement.

Thus the colour part of the baryon's state function is an $SU(3)$ singlet, a completely antisymmetric state of the three colours. The ordinary baryons are made up of u, d, and s quarks and belong to the multiplets on the right side of

$$3 \otimes 3 \otimes 3 = 10 \oplus 8 \oplus 8 \oplus 1.$$

The decuplet is symmetric in flavour, the singlet is antisymmetric and the two octets have mixed symmetry.

Following $SU(3)$, the nine states (nonet) made out of a pair $q\bar{q}'$ (meson) states containing the u, d, and s quarks can be decomposed into the trivial representation of singlet and octet. The notation for this decomposition is

$$3 \otimes 3 = 8 \oplus 1.$$

The parity of a meson state is given by $(-1)^{l+1}$, where l is the orbital angular momentum and it's spin is either 0 (antiparallel quark spins) or 1 (parallel quark spins). The C -parity(charge conjugation), which is defined only for the $q\bar{q}'$ states is given by the relation $C = (-1)^{l+s}$. The C -parity can also be generalised to the G -parity defined by $G = (-1)^{l+l+s}$ for the mesons made of quarks and their own antiquarks, where I is the isospin quantum number.

It can also be noted in this context that the mesons are classified in J^{PC} multiplets. The $l = 0$ states give the pseudoscalar (0^{-+}) and vector (1^{--}) mesons where as $l = 1$ states are the scalars (0^{++}), the axial vectors (1^{++}) and (1^{+-}) and the tensors (2^{++}). Depending upon the quark-antiquark combinations, three types of terminology to categorise the mesons are being widely used in the literature. They are:

- a) Light-light mesons, where both the quark and antiquark are light (u,d or s only). π and K mesons play the dominant role in this sector.

b) Heavy-light mesons, where one quark or antiquark is heavy (c, b or t) and the other is light. D and B mesons are characterised in this category and

c) Heavy-heavy mesons, where both the quark and antiquark are heavy. The particles of the cutting edge study of Charmonium and Bottomonium spectroscopy like η_c , Υ , η_b etc. are studied under this category.

In this thesis work, however, we put our special emphasis on the pseudoscalar heavy-light mesons of $l = 0$ state. In Table 1.2, we show the different heavy-light pseudoscalar mesons with their experimental masses which will be involved in this work.

Table 1.2: The pseudoscalar heavy-light mesons and their experimental masses from PDG [2]. B_c meson is included as a heavy-light meson due to its different flavour.

Mesons	Quark composition	Meson masses(in GeV)
D^0	$c\bar{u}$	1.8649
D^\pm	$c\bar{d}$	1.8696
D_s	$c\bar{s}$	1.9685
B^0	$d\bar{b}$	5.2796
B^\pm	$u\bar{b}$	5.2793
B_s	$s\bar{b}$	5.3668
B_c	$c\bar{b}$	6.277

1.1.3 Role of CKM in the Standard Model

In 1963, N. Cabibbo proposed the Cabibbo theory [9] of quark mixing to explain the suppression of $\Delta S = 0$ decay over $\Delta S = 1$ decay. According to this theory, the weak eigen states can be represented as the combinations of flavour eigen states i.e. the quarks in strong interaction are not the same as the ones in the weak interaction. In 1972, Kobayashi and Masakawa [10] extended the idea of Cabibbo Model to six quarks. Thus in the Standard Model, quark flavour mixing is described by a 3×3 unitary matrix, the so called Cabibbo Kobayashi-Masakawa(CKM) matrix. The CKM matrix can be regarded as a rotation from the quark mass eigenstates d , s , and b to a set of new states d' , s' , and b' with diagonal

couplings to u , c , and t . The standard notation of CKM matrix is

$$\begin{pmatrix} d' \\ s' \\ b' \end{pmatrix} = \begin{pmatrix} V_{ud} & V_{us} & V_{ub} \\ V_{cd} & V_{cs} & V_{cb} \\ V_{td} & V_{ts} & V_{tb} \end{pmatrix} \begin{pmatrix} d \\ s \\ b \end{pmatrix}. \quad (1.2)$$

Although the quark couplings to the W-boson are non-universal, the departure from universality is constrained in the Standard Model by the unitarity of the CKM matrix. Unitarity is the only powerful constraint on CKM matrix V_{CKM} . Without loss of generality, the matrix can be parametrised in terms of three mixing angles $\theta_{12}, \theta_{23}, \theta_{13}$ and one phase δ :

$$V_{CKM} = \begin{pmatrix} C_{12}C_{13} & S_{12}C_{13} & S_{13}e^{-i\delta} \\ -S_{12}C_{23} - C_{12}S_{23}S_{13}e^{-i\delta} & C_{12}C_{23} - S_{12}S_{23}S_{13}e^{-i\delta} & S_{23}C_{13} \\ S_{12}S_{23} - C_{12}C_{23}S_{13}e^{-i\delta} & -C_{12}S_{23} - S_{12}C_{23}S_{13}e^{-i\delta} & C_{23}C_{13} \end{pmatrix}, \quad (1.3)$$

where $C_{ij} \equiv \cos\theta_{ij}$ and $S_{ij} \equiv \sin\theta_{ij}$ for ($ij = 12, 23$ and 13). The phase term δ is the unique source of CP violation in quark flavour changing processes within the Standard Model. This term does not appear for two generation of quarks. The known values of CKM elements motivated Wolfenstein [11] to parametrise the CKM matrix in terms of four independent parameters A, λ, ρ, η :

$$V_{CKM} = \begin{pmatrix} 1 - \frac{1}{2}\lambda^2 & \lambda & A\lambda^3(\rho - i\eta) \\ -\lambda & 1 - \frac{1}{2}\lambda^2 & A\lambda^2 \\ A\lambda^3(1 - \rho - i\eta) & -A\lambda^2 & 1 \end{pmatrix}. \quad (1.4)$$

This parametrisation is based on the expansion of the small parameter $\lambda = \sin\theta_c \simeq 0.22$, where θ_c is the Cabibbo angle. The recent values of these parameters, provided by the CKMfitter and UTfit [12] groups for Particle Data group [2] are $\lambda = 0.22535 \pm 0.00065$, $A = 0.817 \pm 0.015$, $\bar{\rho} = \rho(1 - \frac{\lambda^2}{2} + \dots) = 0.136 \pm 0.018$ and $\bar{\eta} = 0.348 \pm 0.014$.

The unitarity condition of CKM matrix imposes the relations $\sum_i V_{ij}V_{ik}^* = \delta_{jk}$ and $\sum_j V_{ij}V_{kj}^* = \delta_{ik}$. The six vanishing combinations which are valid from these relations are

$$V_{ud}V_{us}^* + V_{cd}V_{cs}^* + V_{td}V_{ts}^* = 0, \quad (1.5)$$

$$V_{us}V_{ub}^* + V_{cs}V_{cb}^* + V_{ts}V_{tb}^* = 0, \quad (1.6)$$

$$V_{ud}V_{ub}^* + V_{cd}V_{cb}^* + V_{td}V_{tb}^* = 0, \quad (1.7)$$

$$V_{ud}V_{cd}^* + V_{us}V_{cs}^* + V_{ub}V_{cb}^* = 0, \quad (1.8)$$

$$V_{cd}V_{td}^* + V_{cs}V_{ts}^* + V_{cb}V_{tb}^* = 0 \quad (1.9)$$

and

$$V_{ud}V_{td}^* + V_{us}V_{ts}^* + V_{ub}V_{tb}^* = 0. \quad (1.10)$$

By using the Wolfenstein parametrisation, these relations can be visualised as triangles of equal area (which are proportional to the magnitude of CP violation) in the complex plane (ρ, η) as illustrated in Fig.1.1 for the most commonly used Eqn.1.7.

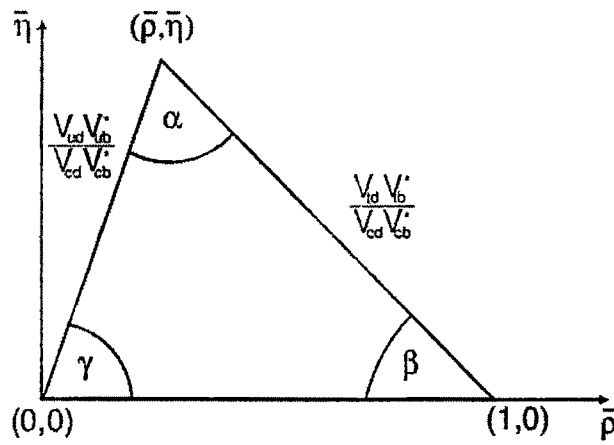


Figure 1.1: Unitarity triangle from Eqn.1.7

The three angles of this triangle are [13]

$$\alpha = \arg \left[-\frac{V_{td} V_{tb}^*}{V_{ud} V_{ub}^*} \right] = \tan^{-1} \left(\frac{\bar{\eta}}{\eta^2 + \bar{\rho}(\bar{\rho} - 1)} \right), \quad (1.11)$$

$$\beta = \arg \left[-\frac{V_{cd} V_{cb}^*}{V_{td} V_{tb}^*} \right] = \tan^{-1} \left(\frac{\bar{\eta}}{1 - \bar{\rho}} \right), \quad (1.12)$$

$$\gamma = \arg \left[-\frac{V_{cd} V_{cb}^*}{V_{cd} V_{cb}^*} \right] = \tan^{-1} \left(\frac{\bar{\eta}}{\bar{\rho}} \right). \quad (1.13)$$

In general, the real side of the triangle from Eqn.1.7, is normalised to one using

$$\bar{p} + i\bar{\eta} = -\frac{V_{ud} V_{ub}^*}{V_{cd} V_{cb}^*} \quad (1.14)$$

and results in sides

$$R_b = \sqrt{\bar{p}^2 + \bar{\eta}^2} = \frac{1 - \lambda^2/2}{\lambda} \left| \frac{V_{ub}}{V_{cb}} \right| \quad (1.15)$$

$$R_t = \sqrt{(1 - \bar{p}^2) + \bar{\eta}^2} = \frac{1}{\lambda} \left| \frac{V_{td}}{V_{cb}} \right|. \quad (1.16)$$

In the Standard Model, R_t is the least known length of unitarity triangle, which can be measured through the mixing¹ of B meson[14]. Considering the experimental average values of the CKM elements, from PDG2012 [2], we can express V_{CKM} as:

$$V_{CKM} = \begin{pmatrix} 0.9742 \pm 0.0002 & 0.2252 \pm 0.0009 & (4.15 \pm 0.49) \times 10^{-3} \\ 0.230 \pm 0.011 & 1.006 \pm 0.023 & (40.9 \pm 1.1) \times 10^{-3} \\ (8.4 \pm 0.6) \times 10^{-3} & (42.9 \pm 2.6) \times 10^{-3} & 0.89 \pm 0.07 \end{pmatrix}. \quad (1.17)$$

The main aim of precession of CKM physics is threefold: (a) to measure the mixing and CP violating parameters of V as accurately as possible; (b) to test the self-consistency of the CKM picture for quark mixing and CP violation and (c) to search for possible new physics beyond the CKM mechanism. It is therefore, important to measure very precisely

¹Mixing of B and B_s mesons are discussed in Chapter 3

the various entries of the CKM matrix.

1.2 Weak decay of Mesons

During a weak decay a fermion (quark or lepton) transforms into its doublet partners by emission of a charged boson W^\pm . The W^\pm can then either materialize into a fermion anti fermion pair or couple to another fermion and transform into its doublet partner. Therefore a weak decay can be represented as the interaction of two fermion currents, mediated by a charged W^\pm bosonic current. Obviously, a weak decay can occur only if the parent fermion has a larger mass than the daughter fermion and hence the u quark and e lepton being the lowest mass quark and lepton do not decay. There are three types of weak decays which are extensively studied in the literature. They are leptonic decay, semileptonic decay and non-leptonic decay. In Table 1.3, we tabulate the three types of weak decays and their product particles.

Table 1.3: The three types of weak decay and their decay products.

Types of weak decay	Products	Example
Leptonic decay	Leptons only	$D^+ \rightarrow l^+ \nu$ $\pi^\pm \rightarrow l^\pm \nu$ $K^\pm \rightarrow l^\pm \nu$ etc.
Semileptonic decay	Both leptons and hadrons	$B^+ \rightarrow D l^+ \nu$ $B^- \rightarrow \pi^0 l^- \bar{\nu}$ $B_c \rightarrow J/\psi l^+ \nu$ etc.
Non-leptonic decay	Hadrons only	$B^0 \rightarrow D^- \pi^+$ $\bar{B}^0 \rightarrow D^+ \rho^-$ $\bar{B} \rightarrow \bar{K} J/\psi$ etc.

1.2.1 Leptonic and Semileptonic decay of mesons

In this section, we present an overview of leptonic and semileptonic decays, which are useful for both charm and bottom hadrons.

In the diverse phenomenology of weak interactions, leptonic and semileptonic decays of hadrons have a special standing, since the final state particles include a single charged lepton, the clearest experimental signature for a weak process mediated by the W-boson. From the theoretical perspective, these decays are relatively simple and provide a means both to measure the fundamental Standard Model parameters and to perform detailed studies of decay dynamics.

Historically, the semileptonic process of nuclear decay opened the era of weak interaction physics and presented physicists with the mystery of the electron's undetected partner, the neutrino [15]. The process underlying β decay is the W-boson mediated weak transition $d \rightarrow uW, W \rightarrow e\bar{\nu}_e$; where the decay of a d-quark into a u-quark transforms a neutron (udd) into a proton (uud). β decay was the only known weak process from the turn of the century until the late 1930s and 1940s, when muons, pions and kaons were discovered in cosmic rays.

A key feature of leptonic and semileptonic decays is their relative simplicity, a consequence of the fact that here the effects of the strong interactions can be isolated. The decay amplitude for either type of decay can be written as the product of a well-understood leptonic current for the system and a more complicated hadronic current for the quark transition. In leptonic decays, the hadronic current describes the annihilation of the quark and antiquark in the initial-state meson, whereas in semileptonic decays it describes the evolution from the initial to final state hadrons. Because strong interactions affect only one of the two currents, leptonic and semileptonic decays are much more tractable theoretically than hadronic decays, in which the decay products of the W are also hadrons. A further complication of hadronic decays is that the hadrons in the final state can interact strongly with each other. Leptonic and semileptonic decays therefore, provide a means for studying the strong interactions in a relatively simple environment. Perhaps more important, the effects of strong interactions in these processes can be understood sufficiently well that the underlying weak couplings of quarks to the W boson can be determined.

The standard model successfully accounts for flavour-changing quark transitions in terms of a V-A charged weak current operator J^μ that couples to the W-boson according to the interaction Lagrangian [17]

$$L_{int} = -\frac{g}{\sqrt{2}}(J^\mu W_\mu^+ + J^{\mu+} W_\mu^-) \quad (1.18)$$

where

$$J^\mu = \sum V_{q_1 q_2} J^\mu = \sum \bar{u}_i \gamma^\mu \frac{1}{2}(1 - \gamma_5) V_{q_1 q_2} d_j. \quad (1.19)$$

The indices i and j run over the three quark generations, so that the field operators u_i ($i = 1, 2, 3$) annihilate (or create their antiparticles) and the d_j annihilate. Thus the amplitudes of the decay processes are proportional to the CKM element $V_{q_1 q_2}$.

Purely leptonic decays are considered to be the simplest and the cleanest decay modes of the pseudoscalar charged meson. To obtain transition amplitudes, the quark and lepton current operators must be sandwiched between physical states [16]. For the leptons, this calculation yields directly an expression in terms of Dirac spinors. The hadronic current, however, cannot be so easily evaluated, since the quarks in the hadrons are not free and nonperturbative strong-interaction effects are important in describing the physical states. In general, the long-distance effects, present in the formation of the bound meson state (hadronisation) in hadronic interactions are parameterised with so called *form factors*. These form factors are functions of the momentum transfer and polarization states of the hadrons involved in the interaction. For leptonic decays, the initial state is unpolarised, and the momentum transfer is constant $q^2 = m^2$ and hence the form factor becomes a constant f_p , the *decay constant* of the meson.

Mathematically, the amplitude for a leptonic decay can be written as [17]

$$\mathcal{A}(M_{Q\bar{q}} \rightarrow l^-\bar{\nu}) = -i \frac{G_F}{\sqrt{2}} V_{qQ} L^\mu H_\mu \quad (1.20)$$

where the leptonic current L^μ can be written in terms of Dirac spinors u_l and ν_v

$$L^\mu = \bar{u}_l \gamma^\mu (1 - \gamma_5) \nu_v. \quad (1.21)$$

The hadronic current for leptonic decay is very simple, since the only four vector available to be constructed with the leptonic current is q^μ . i.e.

$$H^\mu = \langle 0 | \bar{q} \gamma^\mu (1 - \gamma_5) Q | M \rangle = i f_p q^\mu. \quad (1.22)$$

Here f_p is parametrised to absorb all the strong interaction effects, which is called the decay constant. Since the two initial quarks must annihilate, the matrix element is sensitive to f_p , which measures the amplitude for the quarks to have zero separation.

For semileptonic decay of a meson M into a meson X , the amplitude takes the form [18, 19]

$$\mathcal{A}(M_{Q\bar{q}} \rightarrow X_{q\bar{q}} l^-\bar{\nu}) = -i \frac{G_F}{\sqrt{2}} V_{qQ} L^\mu H_\mu. \quad (1.23)$$

Here the hadronic current

$$H^\mu = \langle X | \bar{q} \gamma^\mu (1 - \gamma_5) Q | M \rangle \quad (1.24)$$

is not calculated in a simple manner as is done in leptonic decay, since q^2 is different from event to event. Thus H^μ can be expressed in terms of different form factors, which isolate the effects of strong interactions on the amplitude. Unlike the case of electromagnetic interaction, here the normalisation of weak form factors are in general unknown. However, in the limit of infinitely heavy quark masses $m_Q \rightarrow \infty$, a new heavy flavour symmetry appears in the effective Lagrangian of the standard model which provides the model independent normalisation of the weak form factors and the necessity of HQET(Heavy Quark Effective Theory)[20] enters into the literature. In this heavy quark symmetry, the form factors (two for pseudoscalar to pseudoscalar transition and four for pseudoscalar to vector transition) of heavy-light mesons in semileptonic decay can be expressed in terms a single form factor

which is termed as *Isgur-Wise function* [21].

In heavy-quark decays, semileptonic modes are generally much more accessible experimentally than leptonic modes, simply because semileptonic branching fractions are larger. Considering its simplicity and great importance, Leptonic and semileptonic decays have been widely studied in the literature [22, 23, 24, 25, 26, 27]. For a review one can see the Ref.[16] and the references there in.

1.2.2 Status of decay constant f_p in leptonic decay

Measurement of purely leptonic decay branching ratios of heavy-light mesons are important since it allows an experimental determination of the product $|V_{qQ}|f_p$. If the CKM element V_{qQ} is well known from other measurements, then f_p can be well measured. If, on the other hand, the CKM element is less well or poorly measured, then having the theoretical input on f_p can allow a path to determine the CKM element. These decay constants are accessed both experimentally and through lattice Quantum Chromodynamics (lQCD) simulations. While for f_π , f_K , f_D , experimental measurements agree well with lattice QCD calculations, a discrepancy is seen for the value of f_{D_s} : The 2008 PDG average for f_{D_s} is 273 ± 10 MeV[28], about 3σ larger than the most precise $N_f = 2 + 1$ lQCD result from the HPQCD/UKQCD collaboration [29], 241 ± 3 MeV. On the other hand, experiments and lQCD calculations agree very well with each other on the value of f_D , $f_D(\text{expt}) = 205.8 \pm 8.9$ MeV and $f_D(\text{lQCD}) = 207 \pm 4$ MeV. The discrepancy concerning f_{D_s} is quite puzzling because whatever systematic errors have affected the lQCD calculation of f_D , they should also be expected for the calculation of f_{D_s} [30]. It is being argued that for D_s^+ decays, beyond the Standard Model there is existence of a charged Higgs boson or any other charged object which would modify the decay rates but would not necessarily be true for the D^+ decay [31, 32].

However, the discrepancy is reduced to 2.4σ with the new (updated) data from CLEO

[33, 34] and Babar [35], together with the Belle measurement [36] and the PDG(2010) average is $f_{D_s} = 257.5 \pm 6.1$ MeV [37]. Lately the HPQCD collaboration has also updated its study of the D_s decay constant [37]. By including additional results at smaller lattice spacing along with improved tuning of the charm and strange quark masses, a new value for the D_s decay constant has been reported as $f_{D_s} = 248.0 \pm 2.5$ MeV which has lowered this discrepancy with the latest PDG average $f_{D_s} = 260.0 \pm 5.4$ MeV [2].

In studying the leptonic branching ratio of B meson, the largest uncertainty arises from the unknown decay constant f_B . In principle f_B can be measured in the annihilation process of $B^- \rightarrow l^-\bar{\nu}$, since the decay rate is proportional to the product of $f_B^2 |V_{ub}|^2$. But it is a very difficult process to measure and even if this were done, the uncertainty on $|V_{ub}|$ will not lead to a precise result. Thus the best hope is to rely on unquenched lattice QCD or Potential model, which can use the measurements of the analogous $D^+ \rightarrow \mu^+\nu$ as a check. The knowledge of f_{B_s} is also important, but it cannot be measured directly since B_s does not have leptonic decay and so the violation of $f_{B_s} = f_B$ must be estimated theoretically[2]. The decay of B and B_s mesons is also important for studying CP violation, which has nothing to do with D mesons. Thus determination of f_B and f_{B_s} in conjunction with that of D mesons becomes crucial to study whether there is new physics[NP] [38, 39, 40] beyond the Standard Model or not.

1.2.3 CP violation in meson decays

The CP transformation of a particle refers to the combination of charge conjugation C with parity P. Under C transformation a particle interchange to an antiparticle and vice-versa. Under P transformation, the handedness of space is reversed *i.e* $x \rightarrow -x$. Thus, for example the combined effect of CP transformation a left-handed electron e^- is transformed into a right-handed positron e^+ .

If CP transformation were an exact symmetry, the laws of Nature would be the same for

matter and antimatter. Most of the observed phenomenon are CP symmetric. Particularly, the three interactions gravitational, electromagnetic and strong respects these symmetries. On the other hand, the weak interactions, violate C and P symmetries in the strongest possible way. While C and P symmetries are violated separately, the combined effect of CP is still preserved in most weak interaction processes. However, in certain rare processes, as discovered in neutral K meson decays in 1964 [41] and in neutral B meson decays in 2001 [42, 43], CP symmetry is found to be violated. The decay rate asymmetry for K meson decay is found to be at 0.003 level, whereas this CP violating effect is quite larger for B^0 decays which is about 0.70. Hence the study of CP violation in charmless charged B decays provides a stringent tests of the CKM picture of CP violation in the Standard Model. However, it cannot be excluded for the moment that CP violation is generated by a mechanism beyond the Standard Model [44].

1.2.4 Non-leptonic decay of mesons

Non-leptonic decays, in which only hadrons appear in the final state, are strongly influenced by the confining colour forces among the quarks. Whereas in semileptonic transitions the long-distance QCD effects are explained by some form factors parametrising the hadronic matrix elements of quark currents, non-leptonic processes are complicated by the phenomenon of quark rearrangement which occurs due to the exchange of soft and hard gluons. The theoretical analysis involves matrix elements of local four-quark operators, which are more complex to deal with than current operators. These strong-interaction effects prevented the coherent understanding of non leptonic decays for a long time. However, a factorization prescription for reducing the hadronic matrix elements of four-quark operators to products of current matrix elements provided a path onto the dynamics of non-leptonic processes [45, 46]. Later on, non-leptonic two body decays of B and D mesons were studied in the approximation of factorisation method [47, 48, 49, 26], where the com-

plicated non-leptonic decay amplitudes are related to products of meson decay constants and hadronic matrix elements of current operators, which are similar to those encountered in semileptonic decays.

In many respects, non-leptonic decays of heavy mesons are an ideal instrument for exploring the most interesting aspect of QCD like CP violation. In studying CP violation for mixing of B and D mesons the best bounds come from the measurement of a particular non-leptonic decay. For example, in case of $D - \bar{D}$ mixing the bounds come from the measurements of $D \rightarrow K^+ \pi^-$ [50, 51].

Regarding the recent updates of non-leptonic decay in B meson, in March 2012, the LHCb collaboration reported an observation for CP violation in $B^\pm \rightarrow D K^\pm$ decay. Recently, in 2013 the same collaboration has announced a similar observation for the first time with a significance of more than 5σ marks for the B_s mesons [52].

1.3 Quantum Chromodynamics(QCD)

Quantum Chromodynamics, familiarly called QCD is the sector of the Standard Model(SM) which describes the action of the strong force. It is obtained from the full SM by setting the weak and electromagnetic coupling constants to zero and freezing the scalar doublet to its vacuum expectation value. What remains is a Yang-Mills(YM) theory with local gauge group $SU(3)$ (colour) vectorially coupled to six Dirac fields (quarks) of different masses (flavours). The vector fields in the YM Lagrangian (gluons) live in the adjoint representation and transform like connections under the local gauge group whereas the quark fields live in the fundamental representation and transform covariantly. The QCD Lagrangian reads

$$\mathcal{L}_{\text{QCD}} = -\frac{1}{4} F_{\mu\nu}^a F^{a\mu\nu} + \sum_{\{q\}} \bar{q} (i\gamma^\mu D_\mu - m_q) q, \quad (1.25)$$

where $\{q\} = u, d, s, c, b, t$, $F_{\mu\nu}^a = \partial_\mu A_\nu^a - \partial_\nu A_\mu^a + g f^{abc} A_\mu^b A_\nu^c$, $D_\mu = \partial_\mu - iT^a A_\mu^a$. f^{abc} are the $SU(3)$ structure constants and T^a form a basis of the fundamental representation of the $SU(3)$ algebra. When coupled to electromagnetism, gluons behave as neutral particles whereas u, c and t quarks have charges $+(2/3)e$ and d, s and b quarks have charges $-(1/3)e$.

The main properties of QCD follow:

- It is invariant under Poincaré transformation², parity transformation, time reversal and (hence) charge conjugation. In addition, it conserves quark flavour.
- Being a non-abelian gauge theory, the physical spectrum consists of colour singlet states only. The simplest of these states have the quantum numbers of quark-antiquark pairs (mesons) or of three quarks (baryons), although other possibilities are not excluded.
- The QCD effective coupling constant $\alpha_s(q)$ decreases, as the momentum transfer scale q increases (asymptotic freedom) [53, 54]. This allows perturbative calculations in α_s at high energies.
- At low energies it develops an intrinsic scale, which is usually referred as Λ_{QCD} and provides the main contribution to the masses of most hadrons. At scales $q \sim \Lambda_{\text{QCD}}$, $\alpha_s(q) \sim 1$ and perturbation theory cannot be used. Nonperturbative techniques are being used at this scale, the best established of which is lattice QCD(lQCD).

1.3.1 Perturbative and Non perturbative QCD

Asymptotic freedom turned out to be a useful tool in understanding high energy QCD. The short distance behaviour of quarks and gluons can be described with a perturbative

²Poincaré transformation is the name sometimes (e.g., Misner *et al.*, in Gravitation. San Francisco: W. H. Freeman, 1973.) given to what some other authors (e.g., Weinberg Gravitation and Cosmology: Principles and Applications of the General Theory of Relativity. New York: Wiley, 1972.) term an inhomogeneous Lorentz transformation $x^\mu = \Lambda_\nu^\mu x^\nu + a^\mu$, where Λ_ν^μ is a Lorentz tensor.

expansion in the small value of the coupling constant and allows the calculation of physical properties from first principles. However, understanding of the strong interactions are far from complete. Properties of medium and low energy QCD still present challenges to particle physicists and remain to be understood. Perturbation theory, which proved very useful for the high energy region, is not applicable at low energy scales and no other analytical tool has been developed so far. Quark confinement, chiral symmetry breaking, dynamical mass generation (ie. the hadron spectrum and the origin of the hadron mass), hadron high energy scattering are fundamental strong interaction phenomena at low energy but they are inherently non perturbative and have not yet been proven analytically from the QCD Lagrangian.

The only reliable method of studying the physical properties of low energy QCD is the lattice formulation of gauge theory proposed by Wilson [55] and independently by Polyakov [56, 57] and Wegner [58]. This theory provides a non perturbative description of QCD and indeed numerical simulations of QCD on Euclidean lattices give strong evidence for colour confinement and spontaneous chiral symmetry breaking as well as describing dynamical mass generation from the QCD Lagrangian [59, 60, 61]. But lattice QCD is limited to the Euclidean formulation of QCD and cannot be applied in Minkowski space time to simulate high energy reactions in which the particles are inherently moving near the light cone. It is also difficult to understand from simulations the important QCD mechanisms that lead to colour confinement. The numerical integrations required in this approach are also extremely computationally expensive. Even with the use of efficient Monte Carlo methods, approximations must be made in order to obtain results with the computational technology available today. Even then, however, several lattice gauge theory calculations are being performed and have already made an impact and preliminary understanding has been achieved on the sources of error in these studies.

The only other way to proceed in the non perturbative regime of QCD is by inventing and using phenomenological models that capture the most important features of strong

QCD. A great variety of models have been developed during thirty years of QCD. Among them are the constituent quark models , light cone QCD [62], and various effective field theories such as Heavy Quark Effective Theory (HQET) and Chiral Perturbation Theory (ChPT) [63, 64] besides QCD Sum rules [65, 66].

In Constituent quark models (CQM), hadrons are considered to be bound states of three valence quarks (baryons) and a quark and an antiquark (mesons). Those quarks are quasi-particle degrees of freedom with the same quantum numbers as QCD quarks, but differing from the latter in their masses and in the fact that they could have an internal structure. Among CQM, non-relativistic quark models (NRQM) have shown to be phenomenologically very successful. In these models, constituent quarks are treated non relativistically and they interact through potentials that mimic QCD asymptotic freedom and confinement. In NRQM, the dynamical effects of gluon fields on hadron structure and properties are ignored. The quarks are considered as non relativistic objects interacting via an instantaneous adiabatic potential provided by the gluons. NRQM could account satisfactorily for the magnetic moments of the octet baryons [67]. Isgur and Karl [68, 69, 70, 71, 72, 73] studied baryon spectra within NRQM with the non relativistic point like quarks moving in a flavour independent confining potential and with the help of colour hyperfine interactions was able to explain the main features of the spectra. Meson spectra was explained within NRQM [74] by the generation of colour hyperfine interaction among quarks generated through the one gluon exchange potential introduced in [75].

1.3.2 Effective Field Theory(EFT) and Non-relativistic QCD (NRQCD)

In studying different static and dynamic properties of hadrons, relativistic and non-relativistic treatment of the quarks are found to be equally useful with their own success and failure. However, a proper relativistic treatment of the bound state based on the Bethe-Salpeter equation [76] has been found to be very difficult. The entanglement of all energy modes in

a fully relativistic treatment is more an obstacle than an advantage for the factorization of physical quantities into perturbative and non perturbative contributions. To overcome this problem, semi-relativistic models have been adopted to study the hadronic properties, but due to the uncontrolled approximation it loses contact with QCD.

A non relativistic treatment, offered by the large mass of the heavy quarks on the other hand has clear advantages. The basis of non-relativistic treatment is that in the center of mass frame of the heavy quark-antiquark system, the momenta p of quark and antiquark are dominated by their rest mass. It can also be noted that the relativistic theory, like the light front approach, reproduces the results of non-relativistic potential models under non-relativistic approximation [77].

Within the non-relativistic approach, three scale parameters are found to play an important role in studying the bound states of a heavy quark and antiquark. These scale parameters include the heavy quark mass m (hard scale), the momentum transfer mv (soft scale), which is inversely proportional to the typical size of the system r and the binding energy scale mv^2 (ultrasoft scale), which is proportional to the typical time of the system. Here v is the typical heavy-quark velocity in the center of mass frame and the scales mv and mv^2 are dynamically generated. For a non-relativistic system, $v \ll 1$ and the above scales are hierarchically ordered: $m \gg mv \gg mv^2$. For bottomonium study $v^2 \approx 0.1$ whereas for charmonium $v^2 \approx 0.3$. It is useful to study the physics at each of these scales separately. The wide range of involved energy scales also makes lattice calculation extremely challenging. Generally speaking, lattice QCD(lQCD) can encompass only a limited range of scale and hence, it becomes more tractable after scale separation.

Effective field theories(EFT) are the convenient quantum tool to separate these scales. It describes the low-momentum degrees of freedom in the original theory. To construct an effective field theory, the high momentum degrees of freedom are integrated out in that theory. For low energy EFT, such integration is done in a matching procedure which enforces the equivalence between EFT and QCD at any given order of the expansion in v . Thus a

prediction of the EFT is a prediction of QCD with an error of the size of the neglected order in v .

Non-relativistic QCD (NRQCD) [78, 79] is an effective field theory which follows from QCD and is obtained by integrating out the hard scale m [80, 81]. Taking into account that m is much larger than the remaining scales of the system, the velocity of heavy quark is chosen as the expansion parameter [82] here. Thus, NRQCD has a UV cutoff scale $\Lambda \approx m$. Since $m \gg \Lambda_{QCD}$, it can be made equivalent to QCD at any desired order in $1/m$. In a proper way of speaking, it can reproduce QCD for processes with $p < \Lambda_{QCD}$ where as processes with $p > \Lambda_{QCD}$ are not manifested in NRQCD. Thus Λ_{QCD} becomes the factorization scale between the soft and hard physics.

Following NRQCD, there is another Effective Field Theory known as potential Non-relativistic QCD(pNRQCD), which integrates out the soft scale mv . It distinguishes two situations: 1) weakly coupled pNRQCD when $mv \gg \Lambda_{QCD}$, where the matching from NRQCD to pNRQCD is performed in perturbation theory and 2) strongly coupled pNRQCD when $mv \approx \Lambda_{QCD}$, where the matching is non perturbative [83].

It is not necessary that the heavy quarks Q and Q' in the bound state of mesons have similar masses in NRQCD but the masses must be large compared to Λ_{QCD} . In systems containing a heavy quark with mass much larger than the QCD scale (Λ_{QCD})i.e $m_Q \rightarrow \infty$, a new symmetry known as Heavy Quark Symmetry arises [84, 87, 88, 89, 90, 85, 86].

Heavy Quark Symmetry is an approximate $SU(2N_{HF})$ symmetry of QCD, N_{HF} being the number of heavy flavours (c, b, \dots) that appears in systems containing heavy quarks with masses much larger than the typical quantities ($\Lambda_{QCD}, m_u, m_d, m_s, \dots$) which set up the energy scale of the dynamics of the remaining degrees of freedom. In that limit, the dynamics of the light quark degrees of freedom becomes independent of the heavy quark flavour and spin. This infinite mass limit of QCD leads to another well defined effective field theory-**Heavy Quark Effective Theory (HQET)** [20] that allows a systematic, order by order evaluation of corrections to the infinite mass limit in inverse powers of the heavy

quark masses.

The concept of a new flavour symmetry for hadrons, containing a heavy quark was first introduced by Shuryak in 1980 [91], who later studied many properties of heavy mesons and baryons with QCD sum rules [62]. But a clear model independent formulation of the physical ideas of the spin flavour symmetry was developed by Nussinov and Wetzel [84], Voloshin and Shifman [87, 88], Politzer and Wise [89, 90], Isgur and Wise [85, 86] and Grinstein [92], until finally Georgi [20] reformulated the low energy effective Lagrangian for a heavy quark in a covariant way in a theory called Heavy Quark Effective Theory (HQET). Heavy Quark Symmetry and HQET have proved to be very useful tools to describe the dynamics of systems containing a heavy c or b quark [21, 93].

1.4 QCD Potential

QCD potential between a quark and antiquark has been one of the first important ingredient of phenomenological models to be studied in quarkonium physics. In a non-relativistic potential model, one ignores the dynamical effects of gluon fields on the hadron structure and properties. Quarks are considered as non-relativistic objects interacting via an instantaneous adiabatic potential provided by gluons[94]. The force between a heavy quark and a heavy/light quark is due to the static quark antiquark potential, since the heavy quark is static with respect to the light quark. Vairo [95] defines the potential as the function V into the Schrodinger equation describing the quark-antiquark bound state ψ :

$$E\psi = \left(\frac{p^2}{2m} + V \right) \psi, \quad (1.26)$$

p being the momentum of the quark-antiquark pair in the centre of mass frame and E is its binding energy.

The QCD potential is based on the two important facts of QCD: **confinement**, which

means that the force between quarks does not diminish as they are separated and **asymptotic freedom**, which means that in very high-energy reactions, quarks and gluons interact very weakly.

At low energy or large distance scale, colour confinement one of the prominent feature of QCD comes into play. In case of a quark antiquark pair in the colour singlet state, when one tries to separate the quark from the antiquark by pulling them apart then the interaction between the quarks gets stronger as the distance between them gets larger, similar to what happens in a spring. In fact, when a spring is stretched beyond the elastic limit, it breaks to produce two springs. In the case of the quark pair, a new quark-antiquark pair will be created when pulled beyond a certain distance. Part of the stretching energy goes into the creation of the new pair, and as a consequence, one cannot have quarks as free particles. To understand really what happens, one must make calculations in QCD at large distance scales where, according to the renormalization group equation, the coupling becomes very strong. At present time, such a calculation is found to be very difficult.

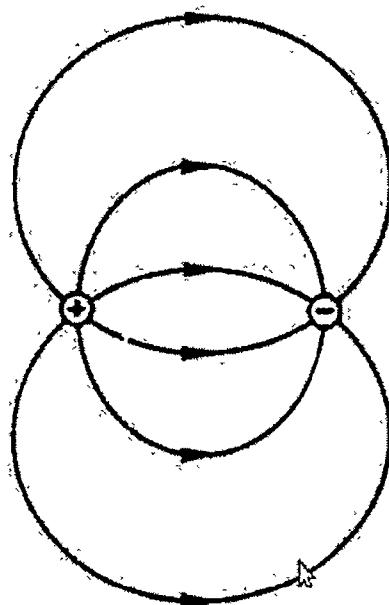


Figure 1.2: Electric lines between the positive and negative charges in QED.

In contrast to QED, where the electric lines between positive and negative charges spread all over the space (as shown in Fig.1.2) and generates a $\frac{1}{r}$ potential, in QCD the vacuum acts like a dual superconductor which squeezes the color electric field to a minimal geometrical configuration-a narrow tube as shown in fig.1.3.

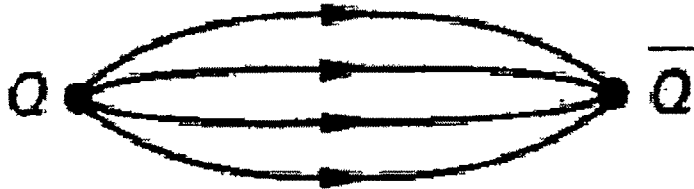


Figure 1.3: Flux tube due to chromoelectric lines of force in QCD.

The tube has approximately a constant cross section and constant energy density. Because of this feature, the energy stored in the flux increases linearly with the length of the flux. The qualitative picture is that the chromo-electric lines of force bunch together into a flux tube which leads to a distance independent force or a potential of the form

$$V(r) \sim \text{constant} \times r \quad (1.27)$$

for $r > M^{-1}$, where M is a typical hadronic mass scale. For hadron size of $1 fm = 5 GeV^{-1}$, $M = 200 MeV$. Nambu provided a connection between linear energy density and a linear Regge trajectory with the string model of hadrons [96] and calculated the potential to be

$$V(r) = br \quad (1.28)$$

where b is known as the QCD string tension which is also known as the slope of the potential. The linear form for the long range part of the QCD potential has been validated by Lattice QCD calculations. Phenomenologically, almost all the potential models have found $b = 0.18 GeV^2$.

At short distance (in the weak-coupling limit), on the other hand quarks are free, which can be represented by a Coulomb potential with an asymptotically free coupling constant. In this scale the quarkgluon interaction is similar to the electronphoton interaction in quantum electrodynamics with the Born term for the qq or $q\bar{q}$ interaction being the familiar $\frac{1}{r}$ form.

$$V(r) \sim \frac{1}{r} \quad (1.29)$$

The naive idea of this Coulomb like potential is that the exchange of a gluon gives rise to a force between the colour states. They are attractive in the color singlet channel and repulsive in the color octet channel but are spin and flavor independent. In contrast with QED the gluon self-coupling results in a slow decrease of the effective coupling strength at short distance. For hadrons, the one gluon exchange contribution in the colour singlet channel is given by:

$$V(r) = -\frac{4}{3} \frac{\alpha_s}{r} \quad (1.30)$$

where α_s is the strong running coupling constant and the factor $\frac{4}{3}$ in Eqn.1.30 arises from the SU(3) colour factors.

It is, however not a proper justification to consider the dominating role of one gluon exchange at short distances. Indeed the studies of the static potential by using LQCD in Ref.[97] suggests that the one gluon exchange can dominate only at very small distances which is hardly accessible from the lattice data and even after including the perturbative higher order correction, only a small part of the static potential is described by perturbative QCD. Generally speaking, Coulomb like potential in phenomenological models covers a large range of distances and should probably be considered only as a phenomenological description that the Coulomb like potential together with the linear contribution provides the medium range potential responsible for the bound states. This is manifested by the fact that $\frac{4\alpha_s}{3}$ is not necessarily small. In the Cornell model of quarkonia, it is in fact large [98].

Numerous variations of the resulting Coulomb plus linear potential exist in the literature. Some of the better known ones are

a) The Cornell potential

The Cornell Potential [99], which was initially proposed to describe masses and decay widths of charmonium states is given by

$$V(r) = -\frac{\beta}{r} + \frac{r}{a^2} + V_0 \quad (1.31)$$

where the coefficients a , β and V_0 are adjusted to fit the charmonium spectrum.

b) Screened Cornell potential

To include the effect of saturation of the strong interaction at long distances, a variation of the Cornell potential, which is called the Screened Cornell potential also appears in Lattice as [100]

$$V(r) = (-\beta/r + r/a^2) \left(\frac{1 - e^{\mu r}}{\mu r} \right) \quad (1.32)$$

where μ is the screening parameter. This potential behaves like a Coulomb potential at short distances but, unlike in the previous model, it tends to a constant value for large r (namely, for $r \gg \mu^{-1}$). β and μ are intrinsic to the model, while a , m_c and m_b were fixed by the authors. In this Potential the linearly growing confining potential flattens to a finite value at large distances, corresponding to the saturation of α_s to a finite value for decreasing Q^2 [101]. This effect should be due to the creation of virtual light quark pairs that screen the interaction between the bound quarks at long distances.

c) Richardson's potential

The Richardson's potential [102] incorporates the features of asymptotic freedom at short distances and linear confinement at long distances with a minimal interpolation between

these two asymptotic behaviours given by:

$$V(r) = \frac{8\pi}{33 - 2n_f} \Lambda \left[\Lambda r - \frac{f(\Lambda r)}{\Lambda r} \right] \quad (1.33)$$

Here n_f is the number of light quarks relevant to the renormalization scale which is taken equal to three, while Λ is the scale interpolation between the two asymptotic regimes.

d) Power law potential

This potential belongs to the special choices of the generality of the potential [103, 104, 105]

$$V(r) = -Cr^\alpha + Dr^\beta + V_0. \quad (1.34)$$

With $V_0 = 0$ and $\alpha = -1$, one gets

$$V(r) = -\frac{C}{r} + Dr^\beta. \quad (1.35)$$

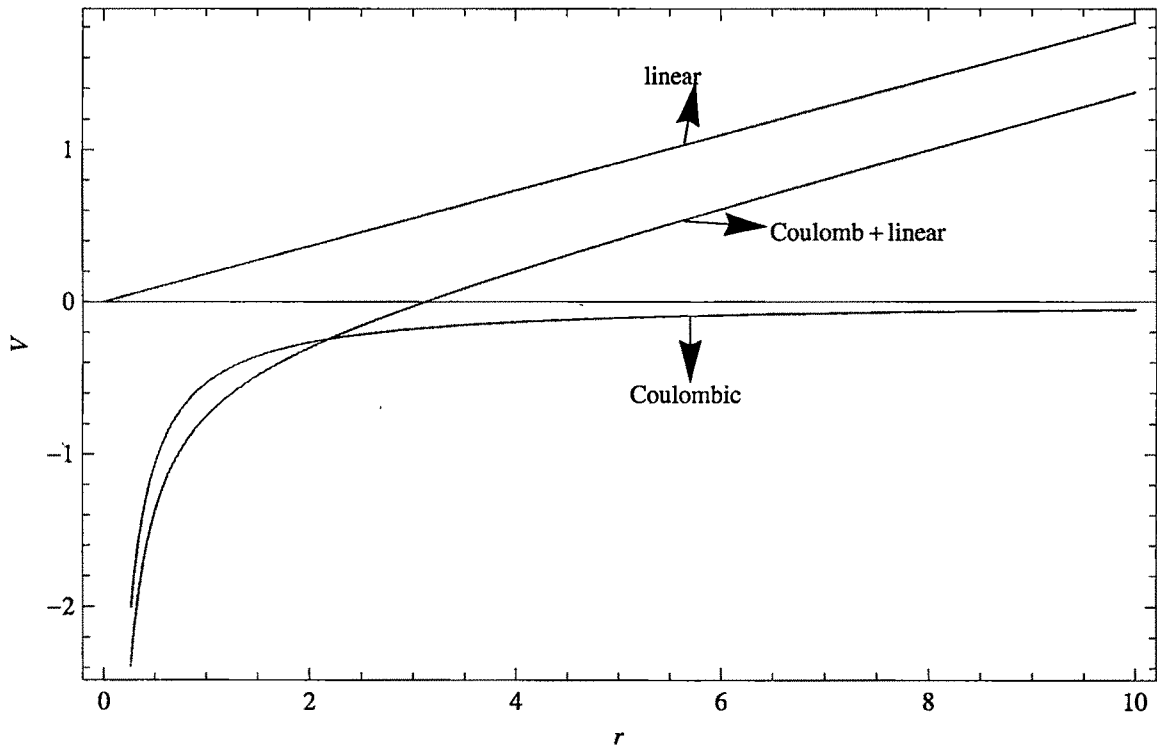
With the power $\beta = 1$, one obtain the simple Cornell potential Eqn.(1.31). However there is variation of β in different models. Martin potential[106] corresponds to $\beta = 0.1$, Heikkila, Tornquisit and Ono [107] potential corresponds to $\beta = 2/3$ where as Vinodkumar *et al* [108] explores within the range $0.5 \leq \beta \leq 2.0$.

Overall, the spin-independent features of quarkonium spectroscopy are well described by the potentials just described. The difficulty resulting from the consideration of different potentials is that the number of parameters to be fixed by comparison with experimental data is almost the same as the number of experimental data. Only qualitative arguments can be made to introduce a new potential form and hence it is more judicious to consider simpler models than to explain experimental data and to find out the limits of the models.

The Coulomb-plus-linear potential, so called the Cornell potential, has received a great deal of attention both in particle physics, more precisely in the context of meson spec-

troscopy where it is used to describe systems of quark and antiquark bound states, and in atomic and molecular physics where it represents a radial Stark effect in hydrogen. The addition of the linear term in the potential makes the “funnel” of the potential narrower and can be seen in Fig.1.4.

Figure 1.4: The potential $\frac{4}{3r}\alpha_s$ (coulombic), br (linear) and the potential $\frac{4}{3r}\alpha_s + br$ (Coulomb+linear), plotted against r (in GeV^{-1}) with $b = 0.183 GeV^2$ and $\alpha_s = 0.4$.



This potential was used with considerable success in models describing systems of bound heavy quarks [109, 110, 111]. All of our results presented in this work will be based on the Cornell potential with a constant shift c

$$V(r) = -\frac{4}{3r}\alpha_s + br + c. \quad (1.36)$$

The parameter c which we call the constant shift of the potential is also known as the quarks self energy[112]. This parameter is needed to reproduce the correct masses for heavy-light

meson system and is found to have a variation in its numerical values. For example in the work of relativistic quark model by Faustov *et al* $c = -0.3\text{GeV}$ [113] is used, in Ref.[99], it is taken to be $c = 0.50805\text{GeV}$, Mao Zhi Yang has taken $c = -0.19\text{ GeV}$ [114], Scora and Isgur [115] obtained $c = -0.81\text{ GeV}$, H M Choi *et al* in Ref.[116] have considered $c = -0.5575, -0.6664\text{GeV}$ where as Grant and Rosner [117] considered a large negative value of $c = -1.305\text{GeV}$ in a power law potential.

1.5 The Work of this Thesis

We mentioned above that perturbative QCD does not work at low energies, and that non-perturbative calculations have yet to produce detailed results.(In fact, the problem arises with any strongly-interacting field theory.) Until we can make quantitative predictions of hadronic properties using QCD, we cannot say that we understand the theory, nor can we make significant headway in this important regime. The main motivation for the present dissertation is to investigate meson properties in the quark model to understand the model applicability and generate possible improvements. Certain modifications to the model are suggested which have been inspired by fundamental QCD properties (such as running coupling or spin dependence of strong interactions). These modifications expand the limits of applicability of the constituent quark model and illustrate its weaknesses and strengths.

The present work is an endeavour to formulate meson wave functions with Coulomb plus linear potential incorporating relativistic correction (in a free Dirac way) and thereby to study the static and dynamic properties of heavy-light flavoured mesons using this wave function. The wave function has been tested initially in Ref.[118, 119] to study the properties of heavy-light mesons such as form factors, decay constants and charge radii. Further, the slope and curvature of Isgur-Wise function were studied in Ref.[120, 121] by incorporating two loop static potential in V-Scheme [122, 123]. However, application of V-Scheme was found to be successful in studying the Isgur-Wise function of D and D_s mesons but

was not so successful in studying the B , B_s and B_c mesons. Also the wave function shows singularity at the origin, which is required to study the leptonic decay constant in the non-relativistic limit.

Considering these two facts, we further improve the wave function and examine two general areas in the quark model: models of meson decay and final state interactions. The meson properties studied include meson masses, decay constants, form-factors and Isgur-Wise functions. The results are then compared to the experimental data, lattice gauge theory calculations (lQCD) and other theories.

Our motivation to study heavy-light mesons, containing at least one heavy quark is natural not only because they are being intensively studied by current experiments, but also because their decay dynamics are significantly different from particles containing only light quarks.

In Chapter 2, we compute the ground state masses and Leptonic decay constants of Open flavour charm Mesons (D D_s and B_c using the QCD Potential model described above. Here we introduce a short distance scale to regularise the wavefunction at the origin and the strong running coupling constant is taken from the \overline{MS} scheme with $\alpha_s = 0.39$ for D and D_s mesons and $\alpha_s = 0.22$ for B_c meson.

In Chapter 3, we try to incorporate the effect of short distance scale into the B sectors of mesons with a scale dependent α_s [125] and compute the Oscillation Frequency of B_d and B_s mesons.

In Chapter 4, we transform the wavefunction from co-ordinate space to momentum space by using Fourier transform and study the masses and Decay constants without applying the short distance scale. We use the same prescription of strong running coupling constant(α_s) as is used in chapter 3 and compute the branching ratio for different leptonic channels to compare with the experimental data.

In Chapter 5, we study the Isgur-Wise function and its derivatives for B and D mesons in this version of our model. We put our special emphasis to study the semileptonic decay of

B meson and compute the CKM element V_{cb} by using HQET. In this chapter, we also show that the leptonic and semileptonic decay are not controlled by the same scale of parameter Λ_{QCD} .

In Chapter 6, we explore B_c meson as a heavy-light meson and study its semileptonic decay to $c\bar{c}$ states. We also use another approach of the model with Coulombic part of the potential as Perturbation to study the same.

In Chapter 7, we present our concluding remarks as well as our future outlook.

Chapter 2

Open Flavour Charmed Mesons in a QCD Potential model

2.1 Introduction

As mentioned in chapter 1, the experimental measurements for the leptonic decay constant of D meson agree well with lattice QCD calculations but a discrepancy is seen for the value of f_{D_s} . A better understanding about the decay properties of D and D_s in this regard is quite important.

The properties of the B_c meson are of special interest [126], since it is the only heavy meson consisting of two heavy quarks with different flavours and due to this special feature, we include B_c meson in the list of heavy-light meson. A peculiarity of B_c decays is that both the quarks may be involved in its weak decays. From an experimental point of view, study of weak decays of B_c meson is quite important for the determination of CKM elements. More detailed information about its decay properties are expected in near future at LHC and other experiments.

In this chapter, we modify the mesonic wavefunction by using a short distance scale r_0 in analogy with hydrogen atom and estimate the values of masses and decay constants

of the open flavour charm mesons D , D_s and B_c within the framework of a QCD Potential model. We also calculate the leptonic decay widths of these mesons to study branching ratios and life time.

2.2 Formalism

2.2.1 The QCD Potential Model

The QCD Potential Model has its origin in the work of de Rujula, Georgi and Glashow [75]. Since then it has been applied to explain schematically the vast body of information available on mesons and baryons [127, 128, 129, 130]. The basis of this model is the Fermi-Breit Hamiltonian. This Hamiltonian, however has terms which are more singular than r^{-2} and is not exactly solvable. Godfrey and Isgur [131] improved upon the model by postulating a relativistic potential $V(\vec{p}, \vec{r})$ which differs from its non relativistic limit in two ways, i) the coordinate (\vec{r}) becomes smeared at over distances of the order of the inverse quark mass and ii) the coefficients of the various potentials become dependent on the momentum of the interacting quarks. The smearing of the potentials results in taming of all their singularities.

The model was phenomenologically satisfactory but can be improved in a different manner. To that end, the original model was improved upon without additional parameters unlike [131].

The basis of the QCD potential model, to be discussed here is the non relativistic two body Schrödinger equation. The Schrödinger equation is then solved perturbatively and the first order wave function is obtained by using Dalgarno's method [132] of perturbation. Relativistic effects are then incorporated in the wave function by using standard Dirac modification in a parameter free way [133, 134].

2.2.2 Wave function in the model

In the ground state ($l = 0$), neglecting the contact term proportional to $\delta^3(r)$ the spin independent Fermi-Breit Hamiltonian with confinement has the simple form,

$$H = -C_F \frac{\alpha_S}{r} + br + c. \quad (2.1)$$

where

$$C_F = \frac{N_C^2 - 1}{2N_C}, \quad (2.2)$$

N_C being the number of colours. Here C_F is the Casimir operator $\lambda^c \cdot \lambda^c = C_F$, λ^c being the generator of $SU(N_C)$. For $N_C = 3$, we obtain

$$H = -\frac{4\alpha_S}{3r} + br + c \quad (2.3)$$

so that

$$H' = br + c \quad (2.4)$$

can be treated as perturbation to the unperturbed Hamiltonian

$$H_0 = \frac{p_1^2}{2m_1} + \frac{p_2^2}{2m_2} - \frac{4\alpha_S}{3r}, \quad (2.5)$$

where H_0 is the Hamiltonian for two quarks of light and heavy flavour m_q and m_Q respectively. The nonrelativistic two body Schrödinger equation then takes the form

$$H|\psi\rangle = (H_0 + H')|\psi\rangle = E|\psi\rangle \quad (2.6)$$

so that the first order perturbed eigenfunction $\psi^{(1)}$ and eigenenergy $W^{(1)}$ can be obtained using the relation

$$H_0\psi^{(1)} + H'\psi^{(0)} = W^{(0)}\psi^{(1)} + W^{(1)}\psi^{(0)}, \quad (2.7)$$

where

$$W^{(1)} = \langle \psi^{(0)} | H' | \psi^{(0)} \rangle. \quad (2.8)$$

From equation (2.7) we calculate $\psi^{(1)}$ by Dalgarno's method [132], which gives

$$\psi^{(1)}(r) = -\frac{1}{2\sqrt{\pi a_0^3}} \mu b a_0 r^2 \exp^{-\frac{r}{a_0}}, \quad (2.9)$$

where μ is the reduced mass defined as

$$\mu = \frac{m_q m_Q}{m_q + m_Q} \quad (2.10)$$

and

$$a_0 = \left(\frac{4\mu\alpha_S}{3} \right)^{-1}, \quad (2.11)$$

α_S being the strong coupling constant. The corresponding eigenfunction $\psi^{(0)}(r)$ with the pure Coulombic potential of Eqn.(2.5) is

$$\psi^{(0)}(r) = \frac{1}{\sqrt{\pi a_0^3}} \exp^{-\frac{r}{a_0}}. \quad (2.12)$$

The normalized wave function with Coulombic plus linear potential is then

$$\psi(r) = \psi^{(0)}(r) + \psi^{(1)}(r) = \frac{N}{\sqrt{\pi a_0^3}} \left(1 - \frac{1}{2} \mu b a_0 r^2 \right) \exp^{-\frac{r}{a_0}} \quad (2.13)$$

with

$$N = \frac{1}{\left(1 - 3\mu b a_0^3 + \frac{45}{8} \mu^2 b^2 a_0^6 \right)^{\frac{1}{2}}}. \quad (2.14)$$

Taking into account the relativistic effects as given in [133, 134], the relativistic version of equation (2.13) takes the form

$$\psi_{rel+conf}(r) = \frac{N'}{\sqrt{\pi a_0^3}} \left(1 - \frac{1}{2}\mu b a_0 r^2\right) \left(\frac{r}{a_0}\right)^{-\epsilon} e^{-\frac{r}{a_0}}. \quad (2.15)$$

For non zero value of c , the wave function with its relativistic correction and confinement effect can be obtained as¹ [121],

$$\psi_{rel+conf}(r) = \frac{N'}{\sqrt{\pi a_0^3}} e^{\frac{-r}{a_0}} \left(C' - \frac{\mu b a_0 r^2}{2}\right) \left(\frac{r}{a_0}\right)^{-\epsilon} \quad (2.16)$$

where

$$N' = \frac{2^{\frac{1}{2}}}{\sqrt{(2^{2\epsilon}\Gamma(3-2\epsilon)C'^2 - \frac{1}{4}\mu b a_0^3 \Gamma(5-2\epsilon)C' + \frac{1}{64}\mu^2 b^2 a_0^6 \Gamma(7-2\epsilon))}} \quad (2.17)$$

$$C' = 1 + c A_0 \sqrt{\pi a_0^3} \quad (2.18)$$

and with a correction [135]

$$\epsilon = 1 - \sqrt{1 - \left(\frac{4}{3}\alpha_s\right)^2} \quad (2.19)$$

2.2.3 The short distance scale and the wave function at the origin

In studying the pseudoscalar leptonic decay constants of mesons, we require the wavefunction at the origin $\psi(0)$. But the wavefunction at the origin, develops a singularity at $r = 0$ (Eqn.2.16). However singularities at $r = 0$, in relativistic and nonrelativistic approaches of quark models [136, 137, 138] are not new and different regularisation procedures are being employed to remove these singularities. Here, in this work we use another way to regularise the wave function at the origin which have the quantum mechanical origin in

¹Derivation in Appendix A

QED. It is well known that relativistic wave function of the hydrogen atom too has such singularities. However such effect is noticeable only for a tiny region[134],

$$2mz\alpha r \leq e^{-(\frac{1}{1-\gamma})} \leq e^{-\frac{2}{z^2\alpha^2}} \sim 10^{-\frac{16300}{z^2}} \quad (2.20)$$

where z is the atomic number, m is the reduced mass of the hydrogen atom, α is the electromagnetic coupling constant and $\gamma = \sqrt{1 - z^2\alpha^2}$. Using such hydrogen like properties in QCD, m , α and $1 - \gamma$ are to be replaced by μ , $\frac{4}{3}\alpha_s$ and ϵ respectively. Here α_s is the strong coupling constant, $\epsilon = 1 - \sqrt{1 - \left(\frac{4}{3}\alpha_s\right)^2}$ [135] and $(mz\alpha r)^{\gamma-1}$ changes to $\left(\frac{r}{a_0}\right)^{-\epsilon}$ leading to a cut off parameter r_0 upto which the model can be extrapolated ($r \geq r_0$). In analogy to the QED calculation (Eqn.2.20), using the typical length scale for the relativistic term $\left(\frac{r}{a_0}\right)^{-\epsilon} \leq \frac{1}{\epsilon}$, we obtain the cut off parameter as

$$r_0 \sim a_0 e^{-\frac{1}{\epsilon}}. \quad (2.21)$$

Unlike QED, r_0 is found to be flavour dependent due to the term a_0 in Eqn.2.21, which carries the flavours of the quark masses (Eqn.2.11).

With this cut-off parameter, we write the normalised and regularised wavefunction [139]

$$\psi(r') = \frac{N'}{\sqrt{\pi a_0^3}} e^{\frac{-r'}{a_0}} \left(C' - \frac{\mu b a_0 (r')^2}{2} \right) \left(\frac{r'}{a_0} \right)^{-\epsilon} \quad (2.22)$$

with

$$r' = r + r_0. \quad (2.23)$$

In the numerical calculations, we adopt $\alpha_s = 0.39$ and $\alpha_s = 0.22$ at charm and bottom mass scale from \overline{MS} scheme [140, 121]. The value of the undetermined factor A_0 , which appears in the series solution is so chosen that the consistency of the value of $cA_0 = 1GeV^{3/2}$ is sustained with the previous work [121]. The other input parameters in the calculations

are $m_u = 0.336\text{GeV} = m_d$, $m_s = 0.483\text{GeV}$, $m_c = 1.550\text{GeV}$ and $m_b = 4.950\text{GeV}$, $b = 0.183\text{GeV}^2$, $c = -0.5\text{GeV}$. With these values, we compute the short distance scale r_0 for open flavour charmed mesons D , D_s and B_c and tabulate in Table (2.1).

Table 2.1: Values of cut-off parameter r_0 for different mesons

Mesons	Reduced mass	Values of r_0 in GeV^{-1}
$D(c\bar{u}/c\bar{d})$	0.2761	0.0073
$D_s(c\bar{s})$	0.3682	0.0055
$B_c(b\bar{c})$	1.1838	3.872×10^{-10}

It is clear from Table. (2.1) that as the masses of the mesons increase, the value of the cut-off parameter r_0 decreases. For heavy-heavy mesons like B_c it becomes as tiny as 10^{-10}GeV^{-1} , which presumably infers that the relativistic effect is too small for this heavy meson.

2.3 Calculation and results

2.3.1 Masses and decay constants of open flavoured charm mesons

As stated in chapter 1, when quark and antiquark annihilate the leptonic decay constant f_P could in principle be measured in the process $q + \bar{q} \rightarrow W^- \rightarrow \mu^- + \nu$. In Fig.2.1, we show the Feynman diagram for the annihilation of quark and antiquark in D and D_s mesons.

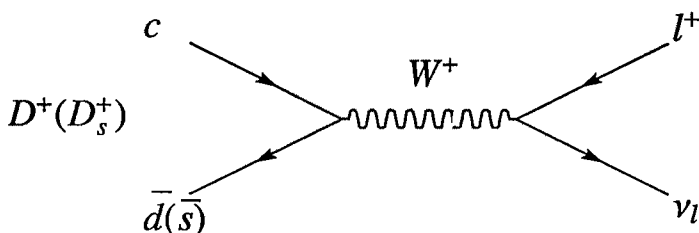


Figure 2.1: The decay diagram for $D_{(s)}^+ \rightarrow l^+ \nu_l$.

In the non-relativistic limit, the pseudoscalar decay constant f_p and the ground state wave function at the origin $\psi(0)$ is related by the Van-Royen-Weisskopf formula²[24].

$$f_p = \sqrt{\frac{12}{M_p} |\psi(0)|^2}. \quad (2.24)$$

With QCD correction factor the decay constant can be written as [25]

$$f_{pc} = \sqrt{\frac{12}{M_p} |\psi(0)|^2 \left[1 - \alpha_s/\pi \left(2 - \frac{m_Q - m_{\bar{Q}}}{m_Q + m_{\bar{Q}}} \ln \frac{m_Q}{m_{\bar{Q}}} \right) \right]}, \quad (2.25)$$

where M_p is the pseudoscalar meson mass in the ground state and can be obtained as [141]

$$M_p = m_Q + m_{\bar{Q}} + \langle H \rangle \quad (2.26)$$

where

$$\langle H \rangle = \langle \frac{p^2}{2\mu} \rangle + \langle V(r) \rangle \quad (2.27)$$

In Table(2.2) and (2.3), we record the prediction of the model for masses and decay constants.

Table 2.2: The masses of heavy-light mesons in GeV.

mesons	masses	experimental values
$D(c\bar{u}/c\bar{d})$	1.860	1.869 ± 0.0016 [37]
$D(c\bar{s})$	1.959	1.968 ± 0.0033 [37]
$B_c(b\bar{c})$	6.507	6.277 ± 0.006 [37]

²The derivation of this formula is given in Appendix.B

Table 2.3: The decay constants of heavy-light mesons with and without QCD correction in GeV

Mesons	Our work		Other work
	f_p	f_{pc}	
$D(c\bar{u}/c\bar{d})$	0.240	0.225	$0.205 \pm 0.085 \pm 0.025$ [142][Exp] 0.206 [143] 0.234 [136] 0.208 [144] 0.201 [145] 0.235 [146]
$D(c\bar{s})$	0.291	0.266	0.254 ± 0.059 [142][Exp] 0.245 [143] 0.268 [136] 0.256 [144] 0.249 [145] 0.266 [146]
$B_c(\bar{b}c)$	0.435	0.413	0.433 [176][Theory] 0.470 [147]

2.3.2 Leptonic decay rate and Branching ratio of D and D_s mesons

There are several reasons for studying the purely leptonic decays of charged mesons. Such processes are rare but they have clear experimental signatures due to the presence of a highly energetic lepton in the final state. The theoretical predictions are very clean due to the absence of hadrons in the final state. The total leptonic decay rate (width) of D , D_s mesons are given by

$$\Gamma(D_q^+ \rightarrow l\nu) = \frac{G_F^2 |V_{cq}|^2 f_{D_q}^2}{8\pi} m_l^2 \left(1 - \frac{m_l^2}{M_{D_q}^2}\right)^2 M_{D_q}, \quad q = d, s. \quad (2.28)$$

where G_F is the Fermi coupling constant, V_{cq} is the Cabibbo-Kobayashi-Maskawa (CKM) matrix element between the two quarks $c\bar{d}(\bar{s})$ in $D^+(D_s^+)$, m_l is the mass of the lepton, and M_{D_q} is the mass of the pseudoscalar D or D_s meson. Equation 2.28 shows an interesting

dependence on the lepton mass m_l . The factor $(1 - \frac{m_l^2}{m_p^2})$ accounts for the phase space suppression when the mass of the lepton is close to the parent mass. In the limit of $m_l = 0$, the D^+ and D_s^+ leptonic decays are forbidden which can occur only for the case of $m_l \neq 0$. This helicity suppression results from the fact that the charged weak interactions only couple the left handed fermions. In leptonic decay, the final state neutrino must be left-handed and hence the final lepton must also be left-handed, since only in this way one can obtain a final state with zero angular momentum component in the direction of motion of the leptons. This helicity suppression of the decay gives a larger decay rate for the final state with the lepton $l = \tau$ and $l = \mu$ than that for the final state with lepton $l = e$. The leptonic decay rate of the charged D and D_s mesons are obtained using Eqn.2.28 and employing the predicted values of the pseudoscalar decay constants f_D and f_{D_s} along with the masses of the M_D and M_{D_s} from our work. The leptonic widths for separate lepton channels by the choice of $m_{l=\tau,\mu,e}$ are computed. Branching ratio of D and D_s mesons are calculated by using the relation

$$BR = \Gamma \times \tau. \quad (2.29)$$

The life time of these mesons $\tau_D = 1.04$ ps and $\tau_{D_s} = 0.5$ ps are taken from the world average value reported by particle data group [37]. The present result of branching ratio, as tabulated in Table (2.4) are in accordance with the available experimental values.

Table 2.4: The leptonic branching ratio of D and D_s mesons. Values within the bracket represent the branching ratio for f_p with QCD correction.

Mesons	$BR_\tau \times 10^{-3}$	$BR_\mu \times 10^{-4}$	$BR_e \times 10^{-8}$
$D(c\bar{u}/c\bar{d})$	0.78(0.68)	4.4(3.89)	1.05(0.92)
Expt.[37]	< 1.2	3.82	
B. Patel et al.,[147]	0.9	6.6	1.5
	$BR_\tau \times 10^{-2}$	$BR_\mu \times 10^{-3}$	$BR_e \times 10^{-7}$
$D(c\bar{s})$	6.4(5.3)	7.0(5.9)	1.67(1.40)
Expt.[37]	5.6 ± 0.4	5.8 ± 0.4	
B. Patel et al.,[147]	8.4	7.7	1.8

2.3.3 Weak decay of B_c^+ meson

Adopting the spectator model for the charm beauty mesons system [148], the total decay width of B_c^+ meson can be approximated as the sum of the widths of \bar{b} -quark decay keeping c-quark as spectator and the c-quark decay with \bar{b} as spectator and the annihilation channel $B_c^+ \rightarrow l\nu_l(c\bar{s}, u\bar{s})$ for $l = e, \mu, \tau$ with no interference assumed between them. Accordingly, the total decay width is written as [148]

$$\Gamma(B_c \rightarrow X) = \Gamma(b \rightarrow X) + \Gamma(c \rightarrow X) + \Gamma(anni). \quad (2.30)$$

Neglecting the quark binding effects, the b and c inclusive widths in the spectator approximation are [148]

$$\Gamma(b \rightarrow X) = \frac{9G_F^2|V_{cb}|^2 m_b^5}{192\pi^3} \quad (2.31)$$

$$\Gamma(c \rightarrow X) = \frac{5G_F^2|V_{cs}|^2 m_c^5}{192\pi^3} \quad (2.32)$$

Here we have used the model quark masses and the CKM matrix elements $|V_{cs}| = 0.957$, $|V_{cb}| = 0.039$ from the particle data group. Employing the computed mass and pseudoscalar decay constant from the present study, the width of the annihilation channel is computed using the expression [141, 148]

$$\Gamma(Anni) = \frac{G_F^2|V_{bc}|^2 f_{B_c}^2 M_{B_c}}{8\pi} m_q^2 \left(1 - \frac{m_q^2}{M_{B_c}^2}\right)^2 C_q, \quad (2.33)$$

where $C_q = 1$ for $\tau\nu_\tau$ channel and $C_q = 3|V_{cs}|^2$ for $c\bar{s}$ channel and m_q is the mass of the heaviest fermions. The computed results of the annihilation decay rate and total decay rate are tabulated in Table 2.5. Our prediction for life time with these results are shown in Table 2.5.

Table 2.5: Decay width(in $10^{-4} eV$) and life time of B_c meson

Meson	$\Gamma(Anni)$	$\Gamma(B_c \rightarrow X)$	$\tau(inps)$
$B_{c\bar{b}}$	1.17(1.06)	19.17(19.06)	0.344(0.346)
[37]			0.453 ± 0.041
[148]	1.40	14.00	0.47
[149]	0.67	8.8	0.75

2.4 Conclusion

In the present work, we have used a short cut-off parameter r_0 to regularise the wave function near the origin. This wave function is then used to compute the masses and decay constants of heavy-light mesons. The short distance scale (or cut-off parameter) as well as the decay parameters are found to be very sensitive to the strong coupling constant α_s in the model. As expected, the magnitude of the short distance scale is far larger than its QED counterpart but still far smaller than the measure of finite size of hadrons or its constituents. It is however well within the reach of LHC [150], where distance down to a scale as short as $5 \times 10^{-20} m - 10^{-21} m$ will be explored. Theoretically, this short distance scale r_0 can be roughly associated with the ultra-violet regularisation scale of QCD.

The analysis with QCD correction is found to be closer to experiments and other theoretical results. In our calculation we have found $\frac{f_{D_s}}{f_D} = 1.18$ (with QCD correction) and $\frac{f_{D_s}}{f_D} = 1.21$ (without QCD correction), which is in accordance with the latest QCD Sum rule result $1.193 \pm 0.025 \pm 0.007$ [143], PDG average $\frac{f_{D_s}}{f_D} = 1.25 \pm 0.06 \pm$ [37], as well as with the recent lattice QCD results $f_{D_s}/f_D = 1.164 \pm 0.011$ [151] and $f_{D_s}/f_D = 1.20 \pm 0.02$ [152].

Present study on the leptonic decay branching ratio of D and D_s mesons with QCD correction for τ and μ leptonic channels, presented in Table 2.4 are as per the available experimental limits. Large experimental uncertainty in the electron channel makes it difficult for any reasonable conclusion. The computed result within the framework of the QCD

potential model for annihilation decay width as well as the lifetime of B_c meson is also found to be in good agreement with the available data as presented in Table 2.5. Probably in future, high luminosity, better statistics and high confidence level data sets will be able to provide more light on the spectroscopy and decay properties of these open charm mesons.

However, with \overline{MS} scheme our results for B_d and B_s mesons are not found to be satisfactory and is shown in Table 2.6.

Table 2.6: Masses and decay constants B_d and B_s mesons

Mesons	Mass	Exp mass	Decay constant(f_p)	Other results
B	7.2351	5.279	0.0264	0.204[37] 0.196[153]
B_s	6.769	5.366	0.0553	0.216[153] 0.218 [136]

Thus the present approach shows a limitation towards the study of the leptonic decay constants of B_d and B_s mesons.

In the next chapter, we will study this feature under an alternative to \overline{MS} scheme.

Chapter 3

Oscillation frequency of B and \bar{B} mesons in the QCD potential model

3.1 Introduction

As stated in chapter 2, while calculating the masses and decay constants of B_d and B_s mesons with \overline{MS} scheme, the results are not found to be satisfactory. The value of α_s in \overline{MS} is taken to be independent of the light quark mass, for example the value of $\alpha_s = 0.39$ for both the D and D_s mesons. It thus paves another way of considering a scale dependent α_s in the model. In this chapter, we use a scale dependent α_s to calculate the pseudoscalar masses M_{B_q} and decay constants f_{B_q} to compute the oscillation frequency Δm_{B_q} , $q = d, s$ within the frame work of the potential model. We also use the same regularisation procedure as is introduced in chapter 2 to regularise the wavefunction at the origin.

In the first part of this chapter, we compute the masses of B_d and B_s mesons with a different mass formula, which in fact depends upon the wavefunction at the origin and study the decay constant and oscillation frequency. However, to maintain a continuous evolution, we also study the same properties with the mass formula of chapter 2 in the second part of this chapter.

3.2 Formalism

3.2.1 Mixing of B_d and B_s mesons

It is found that the weak eigenstates of neutral mesons are different to their mass eigenstates. This leads to the phenomenon of mixing whereby neutral mesons oscillate between their matter and antimatter state. This was first proposed by Gell-man and Pais[154] in 1955 for $K^0 - \bar{K}^0$ system. The first evidence of mixing of neutral B meson was found by the UA1 Collaboration at CERN [155] and thereafter ARGUS[156] Collaboration at DESY observed the mixing of B_d meson, where the production of $e^+e^- \rightarrow \Upsilon(4S) \rightarrow B_d\bar{B}_d$ ended up with two B_d mesons.

The neutral B_d and B_s mesons can mix with their antiparticles by means of box diagram involving exchange of a pair of W bosons and intermediate u, c, t quarks leading to oscillations between the mass eigenstates. Although u, c and t quark exchange occurs, the t quark plays a dominant role mainly due to its mass, as the amplitude of this process is proportional to the mass of the exchanged fermion. A box diagram for mixing of B meson is shown in Fig.5.2.1.

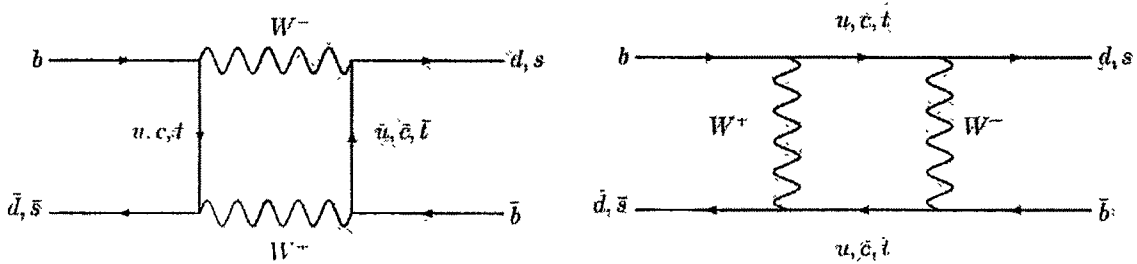


Figure 3.1: Feynman graphs for $B_{d,s} - \bar{B}_{d,s}$ mixing. Quarks are shown as straight lines, while bosons are illustrated by wave-lines.

There are two mass eigenstate for the phenomenon of particle-antiparticle mixing in both the systems $B^0 - \bar{B}^0$ and $B_s^0 - \bar{B}_s^0$, which are linear combinations of the two flavour states B and \bar{B} . This evolution of B^0 or \bar{B}^0 meson with time is given by a Schrödinger like

equation

$$i\frac{d|\psi(t)\rangle}{dt} = M|\psi(t)\rangle.$$

The mass matrix M is not diagonal and is given by,

$$M = m - \frac{i}{2}\Gamma = \begin{pmatrix} m_{11} - \frac{i}{2}\Gamma_{11} & m_{12} - \frac{i}{2}\Gamma_{12} \\ m_{21} - \frac{i}{2}\Gamma_{21} & m_{22} - \frac{i}{2}\Gamma_{22} \end{pmatrix}. \quad (3.1)$$

From the hermiticity condition of matrices, we get

$$m_{21} = m_{12}^* \quad \Gamma_{21} = \Gamma_{12}^* \quad (3.2)$$

and CPT invariance gives the identity,

$$m_{11} = m_{22}, \quad \Gamma_{11} = \Gamma_{22}. \quad (3.3)$$

Diagonalization of mass matrix M in Eqn.(3.1) gives,

$$m_{11} - \frac{i}{2}\Gamma_{11} - pq = m_1 - \frac{i}{2}\Gamma_1 \quad (3.4)$$

$$m_{11} - \frac{i}{2}\Gamma_{11} + pq = m_2 - \frac{i}{2}\Gamma_2 \quad (3.5)$$

where,

$$p^2 = m_{12} - \frac{i}{2}\Gamma_{12}, \quad q^2 = m_{12}^* - \frac{i}{2}\Gamma_{12}^*. \quad (3.6)$$

The eigenstates are given by,

$$|B_{1,2}\rangle = \frac{1}{\sqrt{|p|^2 + |q|^2}} [p|B^0\rangle \mp q|\bar{B}^0\rangle]. \quad (3.7)$$

Considering the real parts of Eqn.(3.5), we have

$$m_1 = m_{11} - Re(pq)$$

$$m_2 = m_{11} + Re(pq).$$

$$\Gamma_1 = \Gamma_{11} + 2Im(pq)$$

$$\Gamma_2 = \Gamma_{11} - 2Im(pq)$$

Thus finally we have

$$\Delta m = m_2 - m_1 = 2Re(pq),$$

$$m = \frac{m_1 + m_2}{2} = m_{11}$$

$$\Gamma = \frac{\Gamma_1 + \Gamma_2}{2} = \Gamma_{11}$$

This mass difference $\Delta m = \Delta m_B$ is a measure of the frequency of the change from a B into a \bar{B} . The probability for a B^0 meson to appear as a \bar{B}^0 , as a function of time is related to the oscillation frequency parameter by the relation [157]

$$P_{\pm}(t) = 0.5\Gamma e^{-\Gamma t} [1 \pm \cos(\Delta m t)]. \quad (3.8)$$

The mass difference Δm_B is a measure of the frequency of the change from a B into a \bar{B} and is called the oscillation frequency. Since the first observation of particle-antiparticle transformations in neutral B mesons in 1987 [155, 156], the determination of $B^0 - \bar{B}^0$ oscillation frequency Δm_B from a time-dependent measurement of $B^0 - \bar{B}^0$ oscillations has been a major objective of experimental particle physics[158].

In the unitarity triangle, the least known length is R_f . This length is proportional to the

CKM matrix element $|V_{td}|$ (Equation 1.16) and can be measured through B_d [14]

$$\Delta m_d = \text{Const.} \times f_{B_d}^2 B_{B_d} |V_{tb}^* V_{td}|^2, \quad (3.9)$$

where, *Const* is a known constant factor, f_{B_d} is the decay constant of B_d and B_{B_d} is the bag parameter.

In the same way, the flavour oscillation in B_s systems can be used to extract the magnitude of $|V_{ts}|$ in the Cabibbo-Kobayashi-Maskawa (CKM) matrix [159]. Most of the uncertainties in the measurement of oscillation frequencies can be cancelled out by calculating their ratio

$$\frac{\Delta m_s}{\Delta m_d} = \frac{M_{B_s}}{M_{B_d}} \xi^2 \frac{|V_{ts}|^2}{|V_{td}|^2}, \quad (3.10)$$

where the constant $\xi = 1.210_{-0.035}^{+0.047}$ has approximately 4% uncertainties left from lattice calculations [14].

It has been argued that recent tension between the Standard Model and flavor physics experiments could be alleviated by the presence of new physics in B mixing [160, 161, 162], while the latest analysis indicate that this may not be the case [163] and precise calculations of the theoretical inputs to B mixing are necessary for a thorough understanding of quark flavor physics [164].

3.2.2 Allowed range of strong running coupling constant α_s in the model

The modified wavefunction 2.16 with linear part of the Cornell Potential as perturbation is discussed in chapter.2. In chapter.2, we see that with \overline{MS} scheme, the masses and decay constants for B and B_s mesons show a large discrepancy with the other theoretical results. This deviation allows us to think of an alternate way of choosing the strong running coupling constant α_s in the model.

The values of α_s and the constant shift c of the potential $V(r)$ are found to vary from model to model. These two parameters are expected to be fitted from the mass spectroscopy of hadrons and then to study its other properties. Thus, a narrow range of the free parameters in a potential model measures its success and applicability as well.

In Ref.[120], it is shown from the momentum transform¹ of Eqn.(2.16) with $C' = 1$, that the confinement part of the potential can be treated as perturbation provided

$$\frac{(4 - \epsilon)(3 - \epsilon)\mu b a_0^3}{2(1 + a_0^2 Q^2)} \ll 1. \quad (3.11)$$

For very low Q^2 , $Q^2 \leq Q_0^2$, the present method of perturbation breaks down, where Q_0^2 is determined from the relation

$$\frac{(4 - \epsilon)(3 - \epsilon)\mu b a_0^3}{2(1 + a_0^2 Q_0^2)} = 1. \quad (3.12)$$

The values of Q_0^2 with $b = 0.183 \text{ GeV}^{-2}$ for B and D mesons are shown in Table 3.1.

Table 3.1: Values of Q_0^2 (in GeV^2) for heavy-light mesons above which linear part can be treated as perturbation [118].

Mesons	$\alpha_s = 0.65$	$\alpha_s = 0.6$	$\alpha_s = 0.5$
D	3.5	4.1	5.5
D_s	3.5	4.2	5.8
B	1.4	1.7	2.3
B_s	3.9	4.4	5.5
B_c	0	0.4	2.0

To reduce the value of Q_0^2 , either one has to consider a very small value of b or to increase the value of α_s . This is obvious, since in both the cases Coulombic part will be more dominant (Eqn.2.1). However, reality condition of ϵ demands that $\alpha_s \leq \frac{3}{4}$ and hence one cannot go beyond $\alpha_s = 0.75$ in this approach. The standard spectroscopic result

¹The wavefunction with momentum space is discussed in chapter.4

$b = 0.183 \text{GeV}^2$ [165] can be accommodated by a proper choice of c [120, 121] so that the perturbative condition of Eqn.(3.11) becomes

$$\frac{(4 - \epsilon)(3 - \epsilon)\mu b a_0^3}{2(1 + a_0^2 Q^2)} \ll C'. \quad (3.13)$$

This possibility arises due to the arbitrariness of A_0 , which appears in the series solution (Ref. Appendix A). With this one can impose $b = 0.183 \text{GeV}^2$ with low Q^2 value. The improved values of Q_0^2 with $b = 0.183 \text{GeV}^2$ for B and D mesons are shown in Table 3.2.

Table 3.2: Values of Q_0^2 (in GeV^2) for heavy-light mesons with linear part as perturbation and $m_{u/d} = 0.33 \text{ GeV}$, $m_s = 0.483 \text{ GeV}$, $m_c = 1.55 \text{ GeV}$, $m_b = 4.97 \text{ GeV}$

Mesons	$\alpha_s = 0.65$	$\alpha_s = 0.5$	$\alpha_s = 0.4$	$\alpha_s = 0.37$
D	-0.0001	0.0264	0.0362	0.037
D_s	-0.0166	0.0304	0.0490	0.052
B	-0.0057	0.0286	0.0412	0.043
B_s	-0.0371	0.0300	0.0530	0.056
B_c	-0.7045	-0.0219	0.0162	0.054

Thus to incorporate lower value of Q^2 ($Q^2 \leq \Lambda_{QCD}^2$), with linear part as perturbation in the improved version one expects a bound of α_s as $0.37 \leq \alpha_s \leq 0.75$.

The results of the slope and curvature of Isgur-Wise function with linear part as perturbation [121] in the Dalgarno method as well as in VIPT method [166], clearly indicates that with $\alpha_s = 0.6$ one can expect high accuracy towards experimental and other theoretical values. Thus to treat linear part of the Cornell potential as perturbation, the allowed range of strong running coupling can be considered as $0.37 \leq \alpha_s \leq 0.75$ with $cA_0 = 1 \text{GeV}^{3/2}$ in the model.

3.2.3 Strong running coupling constant α_s in \overline{MS} scheme

Traditionally, the strength of the quark gluon interaction is characterised by the coupling constant $\alpha_{\overline{MS}}(q^2)$ and is defined in a particular dimensional regularisation scheme such as the \overline{MS} (modified minimal subtraction) regularisation scheme [167]. In \overline{MS} scheme, the higher order effects of QCD are conventionally expressed as a power series in the coupling constant $\alpha_{\overline{MS}}$. In inverse powers of $\ln(\mu^2)$, $\alpha_s(\mu)$ is written as [168]

$$\alpha_s(\mu) = \frac{4\pi}{\beta_0 \ln(\mu^2/\Lambda^2)} \left[1 - \frac{2\beta_1}{\beta_0^2} \frac{\ln[\ln(\mu^2/\Lambda^2)]}{\ln(\mu^2/\Lambda^2)} + \frac{4\beta_1^2}{\beta_0^4 \ln^2(\mu^2/\Lambda^2)} \left(\left(\ln[\ln(\mu^2/\Lambda^2)] - \frac{1}{2} \right)^2 + \frac{\beta_2 \beta_0}{8\beta_1^2} - \frac{5}{4} \right) \right], \quad (3.14)$$

where,

$$\beta_0 = 11 - \frac{2}{3}n_f \quad (3.15)$$

$$\beta_1 = 51 - \frac{19}{3}n_f \quad (3.16)$$

$$\beta_2 = 2857 - \frac{5033}{9}n_f + \frac{325}{27}n_f^2 \quad (3.17)$$

and n_f is the number of quarks with mass less than the energy scale μ . The coefficients β_0 and β_1 of Eqn.3.14 are independent of the choice of renormalisation scheme but the form of β_2 , which is shown here in Eqn.3.17 is from the \overline{MS} scheme. Taking n_f to be respectively 4 and 5, the corresponding value of $\alpha_{\overline{MS}}$ at the scale of the c and b quark mass are taken to be $\alpha_{\overline{MS}}(m_c) = 0.39$ and $\alpha_{\overline{MS}}(m_b) = 0.22$ [169, 121, 140].

\overline{MS} subtraction scheme is however, a quark mass independent renormalisation scheme. The ratios of quark masses are scale independent in such a scheme [168]. Further, there is no definite choice of μ for such a scheme since the higher order corrections do not “fix” the scale, rather they render the theoretical predictions less sensitive to its variation.

3.2.4 An alternate to \overline{MS} scheme

To incorporate the scale dependance of quark masses, we consider the one loop expression for α_s appearing in the potential $V(r)$ which in turn is related to the quark mass parameter as[125, 137]

$$\alpha_s(\mu^2) = \frac{4\pi}{\left(11 - \frac{2n_f}{3}\right) \ln\left(\frac{\mu^2 + M_B^2}{\Lambda^2}\right)} \quad (3.18)$$

where, n_f is the number of flavours, μ is the renormalisation scale related to the constituent quark masses as $\mu = 2 \frac{m_u m_d}{m_u + m_d}$ and Λ is the QCD scale which is taken as 0.200 GeV here.

The background mass M_B appearing in Eqn.3.18 is not an arbitrary parameter, rather it is a characteristic for a process to be considered. It can be calculated in the framework of Lattice QCD or background perturbation theory(BPTh) [170, 171, 172].

We consider that the background mass M_B is related to the confinement term of the potential by the relation $M_B = 2.24 \times b^{1/2} = 0.95 \text{ GeV}$ [125, 137]. An advantage of choosing this relation is that on the perturbation procedure of the model, if one needs to change the confinement parameter b then that will make a change in the background mass M_B which will correspondingly change the coupling α_s . Thus a change in the confinement term of the potential $V(r)$ will contribute a change in the Coulombic term as such. With M_B , thus we are able to incorporate the confinement effect so that with $\mu_0^2 = \Lambda^2$, the strong coupling constant α_s becomes finite and with zero confinement ($b = 0$), Eqn. 3.18 becomes equivalent to that of the \overline{MS} scheme in the leading order(LO).

Within this prescription (Eqn.3.18), we find $\alpha_s = 0.40$ for B_d mesons and $\alpha_s = 0.37$ for B_s mesons, where as the corresponding value for B_d and B_s mesons was $\alpha_s = 0.22$ in \overline{MS} scheme.

3.3 Calculation and results

3.3.1 Masses and Decay constants of B mesons

For studying oscillation frequency of B and \bar{B} mesons the pseudoscalar decay constant and mass are the two important parameters to be predicted in a potential model.

The energy shift of mass splitting due to spin interaction in the perturbation theory reads [173]

$$\Delta E = \int \Psi^* \left(\frac{32\pi\alpha_s}{9} \delta^3(r) \frac{S_i \cdot S_j}{m_i m_j} \right) \psi d^3r, \quad (3.19)$$

so that

$$\Delta E = \frac{32\pi\alpha_s}{9m_i m_j} (S_i \cdot S_j) |\psi(0)|^2. \quad (3.20)$$

Here the hyperfine term $(S_i \cdot S_j)$ is motivated by the corresponding term in the one gluon exchange potential between quarks and the latter is proportional to a delta function at the origin from where we get the $|\psi(0)|^2$ dependence. Taking this energy shift into account, the pseudoscalar meson mass is expressed as [174]

$$M_p = m_i + m_j - \frac{8\pi\alpha_s}{3m_i m_j} |\psi(0)|^2, \quad (3.21)$$

since $(S_i \cdot S_j) = -3/4$ for pseudoscalar meson.

To compute the decay constant of B_d and B_s mesons, we use the non relativistic expression given by equation 2.24 in chapter 2. To use Eqn.3.21 and 2.24, we need the regularisation length r_0 as is defined in Eqn. 2.21 of chapter 2.

The values of r_0 and corresponding wavefunction at the origin for B_d and B_s are calculated to study pseudoscalar masses and are shown in Table 3.3. The corresponding computed values of decay constants for B_d and B_s mesons are presented in Table 3.4. The set of input parameters which are used to compute the results of Table 3.3 and 3.4 are $m_d=0.36 \text{ GeV}$, $m_s=0.46 \text{ GeV}$, $m_b=4.95 \text{ GeV}$, $c = 1 \text{ GeV}$ and $A_0 = 1 \text{ GeV}^{1/2}$ [135].

Table 3.3: Values of r_0 and M_p for B_d and B_s mesons.

Mesons	$ \psi(0) $ in $GeV^{3/2}$	Values of r_0 in GeV^{-1}	M_B in GeV
B_d	0.1266	0.0091	5.273 [This work]
			5.279 [37]
			5.285 [176]
			5.279 [177]
			5.370 [This work]
B_s	0.1778	0.0022	5.369 [37]
			5.373 [176]
			5.375 [177]

3.3.2 Oscillation frequency of $B - \bar{B}$ mesons

In the Standard Model, the oscillation frequency or mixing mass parameter (Δm) is given by [178, 179]

$$\Delta m_B = \frac{G_F^2 m_t^2 M_{B_q} f_{B_q}^2}{8\pi} g(x_t) \eta_t |V_{tq}^* V_{tb}|^2 B, q = d, s \quad (3.22)$$

where η_t is the gluonic correction to the oscillation and is taken to be 0.55 as in ref.[178], the last factor B is the bag parameter which represents the correction to the vacuum insertion and is taken as 1.34 [178]. The function $g(x_t)$ is given by[180]

$$g(x_t) = \frac{1}{4} + \frac{9}{4(1-x_t)} - \frac{3}{2(1-x_t)^2} - \frac{3x_t^2}{2(1-x_t)^3} \quad (3.23)$$

Here, $x_t = \frac{m_t^2}{M_W^2}$. The values $m_t = 174$ GeV , $m_W = 80.403$ GeV and the CKM matrix elements $|V_{tb}| = 1$, $|V_{td}| = 7.4 \times 10^{-3}$, $|V_{ts}| = 40.6 \times 10^{-3}$ are taken from the particle data group [37].

We use the estimated values of masses and decay constants to compute the mixing mass parameters and present them in Table 3.4. The decay constants are found to be comparable with the other theoretical values and mixing mass parameters are found to be in good

agreement with the experimental values.

Table 3.4: Decay constant and oscillation freq. of B mesons

Mesons	f_B (in GeV)	Δm_B (in ps^{-1})
B_d	0.213[This work]	0.55[This work]
	0.189 [136]	0.50[37]
	0.196(29)[153]	0.547[181]
	0.190(7) $^{+24}_{-1}$ [183]	0.515[181]
	0.210(9)[184]	
	0.216(9)(19)(6)[150, 145]	
B_s	0.265[This work]	17.34[This work]
	0.218 [136]	17[37]
	0.216[153]	17.77[185]
	0.217(6) $^{+32}_{-28}$ [183]	
	0.244(21)[184]	
	0.259(32)[150, 145]	

3.3.3 The results with the mass formula 2.26

In the above section, we have computed the masses of B_d and B_s mesons by using the relation (3.21) proposed by Halzen and Martin [174] in a sense to check the sensitivity of the wavefunction at the origin in the formula of mass and decay constant as well. This formula (Eqn.3.21) as is used in Ref.[135], however does not contain the eigenenergy term of the system [175]. Therefore, in addition to the above results, we also compute the masses of B mesons using the formula (Eqn.2.26) of chapter.2, which contain the eigen energy term of the system (but not the hyperfine term). The corresponding change of decay constants and oscillation frequency are shown in the Tables 3.5 and 3.6. In the numerical computation, we use the input parameters as $m_u = m_d = 0.336 \text{ GeV}$, $m_s = 0.465 \text{ GeV}$, $m_b = 4.97 \text{ GeV}$ and $c = -0.4 \text{ GeV}$ with the consistency of $cA_0 = 1 \text{ GeV}^{3/2}$.

Table 3.5: Values of r_0 and M_p with Eqn.2.26 for B_d and B_s mesons (in unit of GeV).

Mesons	Values of r_0 in GeV^{-1}	M_B in GeV
B_d	0.009	5.273[our work with $n_f = 3$]
		5.279 [37]
		5.285 [176]
		5.279 [177]
		5.365[our work with $n_f = 3$]
B_s	0.002	5.369[37]
		5.373[176]
		5.375[177]

Table 3.6: Decay constant and oscillation freq. for B_d and B_s mesons

Mesons	f_B (in GeV)	Δm_B (in ps^{-1})
B_d	0.191[our work with $n_f = 3$]	0.45[our work with $n_f = 3$]
	0.189 [136]	0.50[37]
	0.196(29)[153]	0.547[181]
	0.190(7) ₋₁ ⁺²⁴ [183]	0.515[181]
	0.210(9)[184]	
	0.216(9)(19)(6)[150, 145]	
B_s	0.268[our work with $n_f = 3$]	17.79[our work with $n_f = 3$]
	0.218 [136]	17[37]
	0.216[153]	17.77[185]
	0.217(6) ₋₂₈ ⁺³² [183]	
	0.244(21)[184]	
	0.259(32)[150, 145]	

3.4 Conclusion

In the present work, we have computed the masses using two different formulae and calculated the corresponding results for f_B , f_{B_s} , Δm_B and Δm_{B_s} . The first set of results are shown in Table 3.3, Table 3.4 and the second set of results are tabulated in Table 3.5, Table 3.6. These results are found to be well within the other theoretical and experimental results. However a different set of input parameters needs to be fixed in each case.

· The concluding remarks of this chapter can be summarised as:

- we are able to obtain satisfactory results for B_d and B_s mesons with a scale dependent α_s (Eqn.3.18) for a fixed value of $n_f = 3$ and $\Lambda_{QCD} = 200 \text{ MeV}$.
- The same regularisation procedure(as is used in chapter.2) within a short distance scale is found to be effective in finding the value of the wavefunction at the origin.
- We have found from the calculation that generally the masses are not so sensitive to running coupling constants since the heavy quark constituent masses are dominant here, but the decay constants are very much sensitive to the running coupling constants and therefore a slight change in α_s as well as r_0 deviates the results significantly.

In the second part of the results of this chapter we see that the the oscillation frequency Δm_{B_d} is slightly less [Table 3.6] than the experimental value. Considering this deviation to be a negligible one, we fix the model parameters here from the second part of this work and maintain a continuous evolution with our previous chapter (chapter 2). However, the computed value of ΔM_{B_s} in the two approaches are found to be in good agreement with the available data as well as within the experimental bounds $17 < \Delta m_{B_s} < 21 \text{ ps}^{-1}$ at the 90% C.L.[182].

It would be interesting to test the predictive power of the model with this set of parameters ($m_u = m_d = 0.336 \text{ GeV}$, $m_s = 0.465 \text{ GeV}$, $m_b = 4.97 \text{ GeV}$ and $c = -0.4 \text{ GeV}$, $cA_0 = 1 \text{ GeV}^{3/2}$, $n_f = 3$, $\Lambda_{QCD} = 200 \text{ MeV}$ and $M_B = 0.95$) in the next chapters to study the leptonic and semileptonic decay of heavy-light mesons.

Chapter 4

Leptonic decay of B and D mesons in the QCD potential model with relativistic correction

4.1 Introduction

In chapters 2 and 3, we have studied the masses and leptonic decay constants of heavy-light mesons within a short distance scale r_0 and fixed the model input parameters in chapter 3. However, we are unable to explain the origin of such a scale r_0 , which leads us to adopt an alternate approach to evaluate the leptonic decay constants.

In this chapter, we have used the wavefunction with linear part as perturbation and transformed it to momentum space by applying Fourier transformation. This wavefunction is then used to study the decay constants in a formula with relativistic correction where the necessity of the wavefunction at the origin and hence the short distance scale does not arise. We also compute the leptonic branching ratio of B and D mesons to compare with the experimental and other theoretical works.

4.2 Formalism

4.2.1 Wave function in the model

For completeness, we recall the wavefunction with linear part of the Cornell potential as perturbation (Eqn.2.16) in co-ordinate space from chapter 2.

$$\psi(r) = \frac{N'}{\sqrt{\pi a_0^3}} e^{\frac{-r}{a_0}} \left(C' - \frac{\mu b a_0 r^2}{2} \right) \left(\frac{r}{a_0} \right)^{-\epsilon}. \quad (4.1)$$

The terms involved in the above equation are explained in Chapter 2. The wavefunction in momentum space can be obtained by using the Fourier transform as

$$\psi(p) = \frac{1}{(2\pi\hbar c)^{3/2}} \int d^3r e^{\frac{-ip \cdot r}{\hbar c}} \psi(r). \quad (4.2)$$

Separating the variable-dependence of the momentum space wave function as

$$\psi(\vec{p}) = \psi_l(p) Y_{lm}(\theta, \phi) \quad (4.3)$$

one can obtain for $l = 0$ in the natural unit as [144]

$$\psi(p) = \sqrt{\frac{2}{(\pi p^2)}} \int dr \sin(pr) \psi(r). \quad (4.4)$$

Then using Eqn.4.1, 4.4 and the standard result

$$\int x^{p-1} e^{-ax} \sin(mx) dx = \frac{\Gamma(p) \sin(p\theta)}{(a^2 + m^2)^{1/2}}, \quad (4.5)$$

we obtain the normalised wavefunction in momentum space as

$$\psi(p) = \frac{N\sqrt{2}(2-\epsilon)\Gamma(2-\epsilon)}{\pi(1+a_0^2p^2)^{\frac{3-\epsilon}{2}}} \left[C' - \frac{(4-\epsilon)(3-\epsilon)\mu b a_0^3}{2(1+a_0^2p^2)} \right]. \quad (4.6)$$

This simplified form of the wavefunction gives the momentum distribution of the quark and anti quark.

4.2.2 Masses and Decay constants of D and B mesons

The decay constant with relativistic correction can be expressed through the meson wavefunction $\psi_P(p)$ in the momentum space [186] by

$$f_P = \sqrt{\frac{12}{M_P}} \int \frac{d^3p}{(2\pi)^3} \left(\frac{E_q + m_q}{2E_q} \right)^{1/2} \left(\frac{E_{\bar{q}} + m_{\bar{q}}}{2E_{\bar{q}}} \right)^{1/2} \left(1 + \lambda_P \frac{p^2}{[E_q + m_q][E_{\bar{q}} + m_{\bar{q}}]} \right) \psi_P(p), \quad (4.7)$$

where $\lambda_P = -1$ for pseudoscalar mesons and $E_q = \sqrt{p^2 + m_q^2}$. The pseudoscalar mass M_P of the mesons in Eqn.4.7 are calculated by using the relation Eqn.2.26 and the strong running coupling constant appearing in the potential $V(r)$ in turn is considered to be related to the quark mass parameter by Eqn.3.18. However, in the non relativistic limit $\frac{p^2}{m^2} \rightarrow 0$, this expression (Eqn.4.7) reduces to the well known Van-Royen-Weisskopf formula given by Eqn.2.24¹.

The computed results of the pseudoscalar ground state masses of the heavy-light pseudoscalar mesons are compared with the experimental data in Table 4.1. Again, using these computed masses we employ Eqn.4.7 to obtain the pseudoscalar decay constants. The results are then compared with the available experimental and theoretical values in Table 4.2. The results are found to be compatible with available experimental and theoretical values. The same set of input parameters, as stated in the conclusion part of chapter 3 is used to evaluate the numerical results of this chapter.

¹Appendix.C

We note that the present result, ExchQm [187] and that from LC [188] give $f_{B_s} > 260$ MeV, while other results give $f_{B_s} \leq 240$ MeV. Hence, the experimental measurements for f_{B_s} can be a good testing ground for theoretical reliability of each model as shown here.

Table 4.1: Masses of heavy-light mesons in this work with $m_d = 0.336\text{GeV}$, $m_s = 0.465\text{GeV}$, $m_c = 1.55\text{GeV}$, $m_b = 4.97\text{GeV}$ and comparison with experimental data. All values are in units of MeV.

Mesons	Present work	Experimental masses[37]
$D(\bar{c}u/\bar{c}d)$	1870.82	1869.6 ± 0.16
$D(\bar{c}s)$	1966.62	1968 ± 0.33
$B_u(\bar{b}u)$	5273.50	5279 ± 0.29
$B_s(\bar{b}s)$	5365.99	5366 ± 0.6

Table 4.2: Decay constants of pseudoscalar heavy-light mesons(in MeV) computed in this work and comparison with experimental [188, 192] and theoretical results from (2+1)-flavour asqdat action [193], HPQCD [194], extended chiral quark model(ExChQm) [187], Light cone wavefunction [188], light-front quark model (LQM) [189], field-correlator method (FC) [190], Bethe-Salpeter method (BS) [153, 191], relativistic quark model (RQM) [136], relativistic potential model(RPM) [144]

	f_D	f_{D_s}	f_B	f_{B_s}
Present work	205.14	241.84	201.09	292.04
Experiment [188, 192]	206 ± 8.9	260.0 ± 5.4	204 ± 31	...
LQCD [193]	218.9 ± 11.3	260.1 ± 10.8	196.9 ± 8.9	242 ± 9.5
LQCD [194]	213 ± 4	248 ± 2.5
ExChQm[187]	207.53	262.56	208.13	262.39
LC [188]	206 ± 8.9	267.4 ± 17.9	204 ± 31	281 ± 54
LQM [189]	211	248	189	234
FC [190]	210 ± 10	260 ± 10	182 ± 8	216 ± 8
BS [153, 191]	230 ± 25	248 ± 27	196 ± 29	216 ± 32
RQM [136]	234	268	189	218
RPM [144]	208 ± 21	256 ± 26	198 ± 14	237 ± 17

4.2.3 Leptonic decay rate and Branching ratio of D , D_s and B mesons

The leptonic decay rate of the charged Pseudoscalar mesons are obtained by using Eqn.2.28 and employing the predicted values of the pseudoscalar masses and decay constants f_D , f_{D_s} and f_B . We then use this result of decay rates to compute the branching ratio by using the Eqn.2.29 for separate leptonic channels with the choice of $m_{l=\tau,\mu,e}$. The life time of these mesons $\tau_D = 1.04\text{ps}$, $\tau_{D_s} = 0.5\text{ps}$, $\tau_B = 1.63\text{ps}$ and the CKM elements $V_{cd} = 0.230$, $V_{cs} = 1.023$, $V_{ub} = 3.89 \times 10^{-3}$ are taken from the world average value reported by Particle data group [37]. The present results as tabulated in Table 4.3 are in accordance with the available experimental values.

Table 4.3: Leptonic branching ratio of D , D_s and B mesons for three leptonic channels and comparison with experiment and theoretical results.

mesons	$BR_\tau \times 10^{-3}$	$BR_\mu \times 10^{-4}$	$BR_e \times 10^{-6}$
$D(cd)$ Expt. [37] B. Patel et al.,[195]	1.08 [present work]	3.89 [present work]	0.092 [present work]
	< 1.2	$3.82 \pm 0.32 \pm 0.09$	< 8.8
	0.9	6.6	0.015
	$BR_\tau \times 10^{-2}$	$BR_\mu \times 10^{-3}$	$BR_e \times 10^{-4}$
$D(cs)$ HFAG [142] Expt. [37] B. Patel et al.,[195]	5.43 [present]	5.33 [present]	0.0013 [present]
	5.38 ± 0.32	5.8 ± 0.43	
	5.6 ± 0.4	5.8 ± 0.4	< 1.2
	$BR_\tau \times 10^{-4}$	$BR_\mu \times 10^{-6}$	$BR_e \times 10^{-6}$
$B(bu)$ Wolfgang et al.,[196] Expt. [37]	1.07 [present]	0.48 [present]	0.0001 [present]
	0.80 ± 0.12		
	1.8 ± 0.5	< 1.0	< 1.9

4.3 Summary and Conclusion

In this work, we have computed the Pseudoscalar masses and decay constants of heavy-light mesons (B and D together). We have transformed the wavefunction from co-ordinate (r) space into momentum (p) space and used it to obtain the weak decay constants with

its relativistic effect. The condition of convergence of the model has been discussed in chapter 3, which demands that linear part of the potential can be considered as perturbation provided $\frac{(4-\epsilon)(3-\epsilon)\mu b a_0^2}{2(1+a_0^2 Q^2)} \ll C'$ (Eqn.3.22). The values of the α_s , used in the computation also follows this condition correctly. The computed masses and decay constants are then used to compute the branching ratio of D , D_s and B mesons for the three leptonic channels τ , μ and e . B_s meson being neutral in nature, does not show leptonic decay and hence for B_s meson, we have not computed the leptonic branching ratio. The results of this chapter can be summarised as below.

- The ground state masses of D and B mesons computed in this approach are found to be well consistent with the experimental values.
- Both the values of f_D and f_{D_s} in this work are safely below the upper limits 230 MeV and 270 MeV which have been determined using two point correlation function by Khodjamirian [197].
- We obtain the decay constants as $f_{D,D_s,B,B_s} = (205.14, 241.84, 201.09, 292.04)$ MeV which are qualitatively compatible with available experimental and theoretical values. Except f_{B_s} , other values of the decay constants locate inside the experimental errors. However, with a variation of Λ_{QCD} for D and B mesons one can obtain more compatible results with the data.
- In the present work, the computed value of $\frac{f_{D_s}}{f_D} = 1.178$ is found to be in good agreement within the error limit of the recent Lattice(HPQCD) QCD result $\frac{f_{D_s}}{f_D} = 1.164 \pm 0.018$ [194] and Lattice(FNAL and MILC) $\frac{f_{D_s}}{f_D} = 1.188 \pm 0.025$ [198]. However the result of $\frac{f_{B_s}}{f_B} = 1.45$ are found to be larger than the other theoretical values.
- The leptonic branching ratio calculated in the present work for three leptonic channels are comparable with their empirical and PDG average data. The large experimental uncertainty in the electron channel makes it difficult for any reasonable con-

clusion. Furthermore, the ratio of branching ratio in the present work is found to be $R \equiv \frac{\mathcal{B}(D_s^+ \rightarrow \tau^+ \bar{\nu})}{\mathcal{B}(D_s^+ \rightarrow \mu^+ \bar{\nu})} = 10.18$ which is not far from the experimental result 9.2 ± 0.7 and Standard Model result 9.76[192].

Taking into account of all the results summarized above, we can conclude that the present theoretical framework of potential model is qualitatively successful to study the leptonic decay of heavy-light Pseudoscalar mesons.

From a phenomenological point of view, the present theoretical framework should be considerably useful to investigate various physical quantities for the heavy-light quark systems. In the next chapter, we shall extend the present model with its input parameters to study the semileptonic decay of heavy-light mesons with special emphasis to analyse the Isgur-Wise function.

Chapter 5

Isgur Wise function and CKM matrix

element V_{cb} in the QCD Potential model

5.1 Introduction

In chapter 4, we have reported the results of leptonic decay constants of heavy-light mesons in the QCD potential model with linear part of the potential as perturbation. The technique used was the quantum mechanical perturbation theory with plausible relativistic correction. In this chapter, we extend the QCD potential model with its input parameters towards the semileptonic decays to study the Isgur-Wise function.

Exclusive semileptonic decays of hadrons containing a bottom quark provide a path to measure the Cabibbo-Kobayashi-Maskawa(CKM) matrix elements V_{cb} , an important parameter to test the Standard Model. It is well known in the literature that in case of heavy to heavy transitions like $b \rightarrow c$ decays, all heavy quark bilinear current matrix elements are described in terms of only one form factor, which is called the Isgur-Wise (I-W) function in leading order. The I-W function, particularly its slope ($\xi''(1)$) at the zero recoil point is important since it allows a model independent way to determine the CKM element $|V_{cb}|$ for the semileptonic decays $(B^0 \rightarrow D^* l \nu)$ and $(B^0 \rightarrow D l \nu)$. This method of obtaining the CKM

element within the framework of Heavy Quark Effective Theory (HQET) was proposed by Neubert [199]. He observed that the zero recoil point is suitable for the extraction of CKM element $|V_{cb}|$. The method basically relies on the existence of one universal form factor (Isgur-Wise function) and the fact that the form factor is unaffected from $1/m_Q$ ($Q = b, c$) corrections at zero recoil.

Here, we compute the slope ρ^2 and curvature C of the Isgur-Wise function for B meson and then obtain the CKM element V_{cb} with the input parameters of chapter 4.

5.2 Formalism

5.2.1 The Isgur-Wise function and Semileptonic decay

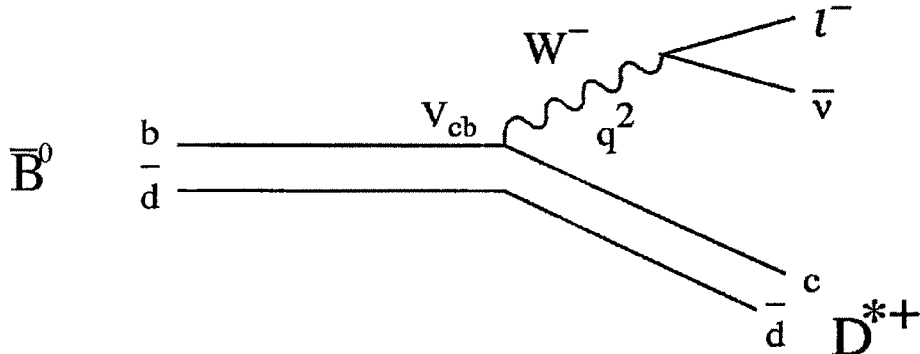


Figure 5.1: Feynmann diagram for semileptonic decay of $B \rightarrow D, D^* l \nu$.

As stated in chapter 1, the amplitude of semileptonic decay like the $B \rightarrow D l \nu$ (shown in Fig.5.1) can be expressed as a product of the hadronic weak current H_μ and the leptonic weak current L_μ with its vector V^μ and axial vector A^μ . Thus we write

$$A = \frac{G_F}{\sqrt{2}} V_{cb} \langle l^-(k_1), \bar{\nu}_l(k_2) | L_\mu | 0 \rangle \times \langle D(P') | H^\mu | \bar{B}(p) \rangle, \quad (5.1)$$

where $H_\mu = \bar{c}\gamma^\mu(1 - \gamma_5)b$ and $L_\mu = \bar{l}\gamma^\mu(1 - \gamma_5)\nu_l$.

Since both the B and D mesons are pseudoscalar ($J^P = 0^-$), so from the consideration of Lorentz covariance and parity one has $\langle D(P')|A^\mu|\bar{B}(p)\rangle = 0$ and there remains the vector part

$$\langle D(p')|V^\mu|B(p)\rangle = f_+(q^2)(p + p')_\mu + f_-(q^2)(p - p')_\mu, \quad (5.2)$$

where $f_+(q^2)$ and $f_-(q^2)$ are two form factors.

Similarly for $B \rightarrow D^*l\nu$, we get another four independent form factors

$$\langle D^*(p', \epsilon)|\bar{u}\gamma^\mu b|B(p)\rangle = 2ie^{\mu\nu\alpha\beta} \frac{\epsilon_\nu p'_\alpha p_\beta}{M_B + M_{D^*}} V(q^2), \quad (5.3)$$

$$\begin{aligned} \langle D^*(p', \epsilon)|\bar{u}\gamma^\mu\gamma_5 b|B(p)\rangle &= (M_B + M_{D^*}) \left[\epsilon^\mu - \frac{\epsilon \cdot q q^\mu}{q^2} \right] A_1(q^2) \\ &\quad - \epsilon \cdot q \left[\frac{(p + p')^\mu}{M_B + M_{D^*}} - \frac{(M_B - M_{D^*})q^\mu}{q^2} \right] A_2(q^2) \\ &\quad 2M_{D^*} \frac{\epsilon \cdot q q^\mu}{q^2} A_0(q^2). \end{aligned} \quad (5.4)$$

These weak form factors can be normalised by applying HQET. In the heavy-quark limit the masses of the heavy quarks and consequently, the masses of the heavy hadrons are taken to be infinite. This leads to an additional symmetry which is known as the heavy flavour symmetry. With the hadron masses their momenta also go to infinity but the hadron 4-velocities stays finite in this symmetry. One is then interested in the dependence of form factors on the (finite) velocity product $v_\mu \cdot v'_\mu$. Moreover, the heavy quark symmetry is an approximate symmetry and correction arises since the quark masses are not infinite. This correction may be studied systematically in the framework of HQET. The leading symmetry-breaking corrections are from terms of order $\frac{1}{m_Q}$ and from the QCD corrections due to the coupling of hard gluons to the heavy quarks. The corrections are given as power series expansions in two small parameters: (a) α_s taken at the scale of the heavy quark (QCD corrections) ie. $\alpha_s(m_Q)$ and (b) the parameter $\frac{\bar{\Lambda}}{m_Q}$, where $\bar{\Lambda}$ is a scale of light degrees

of freedom.

Although the relative corrections can be calculated using perturbative QCD, the m_Q - corrections induce new incalculable functions. For $B \rightarrow D^* l \nu$ decay, there are four such incalculable functions. Hence the predictive power of the theory is reduced. Isgur, Wise, Georgi and others showed that in weak semileptonic decays of $B \rightarrow D l \nu$ or $B \rightarrow D^* l \nu$, all the form factors that describe these decays are expressible in terms of a single universal function of velocity transfer, which is normalized to unity at zero recoil. This universal function is known as the **Isgur-Wise function**. It measures the overlap of the wave functions of the light degrees of freedom in the initial and final mesons moving with four velocities v_μ and v'_μ respectively.

5.2.2 Isgur-Wise function in the model

The universal form factor, Isgur-Wise function, depends only upon the four velocities v_μ and v'_μ of heavy particle before and after decay. This function $\xi(v_\mu, v'_\mu)$ is normalized to unity at zero recoil. If we represent $Y = v_\mu \cdot v'_\mu$ then, for zero recoil i.e $(Y = 1)$, $\xi(v_\mu, v'_\mu) = 1$.

In an explicit form, the Isgur-Wise function can be written as :

$$\begin{aligned} \xi(v_\mu, v'_\mu) &= \xi(Y) \\ &= 1 - \rho^2(Y - 1) + C(Y - 1)^2 + \dots \end{aligned} \quad (5.5)$$

The quantity ρ^2 is the slope of I-W function at $Y = 1$ and known as charge radius :

$$\rho^2 = \frac{\partial \xi}{\partial Y} |_{Y=1} \quad (5.6)$$

The second order derivative is the curvature of the I-W function known as convexity parameter :

$$C = \frac{1}{2} \left(\frac{\partial^2 \xi}{\partial Y^2} \right) |_{Y=1} \quad (5.7)$$

For the heavy-light flavor mesons the I-W function can also be written as [200, 27] :

$$\xi(y) = \int_0^{+\infty} 4\pi r^2 |\psi(r)|^2 \cos pr dr, \quad (5.8)$$

where

$$p^2 = 2\mu^2 (Y - 1). \quad (5.9)$$

Upon integration of Eqn.5.8 one obtains [200, 121]

$$\begin{aligned} \xi(Y) = 1 - \frac{N'^2 a_0^2 \mu^2 (Y - 1)}{2} & \left[\frac{4\Gamma(5 - 2\epsilon)}{2^{4-2\epsilon}} - \frac{4\mu b a_0^3 \Gamma(7 - 2\epsilon)}{2^{6-2\epsilon}} + \frac{\mu^2 b^2 a_0^6 \Gamma(9 - 2\epsilon)}{2^{8-2\epsilon}} \right] \\ & + \frac{4N'^2 a_0^4 \mu^4 (Y - 1)^2}{2^{5-2\epsilon}} \left[\Gamma(4 - 2\epsilon) \left\{ \frac{5 - 2\epsilon}{8} + \frac{3 - 2\epsilon}{3} + \frac{(3 - 2\epsilon)^2}{4} + \frac{(3 - 2\epsilon)^3}{24} \right\} \right. \\ & \quad - \frac{\mu b a_0^3 \Gamma(6 - 2\epsilon)}{4} \left\{ \frac{7 - 2\epsilon}{8} + \frac{5 - 2\epsilon}{3} + \frac{(5 - 2\epsilon)^2}{4} + \frac{(5 - 2\epsilon)^3}{24} \right\} \\ & \quad \left. + \frac{\mu^2 b^2 a_0^6 \Gamma(8 - 2\epsilon)}{64} \left\{ \frac{9 - 2\epsilon}{8} + \frac{7 - 2\epsilon}{3} + \frac{(7 - 2\epsilon)^2}{4} + \frac{(7 - 2\epsilon)^3}{24} \right\} \right]. \quad (5.10) \end{aligned}$$

Here, N' is the normalisation constant of the wavefunction with linear part as perturbation. The normalised wave function naturally follows the zero recoil condition of the I-W function $\xi(1) = 1$ in the model.

5.2.3 The strong coupling constant α_s and determination of Λ_{QCD} for semileptonic decay

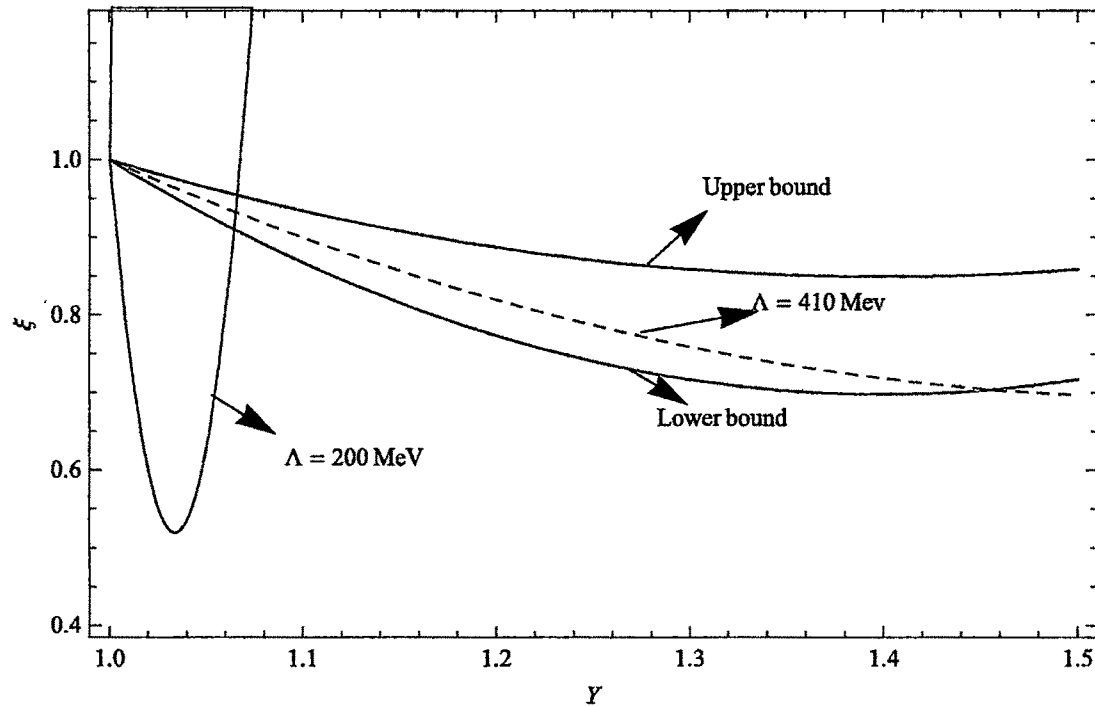
We recall from chapter 3 that the value of α_s is allowed in the range of $0.38 \leq \alpha_s \leq 0.75$ to treat the linear part of the potential as perturbation with its model parameters.

In studying the leptonic decay of heavy-light mesons, the value of $\Lambda_{QCD} = 200\text{MeV}$ was fixed (in chapter 4) in the Eqn.3.18 to obtain the different values of α_s for different values of the renormalisation scale μ . In case of leptonic decay of charged mesons, the

quark and antiquark annihilate to produce a virtual W^* boson so that $q^2 = M^2$ and hence we get only one form factor, the decay constant f_p , which absorbs all the strong interaction effects. In semileptonic decay, however the case is different since q^2 is different from event to event and hence more than one form factor appears. This decrease of q^2 in semileptonic decay leads us to consider a larger value of Λ_{QCD} than that of the leptonic decay which effectively increases the strong coupling constant $\alpha_s(\mu)$.

The physically plausible range of effective Λ_{QCD} should in principle be deduced from the allowed bands of the slope and curvature of the I-W function. Considering the theoretical bounds on slope $3/4 \leq \rho^2 < 1.51$ [202, 203] and curvature $C \geq \frac{5\rho^2}{4}$ [203], we draw a curve for the variation of I-W function for B meson and is shown in Fig.5.2. The allowed range of ρ^2 provides a range of Λ_{QCD} in the model as $382\text{MeV} \leq \Lambda_{QCD} \leq 430\text{MeV}$.

Figure 5.2: Variation of I-W function with Y for B meson.



In Ref.[201], it was analysed in the study of the freezing of QCD coupling effects that

for running background coupling in V scheme, one can choose $\Lambda_V(n_f = 3) = 410 \text{ MeV}$ (Eqn.30 of Ref.[201]) and this value of Λ_V does not contradict with those which are commonly used in \overline{MS} renormalisation scheme and give rise to $\alpha_s(M_Z) = 0.118 \pm 0.001$. Hence we justify ourself to choose $\Lambda_{QCD} = 0.410 \text{ GeV}$ in this work.

The input parameters used in the numerical calculation are the same as is used in our previous chapter 4, which are $n_f = 3$, $m_d = 0.336 \text{ GeV}$, $m_c = 1.55 \text{ GeV}$, $m_b = 4.97 \text{ GeV}$ with $b = 0.183 \text{ GeV}^2$ and $cA_0 = 1 \text{ GeV}^{2/3}$ with $c = -0.4 \text{ GeV}$.

5.3 Results

5.3.1 Isgur-Wise function

Using Eqn.5.5 and Eqn.5.10, we compute the slope and curvature of the I-W function for B and D mesons and tabulate in Table.5.1.

Table 5.1: Slope and curvature of I-W function for B and D mesons.

Slope and Curvature	With $\Lambda_{QCD} = 200 \text{ MeV}$	With $\Lambda_{QCD} = 410 \text{ MeV}$
ρ_D^2	28.53	0.78
$\rho_{D_s}^2$	28.73	1.23
ρ_B^2	28.42	0.993
$\rho_{B_s}^2$	29.847	1.64
C_D	403.18	0.698
C_{D_s}	447.87	1.71
C_B	420.68	1.114
C_{B_s}	504.81	3.07

From Table.5.1, we see that with $\Lambda_{QCD} = 200 \text{ MeV}$, the results overshoots all other theoretical upper bound $3/4 \leq \rho^2 < 1.51$ [202] where as the results with $\Lambda_{QCD} = 410 \text{ MeV}$ are found to lie within this bound. Thus, for the numerical calculation of V_{cb} , we consider the value of ρ_B^2 and C_B with $\Lambda_{QCD} = 410 \text{ MeV}$. We note that both the slope and curvature of the calculated Isgur-Wise function $\rho_B^2 = 0.993$ and $C_B = 1.114$ satisfy all known lower

bounds $-\xi' = \rho^2 \geq \frac{3}{4}$ and $-\xi'' = C \geq \frac{15}{16}$ [202]. A comparison of the slope and curvature of the Isgur-Wise function of B meson in the present work is shown in Table 5.2.

Table 5.2: Comparison of slope and curvature of B mesons with other works.

work	ρ_B^2	C_B
Present	0.993	1.114
Faustov et al; [204]	1.04	1.36
Lattice QCD [205]	0.83^{+15+24}_{-11-22}	..
ALEPH [206]	$0.92 \pm 0.98 \pm 0.36$..
Belle [207]	$1.12 \pm 0.22 \pm 0.14$..
Le Youanc et al [208]	≥ 0.75	≥ 0.47
QCD Sum Rule [209]	0.65	0.47
Relativistic Three Quark Model [210]	1.35	1.75
Neubert [211]	0.82 ± 0.09	..

Considering the theoretical range of $3/4 \leq \rho^2 < 1.51$ from Ref.[202, 203] which corresponds to the scale $382 \text{ MeV} \leq \Lambda_{QCD} \leq 430 \text{ MeV}$, we compute a wide range of the curvature C of the I-W function in the model as $0.563 \leq C \leq 3.52$.

In Fig.5.3 and Fig.5.4, we show the variation of Isgur-Wise function with Y for the two scales $\Lambda_{QCD} = 200 \text{ MeV}$ and $\Lambda_{QCD} = 410 \text{ MeV}$.

Figure 5.3: Variation of I-W function with Y for heavy-light mesons with $\Lambda = 200 \text{ MeV}$.

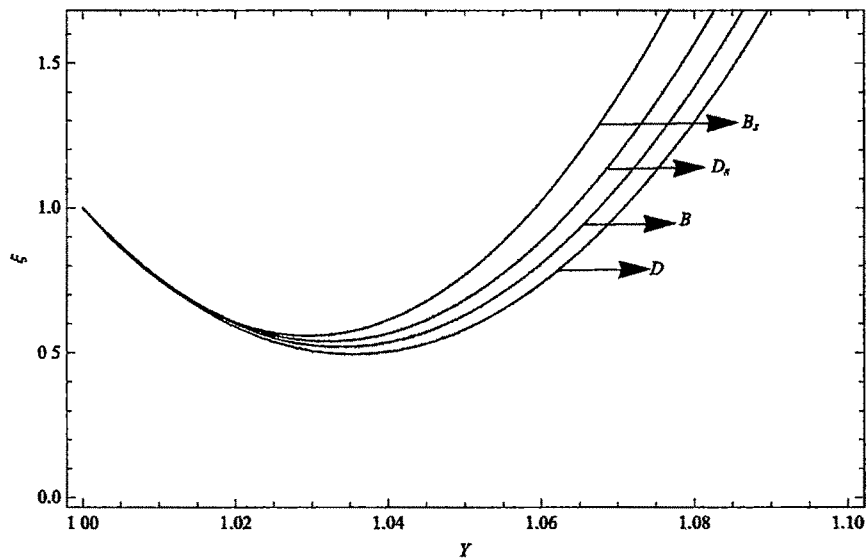
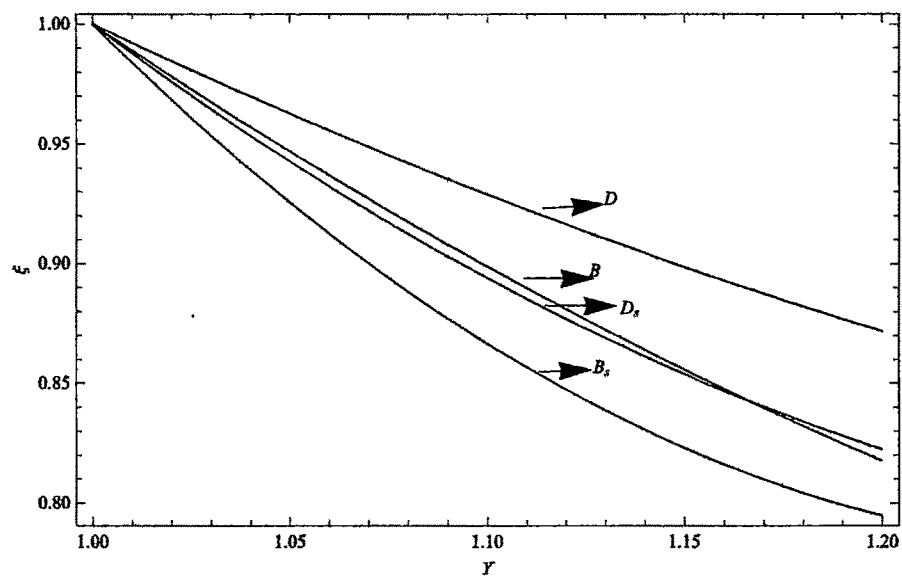


Figure 5.4: Variation of I-W function with Y for heavy-light mesons with $\Lambda = 410 \text{ MeV}$.



5.3.2 Determination of CKM element V_{cb}

The differential semileptonic decay rate $B \rightarrow D l \bar{\nu}$ for the massless leptons is given by [199, 179]

$$\frac{d\Gamma}{dy} = \frac{G_F^2}{48\pi^3} |V_{cb}|^2 M_D^3 (Y^2 - 1)^{3/2} (M_B + M_D)^2 \xi^2(Y), \quad (5.11)$$

where Y lies in the range $1 \leq Y \leq \frac{M_B^2 + M_D^2 - m_l^2}{2M_B M_D}$.

The differential semileptonic decay rate $B \rightarrow D^* l \bar{\nu}$ is defined by

$$\begin{aligned} \frac{d\Gamma}{dY} = & \frac{G_F^2}{48\pi^3} |V_{cb}|^2 (M_B - M_{D^*})^2 M_{D^*}^3 \sqrt{(Y^2 - 1)} (Y + 1)^2 \\ & \times \left[1 + \frac{4Y}{Y + 1} \frac{q^2(Y)}{(M_B - M_{D^*})^2} \right] \xi^2(Y), \end{aligned} \quad (5.12)$$

where $q^2(Y) = M_B^2 + M_{D^*}^2 - 2YM_{D^*}M_B$. By integrating the expressions for the differential decay rates

$$\Gamma = \int \frac{G_F^2}{48\pi^3} |V_{cb}|^2 M_D^3 (Y^2 - 1)^{3/2} (M_B + M_D)^2 \xi^2(Y) dY \quad (5.13)$$

and

$$\begin{aligned} \Gamma = & \int \frac{G_F^2}{48\pi^3} |V_{cb}|^2 (M_B - M_{D^*})^2 M_{D^*}^3 \sqrt{(Y^2 - 1)} (Y + 1)^2 \\ & \times \left[1 + \frac{4Y}{Y + 1} \frac{q^2(Y)}{(M_B - M_{D^*})^2} \right] \xi^2(Y) dY, \end{aligned} \quad (5.14)$$

we get the predictions for the total decay rates in our model as

$$\Gamma(B \rightarrow D l \bar{\nu}) = 6.82 |V_{cb}|^2 \text{ ps}^{-1}, \quad (5.15)$$

$$\Gamma(B \rightarrow D^* l \bar{\nu}) = 28.40 |V_{cb}|^2 \text{ ps}^{-1}. \quad (5.16)$$

Taking the mean values of lifetimes from PDG2012 [2], $\tau_{B^0} = 1.519 \times 10^{-12}$ s and $\tau_{B^+} = 1.641 \times 10^{-12}$ s, and also using the experimental masses, we compute the semileptonic

branching ratio by using the relation $BR = \Gamma \times \tau$ and find

$$\begin{aligned} BR(B^0 \rightarrow D^+ l^- \nu) &= 10.401 |V_{cb}|^2, \\ BR(B^+ \rightarrow D^0 l^+ \nu) &= 11.10 |V_{cb}|^2, \\ BR(B^0 \rightarrow D^{*+} l^- \nu) &= 43.31 |V_{cb}|^2, \\ BR(B^+ \rightarrow D^{*0} l^+ \nu) &= 46.78 |V_{cb}|^2. \end{aligned} \quad (5.17)$$

The comparison of these theoretical results with the experimental branching ratios from the latest PDG average [2], with the propagation of error gives us following values of the CKM matrix element $|V_{cb}|$:

$$\begin{aligned} BR(B^0 \rightarrow D^- l^+ \nu)^{\text{exp}} &= 0.0218 \pm 0.0012 & |V_{cb}| &= 0.0458 \pm 0.0013, \\ BR(B^+ \rightarrow D^0 l^+ \nu)^{\text{exp}} &= 0.0229 \pm 0.0008 & |V_{cb}| &= 0.0454 \pm 0.0008, \\ BR(B^0 \rightarrow D^{*-} l^+ \nu)^{\text{exp}} &= 0.0509 \pm 0.0022 & |V_{cb}| &= 0.0342 \pm 0.0007, \\ BR(B^+ \rightarrow D^{*0} l^+ \nu)^{\text{exp}} &= 0.0558 \pm 0.0026 & |V_{cb}| &= 0.0345 \pm 0.0008. \end{aligned} \quad (5.18)$$

Thus the averaged $|V_{cb}|$ over all presented measurements of semileptonic decays $B \rightarrow D \bar{e} \nu$ and $B \rightarrow D^* \bar{e} \nu$ is equal to

$$|V_{cb}| = 0.0400 \pm 0.0009 \quad (5.19)$$

and is in good agreement with the experimental result [2].

$$|V_{cb}| = 0.0396 \pm 0.0009 \quad (\text{exclusive}).$$

For completeness, we also record the bounds on V_{cb} for the computed bound on Λ_{QCD} due to I-W function of B meson ($382 \text{ MeV} \leq \Lambda_{QCD} \leq 430 \text{ MeV}$):

$$BR(B^0 \rightarrow D^+ l^- \nu) = (9.22 - 11.763) |V_{cb}|^2,$$

$$\begin{aligned}
BR(B^+ \rightarrow D^0 l^+ \nu) &= (9.96 - 12.71) |V_{cb}|^2, \\
BR(B^0 \rightarrow D^{*+} l^- \nu) &= 41.92 - 48.41) |V_{cb}|^2, \\
BR(B^+ \rightarrow D^{*0} l^+ \nu) &= (45.29 - 52.33) |V_{cb}|^2.
\end{aligned} \tag{5.20}$$

Comparing this Eqn.5.20 with Eqn.5.18 and taking the average of V_{cb} , we obtain the range

$$0.0375 \leq |V_{cb}| \leq 0.0410. \tag{5.21}$$

5.4 Conclusion

In this work, we have studied the renormalisation scale dependance of Isgur-wise function by using a wavefunction with linear part of the Cornell Potential as perturbation. Considering the exclusive semileptonic decay of $B \rightarrow D e \nu$ and $B \rightarrow D^* e \nu$, we then compute the CKM element $|V_{cb}|$ in this approach. The result of the CKM element is found to be within the error limits of other results. The following features are observed in this work:

- The renormalization scale of the model was set to be $\Lambda_{QCD} = 410 \text{ MeV}$ with the approximation that the Λ_{QCD} for the heavy-quark effective mass is the same as that for the light quark. In this scale, consideration of a relativistic Hamiltonian seems to be necessary for the light quarks of the meson. However, we consider that the plausible relativistic correction introduced by the term $\left(\frac{r}{a_0}\right)^{-\epsilon}$ is sufficient to overcome this problem.
- The larger value of the effective scale $\alpha_{eff} = 4\alpha_s/3$ for semileptonic decay of B meson does not create any problem in the perturbation procedure, since the increasing value of α_s makes the Coulombic part of the potential more dominant to consider the linear term of the potential as perturbation.
- The slope and curvature of the Isgur-wise function for B meson is found to lie within

all the range of limits found in the literature. For a theoretical bound of $3/4 \leq \rho^2 \leq 1.51$, we predict a wide range of the curvature, C in the model as $0.563 \leq C \leq 3.52$.

- The computed value of the CKM element from the exclusive semileptonic decay of B meson is obtained as $|V_{cb}| = 0.0400 \pm 0.0009$. The result is to be well consistent with the lattice result $|V_{cb}| = 0.0409 \pm 0.0015 \pm 0.0007$ [212].
- It becomes an worthy comment to note that the result with $\Lambda_{QCD} = 200$ MeV (as is done in our previous work)is found to be very poor to study the branching ratio and $|V_{cb}|$, which implies that the decay and interaction process of hadrons are not controlled by the same mechanism.

Chapter 6

B_c meson as a heavy-light meson in the QCD potential model

6.1 Introduction

The B_c meson is a particularly interesting hadron, since it is the lowest bound state of two heavy (b, c) quarks with different flavors. Because of the fact that the B_c meson carries the flavor explicitly, there is no gluon or photon annihilation via strong interaction or electromagnetic interaction but decay only via weak interaction. Since both b and c quarks forming the B_c meson are heavy, the B_c meson can decay through the $b \rightarrow q$ ($q = c, u$) transition with c quark being a spectator as well as through the $c \rightarrow q$ ($q = s, d$) transition with b quark being a spectator. The former transitions correspond to the semileptonic decays to η_c and D mesons, while the latter transitions correspond to the decays to B_s and B mesons.

The CDF Collaboration reported the discovery of the B_c ground state in $p\bar{p}$ collisions already more than fourteen years ago [213]. More experimental data on masses and decays of the B_c meson are expected to come in near future from the Tevatron at Fermilab and the Large Hadron Collider (LHCb) at CERN. The estimates of the B_c decay rates indicate that the c quark transitions give the dominant contribution while the b quark transitions and

weak annihilation contribute less. However, from the experimental point of view the B_c decays to charmonium are easier to identify. Indeed, CDF and D0 observed the B_c meson and measured its mass analyzing its semileptonic decays of $B_c \rightarrow J/\psi l\nu$.

There are many theoretical approaches to study the exclusive semileptonic decay of B_c meson. The paper by Bjorken in 1986, on the decays of long lived B_c meson is considered to be the pioneering work for B_c meson [214]. A lot of efforts was then directed to study this specific meson on the basis of modern understanding of QCD dynamics of heavy flavours in the framework of different approaches. Some of these approaches are: QCD sum rules [215, 216, 217], the relativistic quark model [218, 219, 220], the quasi-potential approach to the relativistic quark model [176, 221, 222], the non-relativistic approach of the Bethe-Salpeter(BS) equation [223], based on the BS equation, the relativistic quark model [224, 225], the QCD relativistic potential model [226], the relativistic quark-meson model [227], the nonrelativistic quark model [228], the covariant light-front quark model [229] and the constituent quark model [230, 231, 232, 149] using BSW(Bauer, Stech, and Wirbel) model [233] and ISGW (Isgur, Scora, Grinstein, and Wise) model [234].

The consequence of heavy quark spin symmetry is that the number of form factors which parametrize the matrix elements is reduced and simplifies the semileptonic transitions. However, spin symmetry does not fix the normalisation of the form factors at any point of the phase space. The normalisation of the form factors near the zero recoil point must be computed by some nonperturbative approach [235]. So far, Jenkins *et al.*, in Ref.[236] estimated the universal form factors of semileptonic decays of B_c meson using non-relativistic meson wavefunctions and in Ref.[237], it is computed by employing the ISGW model at the zero-recoil point . In this chapter, we extend the QCD potential model and check its sensitivity in studying the universal form factor Isgur-Wise function for B_c meson with two different approaches: a) linear part of the Cornell potential as perturbation with Coulombic part as parent and b) Coulombic part as perturbation with linear part as parent.

6.2 Formalism

6.2.1 The wavefunctions in the model

With Cornell potential one obtains the advantage of choosing the Coulombic part as perturbation with linear part as parent as well as linear part as perturbation with Coulombic part as parent. It is expected that a critical role is played by scale the r_0 , where the potential $V(r) = 0$. Aitchison and Dudek in Ref.[239] put an argument that if the size of a state (meson here) measured by $\langle r \rangle < r_0$, then the Coulomb part as the “parent” will perform better and if $\langle r \rangle > r_0$, the linear part as “parent” will perform better. Aitchison’s work also showed that the results with Coulombic part as parent (VIPT) for bottomonium spectra are well explained where as charmonium states are well explained with linear part as parent. Moreover in Ref. [240], we have analysed that the critical distance r_0 is not a constant and can be enhanced by reducing b and c or by increasing α_s . Thus for a fixed value of b and c , α_s plays an important role in choosing the perturbative term. However in this manuscript we allow the same range of α_s obtained from the theoretical bounds of slope and curvature of I-W function and check the applicability of the model wavefunctions in the two approaches for the semileptonic decay of B_c meson into $c\bar{c}(\eta_c, J/\psi)$ states.

The wavefunction computed by Dalgarno method, with Coulombic part $-\frac{4\alpha_s}{3r} + c$ of the potential as perturbation and linear part br as parent has been reported in Ref.[241] and the alternate approach of choosing the linear part $br + c$ as perturbation has been discussed in the previous chapters.

The main equations of the wavefunction with Coulombic part as perturbation and linear part as parent are discussed below.

6.2.2 Wavefunction with Coulombic part as perturbation

The wavefunction with linear part as parent becomes an Airy function, which in fact makes the total wavefunction a complicated one since Airy function is a diverging function. Thus, the total wave function corrected upto first order and considering upto order r^3 are given by[241, 242]

$$\psi_{coul}(r) = \psi^{(0)}(r) + \psi^{(1)}(r) \quad (6.1)$$

$$= \frac{N_1}{2\sqrt{\pi}} \left[\frac{Ai((2\mu b)^{\frac{1}{3}} + \rho_{01})}{r} - \frac{4\alpha_s}{3} \left(\frac{a_0}{r} + a_1 + a_2 r \right) \right] \quad (6.2)$$

where N_1 is the normalisation constant for the total wave function $\psi_{coul}(r)$ where subscript “coul” means Coulombic potential as perturbation and ρ_{0n} are the zeros of the Airy function which is given by [239, 243]:

$$\rho_{0n} = - \left[\frac{3\pi(4n-1)}{8} \right]^{\frac{2}{3}} \quad (6.3)$$

$$a_0 = \frac{0.8808(b\mu)^{\frac{1}{3}}}{(E-c)} - \frac{a_2}{\mu(E-c)} + \frac{4W^1 \times 0.21005}{3\alpha_s(E-c)} \quad (6.4)$$

$$a_1 = \frac{ba_0}{(E-c)} + \frac{4 \times W^1 \times 0.8808 \times (b\mu)^{\frac{1}{3}}}{3\alpha_s(E-c)} - \frac{0.6535 \times (b\mu)^{\frac{2}{3}}}{(E-c)} \quad (6.5)$$

$$a_2 = \frac{4\mu W^1 \times 0.1183}{3\alpha_s} \quad (6.6)$$

$$W^1 = \int_0^{+\infty} r^2 H' |\psi^{(0)}(r)|^2 dr \quad (6.7)$$

where $H' = -\frac{4\alpha_s}{3r} + c$ is the perturbed Hamiltonian and

$$E = - \left(\frac{b^2}{2\mu} \right)^{\frac{1}{3}} \rho_{0n}. \quad (6.8)$$

In the Ref.[241], the value of $c = 1$ Gev was taken where as here in this chapter, we choose

$c = -0.4 \text{ GeV}$ in consistency with the chapters 4 and 5.

6.2.3 The strong coupling constant α_s in the Model

We use the same prescription of α_s as is used in our previous chapters (Eqn.3.18). In chapter 5, we discussed that the physically plausible range of effective Λ_{QCD} can be deduced from the allowed range of the slope and curvature of the I-W function and considering the theoretical bounds on slope $3/4 \leq \rho^2 < 1.51$ [202, 203] and curvature $C \geq \frac{5\rho^2}{4}$ [203] of the I-W function, we obtained an allowed range of Λ_{QCD} in the model as $382 \text{ MeV} \leq \Lambda_{QCD} \leq 430 \text{ MeV}$ for B meson. We extend this theoretical bounds of B meson to B_c meson in its semileptonic decay of charmonium states ($B_c \rightarrow c\bar{c}(\ell^+\nu_\ell)$) and compute the slope and curvature of the Isgur Wise function.

6.2.4 Form factors and Decay rates of $B_c \rightarrow c\bar{c}(\ell^+\nu_\ell)$ transitions

In the semileptonic transitions of $B_c \rightarrow c\bar{c}(\ell^+\nu_\ell)$ states, the hadronic part of the matrix element is contributed by the vector ($V^\mu = \bar{c}\gamma^\mu b$) or axial vector ($A^\mu = \bar{c}\gamma^\mu\gamma_5 b$) current between B_c and $c\bar{c}$ states. For transition between two pseudoscalar mesons ($B_c \rightarrow \eta_c$), axial current A^μ vanishes and vector current V^μ only contributes. This hadronic current, V^μ between the two $J^P = 0^-$ mesons is expressed in terms of two form factors $f_\pm(q^2)$ as [179]

$$\langle \eta_c(p') | V^\mu | B_c(p) \rangle = f_+(q^2)(p + p')_\mu + f_-(q^2)(p - p')_\mu \quad (6.9)$$

where q is the four momentum transfer which varies within the range $m_\ell^2 \leq q^2 \leq (m_{B_c} - m_{\eta_c})^2 = q_{max}^2$ and $f_+(q^2)$ and $f_-(q^2)$ are two weak transition form factors.

For the transition of pseudoscalar to vector mesons ($B_c \rightarrow J/\psi(p', \epsilon)$) both the vector

and axial vector current contributes and we get four independent form factors as,

$$\langle J/\psi(p', \epsilon) | \bar{c} \gamma^\mu b | B_c(p) \rangle = 2i \epsilon^{\mu\nu\alpha\beta} \frac{\epsilon_\nu p'_\alpha p_\beta}{M_{B_c} + M_{J/\psi}} V(q^2) \quad (6.10)$$

$$\begin{aligned} \langle J/\psi(p', \epsilon) | \bar{c} \gamma^\mu \gamma_5 b | B_c(p) \rangle &= (M_{B_c} + M_{J/\psi}) \left[\epsilon^\mu - \frac{\epsilon \cdot q q^\mu}{q^2} \right] A_1(q^2) \\ &\quad - \epsilon \cdot q \left[\frac{(p + p')^\mu}{M_{B_c} + M_{J/\psi}} - \frac{(M_{B_c} - M_{J/\psi}) q^\mu}{q^2} \right] A_2(q^2) \\ &\quad 2M_{J/\psi} \frac{\epsilon \cdot q q^\mu}{q^2} A_0(q^2) \end{aligned} \quad (6.11)$$

In the present study we treat B_c system as a heavy-light one in analogy to D system as the ratio of the constituent quark masses in the B_c meson is very close to that of D meson and extend HQET for the study of B_c meson also. On the basis of HQET, the most general form of the transition discussed by Eqns.6.9 and 6.10 can be expressed as [179, 242],

$$\frac{1}{\sqrt{M_{B_c} M_{\eta_c}}} \langle \eta_c(v') | V^\mu | B_c(v) \rangle = (v + v')^\mu \xi(\omega) \quad (6.12)$$

$$\frac{1}{\sqrt{M_{B_c} M_{J/\psi}}} \langle J/\psi(v', \epsilon_3) | V^\mu | B_c(v) \rangle = i \epsilon^{\mu\nu\alpha\beta} \epsilon_\nu v'_\alpha v_\beta \xi(\omega) \quad (6.13)$$

$$\frac{1}{\sqrt{M_{B_c} M_{J/\psi}}} \langle J/\psi(v', \epsilon_3) | A^\mu | B_c(v) \rangle = [(1 + \omega) \epsilon^\mu - (\epsilon \cdot v) v'^\mu] \xi(\omega), \quad (6.14)$$

where v and v' is the four velocity of B_c meson before and after the transition in the rest frame of the initial meson and $\xi(\omega)$ is the universal form factor known as Isgur Wise function.

For small, nonzero recoil, Isgur-Wise function can be written by the formula (Eqn.5.5 of chapter 5):

$$\begin{aligned} \xi(v \cdot v') &= \xi(Y) \\ &= 1 - \rho^2 (Y - 1) + C (Y - 1)^2 + \dots \end{aligned} \quad (6.15)$$

where Y is given by,

$$Y = \nu \cdot \nu' = \frac{[m_{B_c}^2 + m_{c\bar{c}}^2 - q^2]}{2m_{B_c}m_{c\bar{c}}}. \quad (6.16)$$

For heavy-light mesons, I-W function can also be expressed by another formula [244, 245] :

$$\xi(Y) = \int_0^{+\infty} 4\pi r^2 |\psi(r)|^2 \cos pr dr \quad (6.17)$$

where

$$p^2 = 2\mu^2(Y - 1). \quad (6.18)$$

In Eqn.6.17, we employ the two wavefunctions (Eqn.2.16 and Eqn.6.1) to compute the slope and curvature of the Isgur-Wise function and present the results in Table.6.1. The input parameters used in the numerical calculations are the same as is used in our previous chapters. For the masses of B_c , η_c and J/ψ , we use the experimental masses from PDG2012 [2].

Table 6.1: The slope ρ^2 and curvature C of the I-W function with linear part as perturbation and Coulombic part as perturbation.

Λ	Linear part as perturbation		Coulombic part as perturbation	
	ρ^2	C	ρ^2	C
382 MeV	9.59	117.783	3.78	0.057
430 MeV	5.45	31.39	3.83	0.051

In Ref.[235], the slope and curvature of the universal form factor for B_c meson is computed in the framework of QCD relativistic potential model and is shown in Table.6.2.

Table 6.2: Parameters of the form factors for the channel of $B_c \rightarrow \eta_c(J/\psi)$ with $\Lambda = 397\text{MeV}$ (from ref.[235]).

Channel	F(1)	ρ^2	C
$B_c \rightarrow \eta_c(J/\psi)$	0.94	2.9	3

The result of Table.6.1 is found to be closer to that of Ref.[235] in one of the approach of our model with Coulombic part as perturbation. Interestingly, the scale $\Lambda = 397\text{MeV}$ (used in Ref.[235]) lies within our range of $382\text{MeV} \leq \Lambda_{QCD} \leq 430\text{MeV}$. In Fig.6.1 and Fig.6.2, we show the variation of Isgur-Wise function with its four velocity transfer ($Y=v.v'$) in the two different approaches.

Figure 6.1: Variation of I-W function with Y for different scales of Λ with linear part as perturbation.

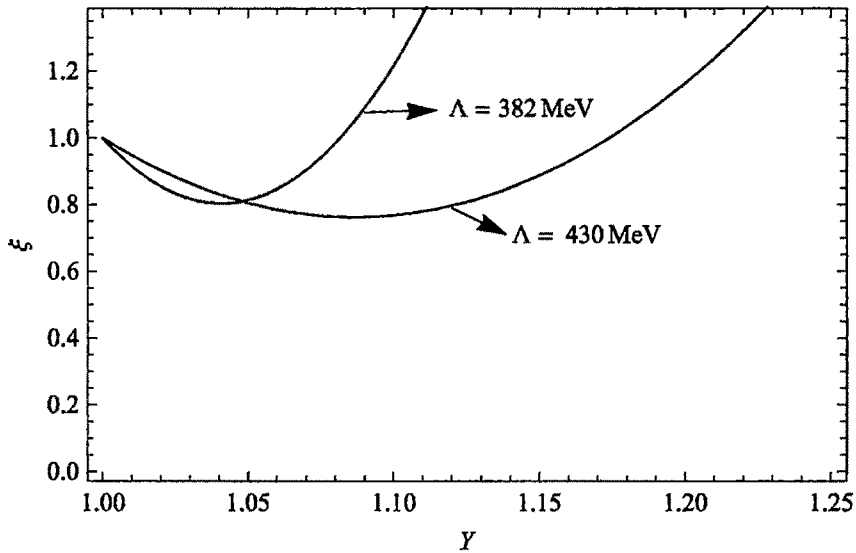
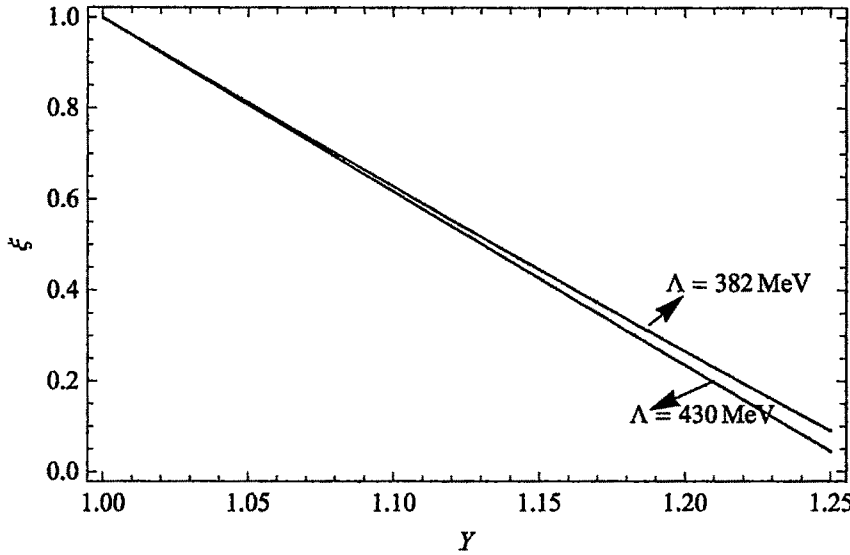


Figure 6.2: Variation of I-W function with Y for different scales of Λ with Coulombic part as perturbation.



Applying HQET, the most general form of the transition discussed by Eqns.6.9 and 6.10 can be expressed in terms of Isgur Wise function as [179]

$$f_{\pm}(q^2) = \xi(Y) \frac{m_{B_c} \pm m_{\eta_c}}{2 \sqrt{m_{B_c} m_{\eta_c}}} \quad (6.19)$$

and

$$V(q^2) = A_2(q^2) = A_0(q^2) = \left[1 - \frac{q^2}{(M_{B_c} + M_{J/\psi})^2} \right]^{-1} A_1(q^2) = \frac{(M_{B_c} + M_{J/\psi})^2}{4 M_{B_c} M_{J/\psi}} \xi(Y) \quad (6.20)$$

Here, we have applied the HQET to relate the form factors of the semileptonic transitions of $B_c \rightarrow c\bar{c}$ states with the Isgur-Wise function in Eqn.6.19 and Eqn.6.20. These equations are based on the heavy flavour symmetry and is broken in the case of mesons containing two heavy quarks[236]. Spin symmetry breaking effects can occur when the c-quarks recoil momentum is larger than m_c . However, we expect that the equations are applicable to other

kinematic point since the recoil momentum of $c\bar{c}$ state is small ($y_{max} - 1 = 0.26$) due to its heavy mass [246]. In Ref.[235], Pietro Colangelo and Fulvia De Fazio showed that the normalization of the form factor Δ describing the transition $B_c \rightarrow J/\psi \ell^+ \nu_\ell$ is close to 1 ($\simeq 0.94$) at the zero-recoil point, as being the overlap of wave-functions, although it is not constrained by symmetry arguments.

The differential semileptonic decay rates can be expressed in terms of these form factors by

(a) $B_c \rightarrow Pe\nu$ decay ($P = \eta_c$)

$$\frac{d\Gamma}{dq^2}(B_c \rightarrow Pe\nu) = \frac{G_F^2 \Delta^3 |V_{qb}|^2}{24\pi^3} |f_+(q^2)|^2. \quad (6.21)$$

(b) $B_c \rightarrow Ve\nu$ decay ($V = J/\psi$) The decay rate in transversely(T) and longitudinally(L) polarized vector mesons are defined by [247]

$$\frac{d\Gamma_L}{dq^2} = \frac{G_F^2 \Delta |V_{qb}|^2}{96\pi^3} \frac{q^2}{M_B^2} |H_0(q^2)|^2, \quad (6.22)$$

$$\frac{d\Gamma_T}{dq^2} = \frac{d\Gamma_+}{dq^2} + \frac{d\Gamma_-}{dq^2} = \frac{G_F^2 \Delta |V_{qb}|^2}{96\pi^3} \frac{q^2}{M_B^2} (|H_+(q^2)|^2 + |H_-(q^2)|^2). \quad (6.23)$$

where helicity amplitudes are given by the following expressions

$$H_\pm(q^2) = \frac{2M_{B_c}\Delta}{M_{B_c} + M_V} \left[V(q^2) \mp \frac{(M_{B_c} + M_V)^2}{2M_{B_c}\Delta} A_1(q^2) \right], \quad (6.24)$$

$$H_0(q^2) = \frac{1}{2M_V \sqrt{q^2}} \left[(M_{B_c} + M_V)(M_{B_c}^2 - M_V^2 - q^2) A_1(q^2) - \frac{4M_B^2 \Delta^2}{M_{B_c} + M_V} A_2(q^2) \right]. \quad (6.25)$$

Thus the total semileptonic decay rate is given by

$$\frac{d\Gamma}{dq^2}(B_c \rightarrow Ve\nu) = \frac{G_F^2 \Delta |V_{cb}|^2}{96\pi^3} \frac{q^2}{M_{B_c}^2} (|H_+(q^2)|^2 + |H_-(q^2)|^2 + |H_0(q^2)|^2), \quad (6.26)$$

where G_F is the Fermi constant, V_{cb} is CKM matrix element,

$$\Delta \equiv |\Delta| = \sqrt{\frac{(M_{B_c}^2 + M_{P,V}^2 - q^2)^2}{4M_{B_c}^2} - M_{P,V}^2}$$

Integrating over q^2 of these formulas (Eqn.6.21 and Eqn.6.26), we compute the total decay rate of the corresponding semileptonic decay and present the results in Table.6.4. In Fig.6.3, Fig.6.3, Fig.6.5 and Fig.6.6, we plot the differential semileptonic decay rates $d\Gamma/dq^2$ for semileptonic decays $B_c \rightarrow \eta_c e \bar{\nu}$ and $B_c \rightarrow J/\psi e \bar{\nu}$ within the two approaches of our model.

Figure 6.3: Differential decay rates $(1/|V_{cb}|^2)d\Gamma/dq^2$ of $B_c \rightarrow \eta_c e \bar{\nu}$ (in GeV^{-1}) with linear part as perturbation. The red and blue curves correspond to $\Lambda = 382 MeV$ and $430 MeV$ respectively.

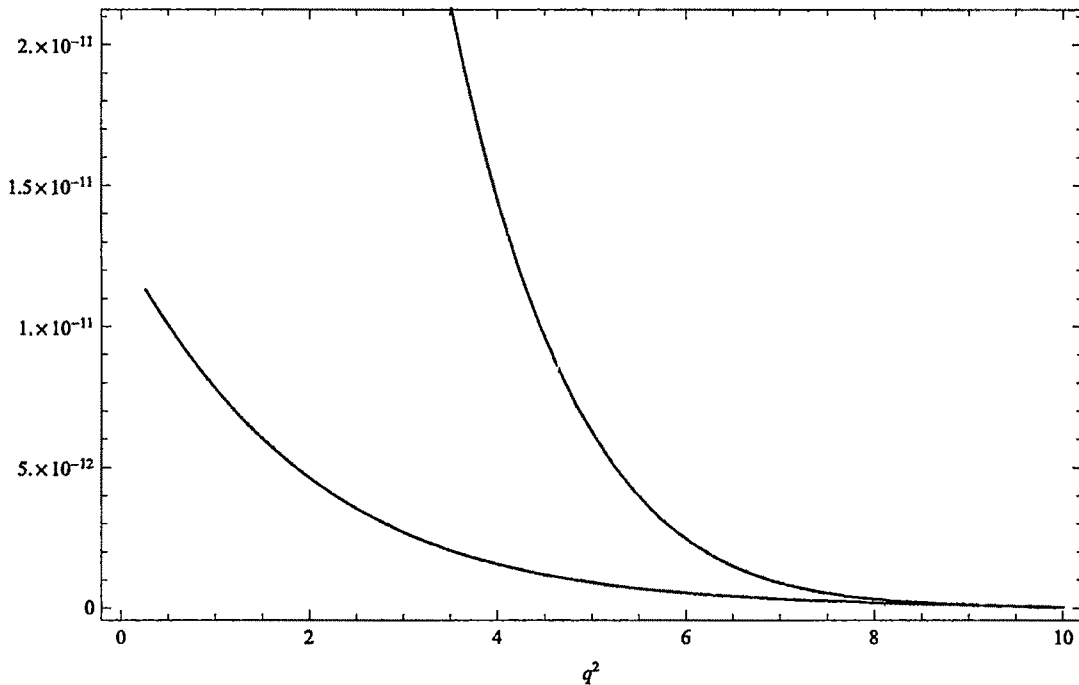


Figure 6.4: Differential decay rates $(1/|V_{cb}|^2)d\Gamma/dq^2$ of $B_c \rightarrow \eta_c e \bar{\nu}$ (in GeV^{-1}) with coulombic part as perturbation. The red and blue curves correspond to $\Lambda = 382 MeV$ and $430 MeV$ respectively.

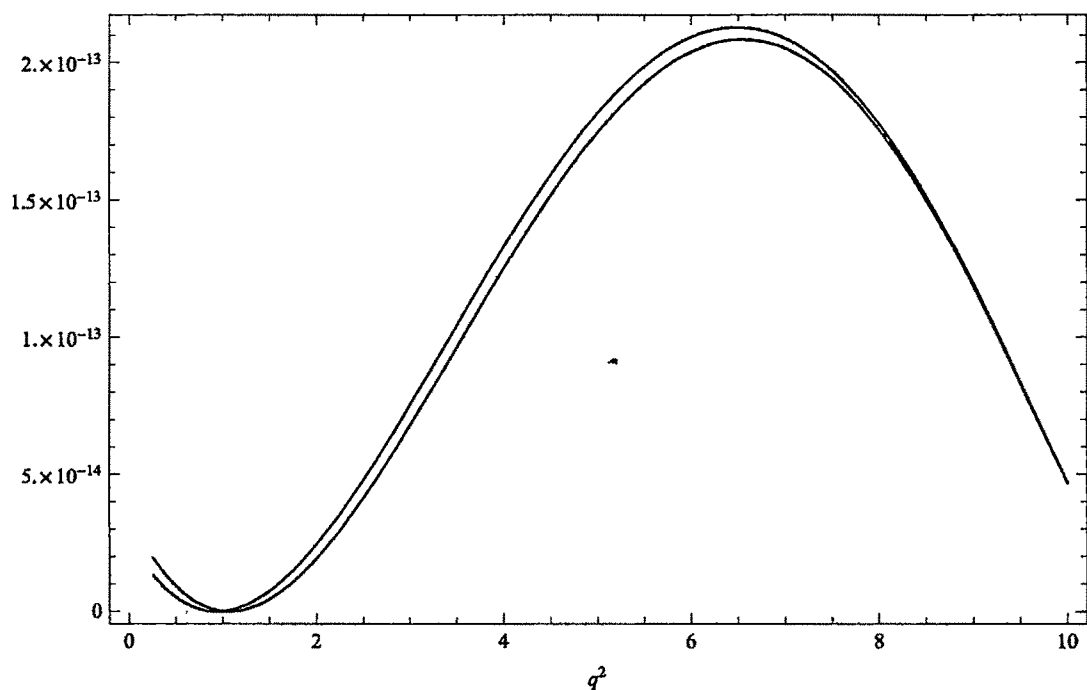


Figure 6.5: Differential decay rates $(1/|V_{cb}|^2)d\Gamma/dq^2$ of $B_c \rightarrow J/\psi ev$ (in GeV^{-1}) with linear part as perturbation. The red and blue curves correspond to $\Lambda = 382 MeV$ and $430 MeV$ respectively.

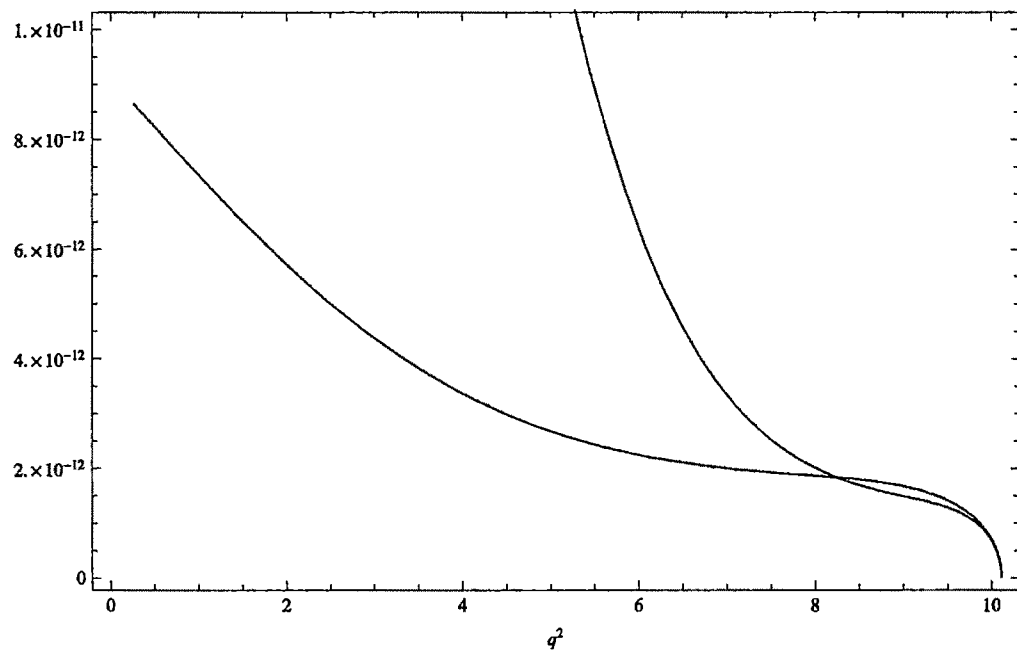


Figure 6.6: Differential decay rates $(1/|V_{cb}|^2)d\Gamma/dq^2$ of $B_c \rightarrow J/\psi \bar{e} \nu$ (in GeV^{-1}) with Coulombic part as perturbation. The red and blue curves correspond to $\Lambda = 382 \text{ MeV}$ and 430 MeV respectively.

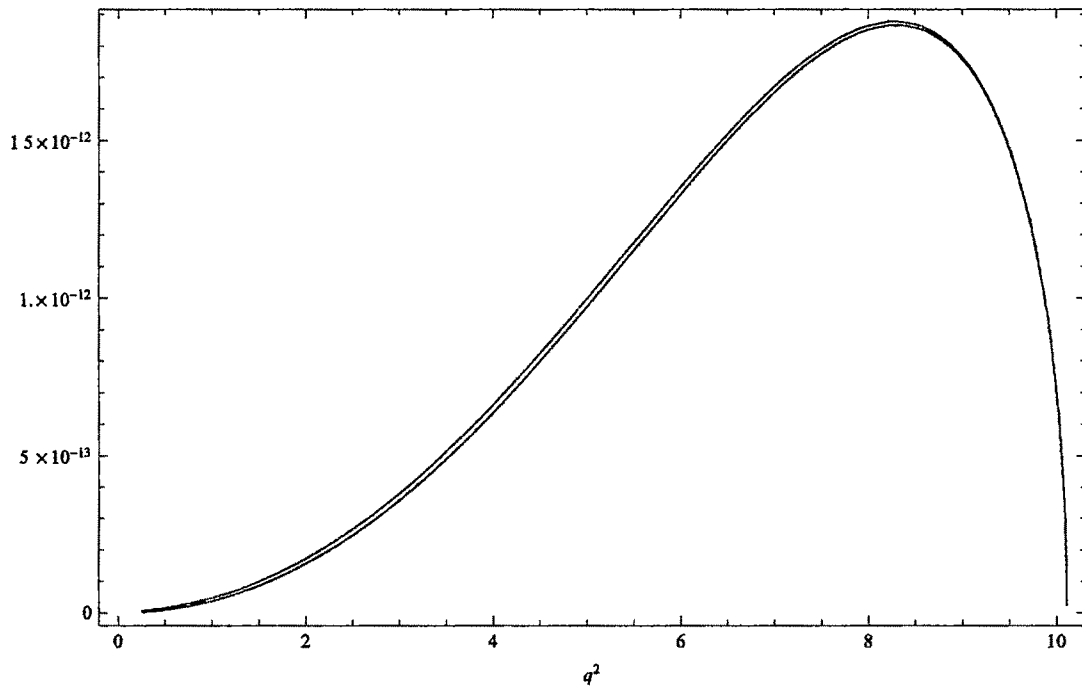


Table 6.3: Decay width for $B_c \rightarrow c\bar{c}(\ell^+ \nu_\ell)$ decay. In the braces “*linear*” means the result with linear part as perturbation and “*coul*” means Coulombic part as perturbation.

Channel	Decay width(Γ) $\times 10^{-15} \text{ GeV}$		Others
	$\Lambda = 382 \text{ MeV}$	$\Lambda = 430 \text{ MeV}$	
$B_c \rightarrow \eta_c(\ell^+ \nu_\ell)$	415 (linear) 1.8 (coul)	32 (linear) 1.7 (coul)	10.7 [219] 5.9 [221] 14.2 [248] 11.1 [225] 11 \pm 1 [249]
$B_c \rightarrow J/\psi(\ell^+ \nu_\ell)$	424 (linear) 15 (coul)	51 (linear) 14 (coul)	28.2 [219] 17.7 [221] 34.4 [248] 30.2 [225] 28 \pm 5 [249]

Table 6.4: Branching ratio for $B_c \rightarrow c\bar{c}(\ell^+\nu_\ell)$ decay. In the braces “*linear*” means the result with linear part as perturbation and “*coul*” means Coulombic part as perturbation.

Channel	Branching ratio(BR) $\times 10^{-2}$		Others
	$\Lambda = 382\text{MeV}$	$\Lambda = 430\text{MeV}$	
$B_c \rightarrow \eta_c(\ell^+\nu_\ell)$	28(linear) 0.12 (coul)	2.3(linear) 0.11 (coul)	0.81[220] 0.42[221] 0.76[225] 0.15[226] 0.51[227]
$B_c \rightarrow J/\psi(\ell^+\nu_\ell)$	29 (linear) 1.0 (coul)	3.5 (linear) 0.98(coul)	2.07[220] 1.23[221] 2.01[225] 1.47[226] 1.44[227]

The computed decay rates and branching ratios for the semileptonic decay of $B_c \rightarrow c\bar{c}(\ell^+\nu_\ell)$ shows that the results overshoot in case of linear part as perturbation and falls short with Coulombic part as perturbation. With Coulombic part as perturbation, the decay rate and branching ratio for $B_c \rightarrow J/\psi(\ell^+\nu_\ell)$ semileptonic decay give comparable results with that of Ref.[221] for both $\Lambda = 382\text{MeV}$ and $\Lambda = 430\text{MeV}$. However, with $\Lambda = 382\text{MeV}$ the numerical result is more comparable to that of Ref.[221] and we consider this small difference of decay rate for $\Lambda = 382\text{MeV}$ and $\Lambda = 430\text{MeV}$ significantly. This is because the smaller value of the QCD scale Λ in Eqn.3.18 provides a smaller value in α_s and hence weakens the Coulombic part of the potential to treat the latter as perturbation. Thus the results with $\Lambda = 382\text{MeV}$ for Coulombic part as perturbation is considered to be more comparable. This fact is even more clear when we check the status of perturbation in Table.6.5, where we show the dominance of parent term over the perturbation by comparing the numerical values for I-W function for the total wave function and parent term only. The result shows that, with linear part as perturbation the condition of $\xi_{total}(Y) > \xi_{parent}(Y)$ is sustained for a narrow range of Y ($1 \leq Y \leq 1.06$) where as with Coulombic part as perturbation the range of Y is quite large Y ($1 \leq Y \leq 1.22$).

Table 6.5: Variation of I-W function with total wavefunction and parent wavefunction only for $\Lambda = 382 \text{ MeV}$.

Y	Linear part as perturbation		Coulombic part as perturbation	
	$\xi_{total}(Y)$	$\xi_{parent}(Y)$	$\xi_{total}(Y)$	$\xi_{parent}(Y)$
1.01	0.916	0.509	0.962	0.959
1.06	0.848	0.772	0.773	0.757
1.08	0.9865	2.145	0.697	0.676
1.20	3.79	25.06	0.246	0.192
1.24	-	-	0.096	0.031

6.3 Results and Discussion

In this chapter, we have computed the slope and curvature of Isgur Wise function for B_c meson, considering the Coulombic part of the Cornell potential as perturbation in one approach and linear part as perturbation in the other. The numerical calculations are done for two different scales of QCD $\Lambda = 382 \text{ MeV}$ and $\Lambda = 430 \text{ MeV}$. The values of slope and curvature of the I-W function seems to be acceptable with Coulombic part as perturbation whereas with linear part as perturbation, the result overshoot the possible values. The former is also closer to the result of Ref.[235] obtained in a QCD relativistic potential model [250, 251]. For a slight lower value of $\Lambda_{QCD} < 382 \text{ MeV}$ ($\Lambda \approx 280 \text{ MeV}$), one can obtain the values of slope ρ^2 at par with the Ref.[235] ($\rho^2 = 2.9$), which lies outside the range.

Moreover, it conforms to the expectation of perturbation since with higher value of Λ , the coupling constant α_s increases making the Coulombic term of the potential more dominant to treat the linear part as perturbation. Similarly, with lower value of Λ (hence lower value of α_s), the Coulombic part of the potential becomes less dominant so as to be considered as perturbation.

To conclude, within the prescription of the strong coupling constant of Ref.[201, 137], the predicted behaviour of B_c meson is closer to typical heavy-light mesons like B and D ,

if the linear part of the potential is more dominant than the Coulombic part. It will be interesting to see if this feature is scheme invariant.

In a sense, the present work is complimentary to the work on leptonic decays (chapter 4), where $\Lambda_{QCD} = 200 \text{ MeV}$ was chosen with linear part as perturbation within the same prescription of running coupling constant [201, 137]. The apparent change of Λ_{QCD} (and hence equivalent strong coupling constant) in the present case is attributed to the decrease of available momentum transfer in semileptonic decays compared to leptonic ones.

Chapter 7

Summary and Outlook

The present work is devoted to a study of heavy and light flavoured pseudoscalar mesons in a QCD potential model. The model uses the non relativistic Schrödinger equation which is solved perturbatively and the first order wave function is obtained using Dalgarno's method [132]. Relativistic effects are then incorporated in the wave function by using standard Dirac modification in a parameter free way [133, 134]. The model is then used to calculate the masses, Leptonic decay constants and Isgur Wise function and its derivatives-the convexity parameter and charge radius of heavy and light flavoured pseudoscalar mesons. The results are compared with available experimental data and also with the predictions of other models.

In chapter 2, we have calculated the masses and pseudoscalar decay constants of D , D_s and B_c mesons using the QCD potential model. The singularity of the wavefunction at the origin was removed by introducing a short distance scale r_0 in analogy with QED. For strong coupling constant α_s , we use the standard values in \overline{MS} scheme- $\alpha_{\overline{MS}}(m_c) = 0.39$ and $\alpha_{\overline{MS}}(m_b) = 0.22$ [140] at the scale of the c quark and b quark masses $m_c = 1.55\text{GeV}$ and $m_b = 4.88\text{GeV}$ [252] respectively. The results are found to be in good agreement with the experimental and theoretical results. However, with \overline{MS} scheme, the results of B and B_s mesons fall short in comparison with the other theoretical results. This aspect requires

further study and modifications in the model.

The force between a heavy quark and a heavy/light quark is due to the static quark antiquark potential, since the heavy quark is static with respect to the light quark. An important ingredient of phenomenological models is the proper choice of the running of the coupling constant α_s , which we discuss in following chapters.

In chapter 3, we have reported the results of masses and decay constants of B and B_s mesons by incorporating a scale dependent α_s of Ref.[201, 137] (Eqn.3.18) which is different from the standard \overline{MS} scheme. We have also reported the oscillation frequencies of B and B_s mesons and compare the results with the experimental results.

In chapters 2 and 3, we used the non-relativistic Van-Royen formula to compute the decay constants of pseudoscalar heavy-light mesons where the cut-off scale r_0 is required to remove the singularity of the wavefunction at the origin. However, we are unable to explain the origin of such a scale and an alternate way of finding the decay constants without such a scale becomes important for the model.

In chapter 4, we have studied the consequences of applying the scale dependent α_s by computing decay constants of D and B mesons together in Eqn.4.7 with its relativistic effect. This formula however, does not carry any singular terms and the need of a cut-off scale r_0 was removed from the wave-function. In this study, the renormalisation scale was set to be $\Lambda_{QCD} = 200 \text{ MeV}$

In chapter 5, we have studied the semileptonic decay of heavy-light mesons and computed the CKM element V_{cb} in the QCD potential model. We have found in this analysis that a further increment of α_s is required to obtain the experimental branching ratio. We also compute an allowed range of Λ ($382 \text{ MeV} \leq \Lambda \leq 430 \text{ MeV}$) from the theoretical bound of I-W function [202, 203] and obtain a range for V_{cb} ($0.0375 \leq |V_{cb}| \leq 0.0410$).

In chapter 6, we explored the possibility of treating B_c meson as a typical heavy-light meson like B or D within a QCD potential model, considering the Coulombic part as perturbation in one approach and linear part as perturbation in the other. As in chapter-5, we

have taken the prescription of the strong coupling constant given by Eqn.3.18 with Λ_{QCD} constrained in the range $382 \text{ MeV} \leq \Lambda_{QCD} \leq 430 \text{ MeV}$.

When one chooses the perturbative term, there should be an underlying assumption that perturbative term should not have dominant impact, otherwise the result is not stable. To that end, we have calculated the I-W function for a different Y with contribution of linear parent and Coulomb parent alone for $\Lambda = 382 \text{ MeV}$ and $\Lambda = 430 \text{ MeV}$. We see that both the process of perturbative is viable for a different range of Y . The linear parent dominates within the range $1 \leq Y \leq 1.22$ where as Coulombic parent dominates very near to zero recoil ($1 \leq Y \leq 1.06$, refer Table.6.5). It indicates that the former one is perturbatively more stable than the latter (which is marginally stable). For Coulombic part to be progressively stable, one would expect a large scale of $\Lambda > 430 \text{ MeV}$ (or equivalently larger strong coupling constant) beyond the theoretical constraint discussed in this work. The reality condition of the model parameter (Eqn.2.19), however permits us to consider $\alpha_s(\mu) \leq 3/4$ and hence $\Lambda \leq 460 \text{ MeV}$ is the allowed limit in the model.

The necessity of two scales of Λ_{QCD} (or equivalent two scales of strong coupling constant) for heavy-light mesons was noticed earlier within V-scheme[122; 123] in Ref.[121] with linear term as perturbation. The present work too conforms to this conclusion in the scheme of Ref.[201, 137] and hence appears to be a scheme invariant feature of the potential.

To summarise, an work in the context of the QCD potential model suggests a two scale picture of the strong coupling constant to accommodate both the leptonic and semileptonic decays of heavy-light mesons with the model parameters $c = -0.4 \text{ GeV}$, $b = 0.183 \text{ GeV}^2$, $n_f = 3$, $m_{u,d} = 0.336 \text{ GeV}$, $m_s = 0.465 \text{ GeV}$, $m_c = 1.55 \text{ GeV}$, $m_b = 4.97 \text{ GeV}$ and $cA_0 = 1 \text{ GeV}^{3/2}$.

Let us now discuss the future scope of the present work. In chapter 5 and 6, we have taken the experimental masses of pseudoscalar mesons to study the semileptonic decays since, the same mass input parameters and c (as is used in chapter 2,3 and 4) cannot

reproduce the experimental masses or nearest to the experimental masses. This, in fact arises due to the two scale pictures of Λ in leptonic decay and semileptonic decay. With the same mass input parameters, however with a different scale of c ($c = 0.02$ GeV and $\Lambda_{QCD} = 410$ MeV), we can reproduce a satisfactory results for masses (Ref. Appendix.D). Thus a question arises that in this two scale picture where shall we put the mass, in $\Lambda_{QCD} = 200$ MeV or in the range 382 $MeV \leq \Lambda \leq 430$ MeV or in an average of both the two scales? This needs attention in future.

In this work, spin-spin interactions which give mass splitting between pseudoscalar and vector mesons have been neglected since we have studied only pseudoscalar mesons. We have also not considered the orbitally and radially excited states of heavy-light mesons in this work. Properties of these mesons will be an important area of study in future.

In this work, we are also unable to use the relativistic Hamiltonian in the perturbation procedure of Dalgarno method, which in fact seems to be necessary for at least the light quark in the $q\bar{q}$ states. The model can be studied with a relativistic or semi-relativistic Hamiltonian not only with the Dalgarno method of perturbation but also in VIPT(Variationally Improved perturbation theory)[239, 253], WKB approximation (Wentzel-Kramers-Brillouin) [133] and FLZ(Friedberg-Lee and Zhao)[254] method of perturbation.

In the future, it will also be interesting to explore the feasibility of applying and renovating the model to study baryons, pentaquarks, glueballs and other exotic hadrons which have received attention in recent years [255, 256, 257].

Appendix A

Calculation of the wavefunction with linear part as perturbation

The Coulomb plus linear potential is given by

$$V(r) = -\frac{4\alpha_s}{3r} + br + c \quad (\text{A.1})$$

The first order perturbed eigenfunction $\psi^{(1)}$ and first order eigenenergy $W^{(1)}$ using quantum mechanical perturbation theory (Dalgarno's method) can be obtained using the relation

$$H_0\psi^{(1)} + H'\psi^{(0)} = W^{(0)}\psi^{(1)} + W^{(1)}\psi^{(0)}, \quad (\text{A.2})$$

where

$$W^{(1)} = \langle \psi^{(0)} | H' | \psi^{(0)} \rangle. \quad (\text{A.3})$$

and

$$H' = br + c \quad (\text{A.4})$$

Then from (A.2),

$$(H_0 - W^{(0)})\psi^{(1)} = (W^{(1)} - H')\psi^{(0)}, \quad (\text{A.5})$$

Putting

$$A = \frac{4\alpha_s}{3}, \quad (\text{A.6})$$

we obtain

$$H_0 = -\frac{\hbar^2}{2r} \nabla^2 - \frac{A}{r}, \quad (\text{A.7})$$

$$\begin{aligned} W^{(0)} &= -\frac{\mu A^2}{2} \\ &= -\frac{8\mu\alpha_s^2}{9} \end{aligned} \quad (\text{A.8})$$

and

$$\begin{aligned} \psi^{(0)} &= \frac{1}{\sqrt{\pi}} (\mu A)^{\frac{3}{2}} e^{-\mu Ar} \\ &= \frac{1}{\sqrt{\pi a_0^3}} e^{-\frac{r}{a_0}}. \end{aligned} \quad (\text{A.9})$$

where $\psi^{(0)}$ is the unperturbed wave function in the zeroth order of perturbation and a_0 is given by equation . Also, we put $W = W^{(1)}$, where

$$W^{(1)} = \int \psi_{100}^* H' \psi_{100} d\tau \quad (\text{A.10})$$

Then taking $\hbar^2 = 1$, equation (A.5) =>

$$\begin{aligned} \left(-\frac{1}{2\mu} \nabla^2 - \frac{A}{r} + \frac{\mu A^2}{2} \right) \psi^{(1)} &= (W - br - c) \frac{1}{\sqrt{\pi}} (\mu A)^{\frac{3}{2}} e^{-\mu Ar} \\ \rightarrow \left(\nabla^2 + \frac{2\mu A}{r} - \mu^2 A^2 \right) \psi^{(1)} &= \frac{2\mu}{\sqrt{\pi}} (\mu A)^{\frac{3}{2}} (br + c - W) e^{-\mu Ar} \\ \rightarrow \left(\nabla^2 + \frac{2}{a_0 r} - \frac{1}{a_0^2} \right) \psi^{(1)} &= \frac{2\mu}{\sqrt{\pi a_0^3}} (br + c - W) e^{-\frac{r}{a_0}} \end{aligned} \quad (\text{A.11})$$

Let

$$\psi^{(1)} = (br + c)R(r) \quad (\text{A.12})$$

$$(A.11) \Rightarrow \left(\frac{d^2}{dr^2} + \frac{2}{r} \frac{d}{dr} + \frac{2}{a_0 r} - \frac{1}{a_0^2} \right) (br + c)R(r) = D(br + c - W)e^{-\frac{r}{a_0}} \quad (\text{A.13})$$

where we put

$$D = \frac{2\mu}{\sqrt{\pi a_0^3}}. \quad (\text{A.14})$$

Now,

$$\frac{d}{dr}(br + c)R(r) = br + (br + c)\frac{dR}{dr} \quad (\text{A.15})$$

$$\frac{d^2}{dr^2}(br + c)R(r) = (br + c)\frac{d^2R}{dr^2} + 2b\frac{dR}{dr} \quad (\text{A.16})$$

Using (A.15) and (A.16) in (A.13), we obtain

$$\begin{aligned} (br + c)\frac{d^2R}{dr^2} + 2b\frac{dR}{dr} + \frac{2bR}{r} + \frac{2}{r}(br + c)\frac{dR}{dr} + \frac{2}{a_0}(br + c)R(r) - \frac{1}{a_0^2}(br + c)R(r) \\ = D(br + c - W)e^{-\frac{r}{a_0}} \quad (\text{A.17}) \end{aligned}$$

Putting

$$R(r) = F(r)e^{-\frac{r}{a_0}} \quad (\text{A.18})$$

$$\frac{dR}{dr} = F'e^{-\frac{r}{a_0}} - \frac{1}{a_0}F(r)e^{-\frac{r}{a_0}} \quad (\text{A.19})$$

$$\frac{d^2R}{dr^2} = F''(r)e^{-\frac{r}{a_0}} - \frac{2}{a_0}F'(r)e^{-\frac{r}{a_0}} + \frac{1}{a_0^2}F(r)e^{-\frac{r}{a_0}} \quad (\text{A.20})$$

$$\begin{aligned} (A.17) \Rightarrow (br + c) \left\{ F''(r) - \frac{2}{a_0}F'(r) + \frac{1}{a_0^2}F(r) \right\} + 2b \left\{ F'(r) - \frac{1}{a_0}F(r) \right\} \\ + \frac{2b}{r}F(r) + \frac{2}{r}(br + c) \left\{ F'(r) - \frac{1}{a_0}F(r) \right\} + \frac{2}{a_0 r}(br + c)F(r) \\ - \frac{1}{a_0^2}(br + c)F(r) = D(br + c - W) \quad (\text{A.21}) \end{aligned}$$

$$\begin{aligned} \Rightarrow (br + c)F''(r) + \left\{ 2b + \frac{2}{r}(br + c) - \frac{2}{a_0}(br + c) \right\} F'(r) \\ + \left(\frac{2b}{r} - \frac{2b}{a_0} \right) F(r) = D(br + c - W) \end{aligned} \quad (\text{A.22})$$

Let

$$F(r) = \sum_{n=0}^{\infty} A_n r^n \quad (\text{A.23})$$

Then,

$$F'(r) = \sum_{n=0}^{\infty} n A_n r^{n-1} \quad (\text{A.24})$$

and

$$F''(r) = \sum_{n=0}^{\infty} n(n-1) A_n r^{n-2} \quad (\text{A.25})$$

$$\begin{aligned} (\text{A.22}) \Rightarrow (br + c) \sum_{n=0}^{\infty} n(n-1) A_n r^{n-2} + \left\{ 2b + \frac{2}{r}(br + c) \right. \\ \left. - \frac{2}{a_0}(br + c) \right\} \sum_{n=0}^{\infty} n A_n r^{n-1} + \left(\frac{2b}{r} - \frac{2b}{a_0} \right) \sum_{n=0}^{\infty} A_n r^n = D(br + c - W) \end{aligned} \quad (\text{A.26})$$

$$\begin{aligned} \Rightarrow \left\{ c \sum_{n=0}^{\infty} n(n-1) A_n + 2c \sum_{n=0}^{\infty} n A_n \right\} r^{n-2} + \left\{ b \sum_{n=0}^{\infty} n(n-1) A_n + 4b \sum_{n=0}^{\infty} n A_n - \right. \\ \left. \frac{2c}{a_0} \sum_{n=0}^{\infty} n A_n + 2b \sum_{n=0}^{\infty} A_n \right\} r^{n-1} + \left(-\frac{2b}{a_0} \sum_{n=0}^{\infty} n A_n - \frac{2b}{a_0} \sum_{n=0}^{\infty} A_n \right) r^n \\ = D(br + c - W) \end{aligned} \quad (\text{A.27})$$

Equating coefficients of r^{-1} on both sides of the above identity (A.27),

$$2cA_1 + 2bA_0 = 0 \quad (\text{A.28})$$

$$\implies (cA_1 + bA_0) = 0 \quad (\text{A.29})$$

Equating coefficients of r^0 on both sides of the identity (A.27),

$$2cA_2 + 4cA_2 + 4bA_1 - \frac{2c}{a_0}A_1 + 2bA_1 - \frac{2b}{a_0}A_0 = D(c - W) \quad (\text{A.30})$$

$$\implies 6(cA_2 + bA_1) - \frac{2}{a_0}(cA_1 + bA_0) = D(c - W) \quad (\text{A.31})$$

$$\implies cA_2 + bA_1 = \frac{1}{6}D(c - W) \quad (\text{A.32})$$

Equating coefficients of r^1 on both sides of the identity (A.27),

$$12cA_3 + 12bA_2 - \frac{4c}{a_0}A_2 - \frac{4b}{a_0}A_1 = Db \quad (\text{A.33})$$

$$\implies 12(cA_3 + bA_2) - \frac{4}{a_0}(cA_2 + bA_1) = Db \quad (\text{A.34})$$

Using (A.32),

$$12(cA_3 + bA_2) - \frac{2}{3a_0}D(c - W) = Db \quad (\text{A.35})$$

$$\implies cA_3 + bA_2 = \frac{D}{12} \left\{ b + \frac{2}{3a_0}D(c - W) \right\} \quad (\text{A.36})$$

Equating coefficients of r^2 on both sides of the identity (A.27),

$$20(cA_4 + bA_3) - \frac{6}{a_0}(cA_3 + bA_2) = 0 \quad (\text{A.37})$$

Using (A.36),

$$cA_4 + bA_3 = \frac{D}{120a_0} \left\{ b + \frac{2}{3a_0}D(c - W) \right\} \quad (\text{A.38})$$

From (A.23),

$$F(r) = A_0r^0 + A_1r^1 + A_2r^2 + A_3r^3 + A_4r^4 + \dots \quad (\text{A.39})$$

Also, from (A.12) and (A.18),

$$\begin{aligned}
 \psi^{(1)} &= (br + c)F(r)e^{-\frac{r}{a_0}} \\
 &= (br + c)(A_0 r^0 + A_1 r^1 + A_2 r^2 + A_3 r^3 + A_4 r^4 + \dots)e^{-\frac{r}{a_0}} \\
 &= \left\{ cA_0 r^0 + (cA_1 + bA_0) r^1 + (cA_2 + bA_1) r^2 + (cA_3 + bA_2) r^3 \right. \\
 &\quad \left. + (cA_4 + bA_3) r^4 + \dots \right\} e^{-\frac{r}{a_0}} \tag{A.40}
 \end{aligned}$$

Applying (A.29), (A.32), (A.36) and (A.38) to (A.40)

$$\begin{aligned}
 \psi^{(1)} &= \left[cA_0 + \frac{1}{6}D(c - W)r^2 + \frac{D}{12} \left\{ b + \frac{2}{3a_0}D(c - W) \right\} r^3 \right. \\
 &\quad \left. + \frac{D}{120a_0} \left\{ b + \frac{2}{3a_0}D(c - W) \right\} + \dots \right] e^{-\frac{r}{a_0}} \tag{A.41}
 \end{aligned}$$

Again, from (A.10),

$$\begin{aligned}
 W &= \int \psi_{100}^*(br + c)\psi_{100} d\tau \\
 &= \frac{1}{\pi a_0^3} \int_0^\infty (br + c)e^{-\frac{2r}{a_0}} r^2 dr \int_0^\pi \sin \theta d\theta \int_0^{2\pi} d\phi \\
 &= \frac{4}{a_0^3} \left[b \int_0^\infty r^3 e^{-\frac{2r}{a_0}} dr + c \int_0^\infty r^2 e^{-\frac{2r}{a_0}} dr \right] \\
 &= \frac{4}{a_0^3} \left[b \frac{6a_0^4}{16} + c \frac{2a_0^3}{8} \right] \\
 &= \frac{3}{2}ba_0 + c \tag{A.42}
 \end{aligned}$$

Hence

$$b + \frac{2}{3a_0}D(c - W) = 0 \tag{A.43}$$

Therefore, (A.41) reduces to

$$\begin{aligned}
 \psi^{(1)} &= \left\{ cA_0 + \frac{1}{6}D(c - \frac{3}{2}ba_0 - c)r^2 \right\} e^{-\frac{r}{a_0}} \\
 &= \left\{ cA_0 - \frac{1}{4}Db a_0 r^2 \right\} e^{-\frac{r}{a_0}} \\
 &= \left\{ cA_0 - \frac{\mu b a_0}{2\sqrt{\pi a_0^3}} r^2 \right\} e^{-\frac{r}{a_0}}
 \end{aligned} \tag{A.44}$$

where A_0 is an undeterminable factor appearing in the series solution of the differential equation. Hence, the total wave function correct upto first order of perturbation using Dalgarno's method is given by

$$\psi_1^{(1)} = \psi^{(0)} + \psi^{(1)}$$

where $\psi^{(0)}$ and $\psi^{(1)}$ are given by equations (A.9) and (A.44) respectively. Therefore,

$$\psi_1^{(1)}(r) = \frac{1}{\sqrt{\pi a_0^3}} \left\{ 1 + cA_0 \sqrt{\pi a_0^3} - \frac{1}{2} \mu b a_0 r^2 \right\} e^{-\frac{r}{a_0}} \tag{A.45}$$

Putting

$$C'(c) = 1 + cA_0 \sqrt{\pi a_0^3} \tag{A.46}$$

we have finally

$$\psi_1^{(1)}(r) = \frac{1}{\sqrt{\pi a_0^3}} \left(C'(c) - \frac{1}{2} \mu b a_0 r^2 \right) e^{-\frac{r}{a_0}} \tag{A.47}$$

Appendix B

Derivation of Van Royen

formula(Eqn.2.24) in chapter 2

We give a short derivation to show how the factor $\psi(0)$ enters the matrix element for the annihilation of a bound state. The creation operator for a bound system of a quark-antiquark pair

$$d_m^*(0) = \sum \int d^3 p f(p) \psi(r, s) a_r^*(p) b_s^*(-p) \quad (B.1)$$

where $d_m^*(0)$ describes the creation operator for the meson of zero momentum and $a_r^*(p) b_s^*(-p)$ the quark and antiquark with spin-unitarity spin components r,s. $f(p)$ is the bound state wavefunction and the normalisation requires

$$\int d^3 p |f(p)|^2 = 1 \quad (B.2)$$

Now $(2\pi)^{3/2} d_M^*(0) |0\rangle$ is the correct normalised state vectors to calculate the decay of the meson if we require that there is one particle per unit volume. The amplitude for the annihilation is then

$$A = (2\pi)^{3/2} \langle 0 | H_{int} d_M^*(0) \rangle = (2\pi)^{3/2} \sum \int d^3 p f(p) \psi(r, s) \langle 0 | H_{int} a_r^*(p) b_s^*(-p) \rangle. \quad (B.3)$$

If the quarks move nonrelativistically in the bound state, then we can make a series expansion of the matrix element in p and keep only the leading term, i.e.

$$\langle 0 | H_{int} a_r^*(p) b_s^*(0) \rangle. \quad (\text{B.4})$$

we then find

$$A \simeq (2\pi)^{3/2} \sum \int d^3 p f(p) \psi(r, s) \langle 0 | H_{int} a_r^*(p) b_s^*(0) \rangle. \quad (\text{B.5})$$

Now from

$$\psi(r) = \frac{1}{(2\pi)^{3/2}} \int f(p) \exp[ipr] d^3 p \quad (\text{B.6})$$

it follows then that

$$A \simeq (2\pi)^3 \psi(0) \sum \psi(r, s) \langle 0 | H_{int} a_r^*(p) b_s^*(0) \rangle. \quad (\text{B.7})$$

For mesons with zero spin the interaction Hamiltonian contributes only from its axial vector part and then this matrix elements are of the form

$$A = G_A \psi_m(0) \sqrt{2} (\cos\theta, \sin\theta) \bar{u}_l(p) \gamma_0 (1 + \gamma_5) u_\nu(-p) \quad (\text{B.8})$$

Here $\cos\theta$ stands for strangeness conserving, $\sin\theta$ stands for strangeness changing transitions.

It is interesting to compare this matrix element with the phenomenological one which is usually used for these reactions. One writes

$$A = G_\nu f_m(\cos\theta, \sin\theta) \frac{p_\alpha}{\sqrt{2p_0}} \bar{u}_l(p) \gamma_0 (1 + \gamma_5) u_\nu(-p) \quad (\text{B.9})$$

Where p_α is the momentum four vector of the meson and f_m is a constant with the dimension of mass. Comparing the above equations we get the decay constant

$$f_m = \frac{G_A}{G_\nu} 2 \frac{\psi_m(0)}{m^{\frac{1}{2}}} = 1.4 \frac{\psi_m(0)}{m^{\frac{1}{2}}} \quad (\text{B.10})$$

Appendix C

Derivation of Eqn. 2.23 from Eqn.4.7

Here, we show how the non relativistic limit of Eqn.4.7 reproduce Eqn.2.23.

From Eqn.4.7, we get

$$f_P = \sqrt{\frac{12}{M_P}} \int \frac{d^3 p}{(2\pi)^3} \left(\frac{E_q + m_q}{2E_q} \right)^{1/2} \left(\frac{E_{\bar{q}} + m_{\bar{q}}}{2E_{\bar{q}}} \right)^{1/2} \left(1 + \lambda_P \frac{p^2}{[E_q + m_q][E_{\bar{q}} + m_{\bar{q}}]} \right) \psi_P(p) \quad (C.1)$$

We know from the relativistic formula of energy,

$$E_q^2 = p^2 c^2 + m^2 c^4. \quad (C.2)$$

In the natural unit $c=1$,

$$E_q = \sqrt{p^2 + m^2} \quad (C.3)$$

In the non-relativistic limit $m^2 \gg p^2$,

$$E_q = \sqrt{m^2} = m. \quad (C.4)$$

Now replacing $E_q = m_q$ and $E_{\bar{q}} = m_{\bar{q}}$ and $\lambda_P = -1$ for pseudoscalar meson in Eq. C.1

$$f_P = \sqrt{\frac{12}{M_P}} \int \frac{d^3 p}{(2\pi)^3} \left(\frac{m_q + m_{\bar{q}}}{2m_q} \right)^{1/2} \left(\frac{m_{\bar{q}} + m_{\bar{q}}}{2m_{\bar{q}}} \right)^{1/2} \left(1 - \frac{p^2}{[m_q + m_{\bar{q}}][m_{\bar{q}} + m_{\bar{q}}]} \right) \psi_P(p). \quad (\text{C.5})$$

Neglecting the last term in the non-relativistic limit $\frac{p^2}{m^2} \rightarrow 0$, we get

$$f_P = \sqrt{\frac{12}{M_P}} \int \frac{d^3 p}{(2\pi)^3} \psi_P(p). \quad (\text{C.6})$$

Again from the Fourier transformation

$$\psi(r) = \frac{1}{(2\pi)^{3/2}} \int \psi(p) \exp[ipr] d^3 p \quad (\text{C.7})$$

putting $r = 0$, we get

$$2\pi^{3/2} \psi(0) = \int \psi(p) d^3 p. \quad (\text{C.8})$$

Hence from Eq.C.6 and Eq.C.8, we obtain the Eq.2.24

$$f_P = \sqrt{\frac{12}{M_P} |\psi(0)|^2}. \quad (\text{C.9})$$

Appendix D

Masses of heavy-light mesons with

$$\Lambda_{QCD} = 410 \text{ MeV}$$

Here, we tabulate the computed masses of heavy-light mesons for $\Lambda = 410 \text{ MeV}$ with $c = 0.02 \text{ GeV}$ and $cA_0 = 1 \text{ GeV}^{3/2}$

Table D.1: Masses of heavy-light mesons in this work with $m_d = 0.336 \text{ GeV}$, $m_s = 0.465 \text{ GeV}$, $m_c = 1.55 \text{ GeV}$, $m_b = 4.97 \text{ GeV}$ and comparison with experimental data. All values are in units of MeV.

Mesons	Present work	Experimental masses[37]
$D(c\bar{u}/c\bar{d})$	1873.02	1869.6 ± 0.16
$D(c\bar{s})$	1674.20	1968 ± 0.33
$B_u(b\bar{u})$	5271.55	5279 ± 0.29
$B_s(b\bar{s})$	5340.20	5366 ± 0.6
$B_c(b\bar{c})$	6566.12	6277 ± 0.6

Bibliography

- [1] J.J. Thomson, in "Cathode rays", *Philosophical Magazine* **44**:293, (1897).
- [2] J. Beringer *et al.*, (Particle Data Group), *Phys. Rev. D* **86**:010001, (2012).
- [3] Alan Boyle, *NBC News.com-cosmic log*. Retrieved 20 February 2013.
- [4] Lucas Taylor in *Observation of a New Particle with a Mass of 125 GeV. CMS Public Website. CERN*. Retrieved 4 July 2012.
- [5] ATLAS Collaboration, *ATLAS-CONF-2012-093*, July 5, (2012).
- [6] M. Gell-Mann, *Phys. Lett.* **8**:214, (1964).
- [7] G. Zweig, CERN Report No. TH 412 (Geneva, 1964).
- [8] G. Zweig, *Fractionally Charged particles and SU₆ in symmetries in elementary particle physics*, Academic Press, New York, (1962), p.192.
- [9] N. Cabibbo, *Phys. Rev. Lett.* **10**:531, (1963).
- [10] M. Kobayashi and T. Masakawa, *Prog. Theor. Phys.* **49**:652, (1973).
- [11] L. Wolfenstein, *Phys. Rev. Lett.* **51**:1945, (1983).
- [12] M. Bona *et al.*, JHEP (UTfit Collaboration), **0803**:049, (2008).
- [13] Gernot A. Weber, in the Thesis entitled "Measurement of the Oscillation Frequency of B_s Mesons in the Hadronic Decay Mode $B_s \rightarrow \pi D_s(\phi\pi)X$ with the D0 Detector at the Fermilab Tevatron Collider", Johannes Gutenberg-University, (2009).
- [14] M. Okamoto, *POS,LAT2005*, p.013, (2005).
- [15] A. Pais, *Inward Bound* (Oxford University Press, Oxford), pp. 142-161 and pp. 309-323, (1986).

- [16] J. D. Richman and Patricia R. Burchat, *Review of Modern Physics*, **64**: no.4, pp-893-976, (1995).
- [17] P. Renton, *Interactions (Cambridge University Press, New York), 1990.*
- [18] F.J. Gilman and R. L. Singleton, *Phys.Rev.* **D41**:93, (1990).
- [19] K. Hagiwara, A. D. Martin and J. F. Wade, *Nucl.Phys.* **B327**:569, (1989).
- [20] H. Georgi, *Phys. Lett.* **B240**:447, (1990).
- [21] M. Neubert, *Phys. Rep.*, **245**:259, (1994).
- [22] S. S. Gershtein and M. Yu. Khlopov, *Pisma v ZhETF* **23**:374 (1976) [English translation: *JETP Lett.* **23**, 338 (1976)].
- [23] M. Yu. Khlopov, *Sov.J.Nucl.Phys.* **28**:583, (1978).
- [24] R. Van Royen and V.F. Weisskopff. *Nuovo Cimento*, **50A**:617, (1967).
- [25] E. Braaten and S. Fleming, *Phys. Rev* **D52**:181, (1995).
- [26] D. Ebert, R.N. Faustov and V.O. Galkin, preprint HUB-EP-96-67, HEP-ph/9701218.
- [27] F. E. Close and A. Wambach, *Nucl.Phys.* **B412**:169, (1994).
- [28] C. Amsler *et al.*, (*Particle data group*), *Phys. Lett.* **B1**: (2008).
- [29] E. Follana *et al.*, (*HPQCD Collaboration and UKQCD Collaboration*), *Phys. Rev. Lett.* **100**:062002, 2008).
- [30] L. S. Geng, M. Altenbuchinger and W. Weise, arXiv:hep-ph/1012.0666,(2010).
- [31] W. S. Hou, *Phys. Rev.* **D48**:2342, (1993).
- [32] A. G. Akeroyd, *Prog. Theor. Phys.* **111**:295, (2004).

- [33] P. U. E. Onyisi *et al.*, (*CLEO Collaboration*), *Phys. Rev.* **D79**:052002, (2009).
- [34] P. Naik *et al.*, (*CLEO Collaboration*), *Phys. Rev.* **D80**:112004, (2009).
- [35] J. P. Lee *et al.*, (*The BABAR Collaboration*), arXiv:hep/ex-1003.3063 (2010).
- [36] L. Widhalm *et al.*, (*Belle Collaboration*), *Phys. Rev. Lett.* **100**:241801, (2008).
- [37] K. Nakamura *et al.*, (*Particle Data Group*), *J. Phys.* **G37**:075021, (2010).
- [38] S. Dimopoulos and H. Georgi, *Nucl. Phys.* **B193**:150, (1981).
- [39] H. P. Nilles, *Phys. Rept.* **110**:1, (1984).
- [40] S. P. Martin, *arXiv:hep-ph/9709356*, (1997).
- [41] J.H. Christenson *et al.*, *Phys. Rev. Lett.* **13**:138, (1964).
- [42] B. Aubert *et al.*, [*BABAR Collab.*], *Phys. Rev. Lett.* **87**:091801, (2001).
- [43] K. Abe *et al.*, [*Belle Collab.*], *Phys. Rev. Lett.* **87**:091802, (2001).
- [44] Tatsuya Nakada *arXiv:HEP-Ex/9502005*, (1995)
- [45] M. Bauer and B. Stech, *Phys. Lett.* **B152**:380, (1985).
- [46] M. Bauer, B. Stech and M. Wirbel, *Z. Phys.* **C34**:103, (1987).
- [47] H.Y. Cheng, *Phys. Lett.* **B335**:428, (1994).
- [48] J.M. Soares, *Phys. Rev.* **D51**:3518, (1995).
- [49] A. Le Yaouanc, *et al.*, *Phys. Rev.* **D52**:2813, (1995).
- [50] Yosef Nir, *arXiv:HEP-ph/950729*, (1995).
- [51] J.C. Anjos *et al.*, *Phys. Rev. Lett.* **60**:1239, (1988).

- [52] *IJHEP, CERN COURIER* Vol53, No.5, p-07, (2013).
- [53] D. J. Gross and F. Wilczek, *Phys. Rev. Lett.* **30**(26):13431346, (1973).
- [54] D. J. Gross, *Nucl. Phys.* **B74**:426446 (1998)-Proceedings Supplements.
- [55] K. G. Wilson, *Phys. Rev.*, **D10**:2445, (1974).
- [56] A. M. Polyakov, *Phys. Lett.*, **B59**:79, (1975).
- [57] A. M. Polyakov, *Phys. Lett.*, **B59**:82, (1975).
- [58] F. J. Wegner, *J. Math. Phys.*, **12**:2259, (1971).
- [59] H. J. Rothe, *World Sc. Lect. Notes. Phys.*, **59**:1, (1997).
- [60] A. S. Kronfeld, hep-lat/0205021.
- [61] M. Müller-Preussker *et al.*, Proc. 19th Int. Symp. Lattice 2001, Berlin, Germany. (2001).
- [62] E. V. Shuryak, *Nucl. Phys.*, **B198**:83, (1982).
- [63] B. Stech, M. Wirbel and M. Bauer, *Z. Phys.*, **C29**:637, (1985).
- [64] S. J. Brodsky and G. P. Lepage, *Phys. Rev.*, **D22**:2157, (1980).
- [65] A. Vainshtein, M. Shifman and V. Zakharov, *Nucl. Phys.*, **B147**:385, (1979).
- [66] E. Jenkins, arXiv:hep-ph/9212295.
- [67] F. E. Close, *An introduction to Quarks and Partons*. Academic Press, London, (1979).
- [68] N. Isgur and G. Karl, *Phys. Lett.*, **B72**:109, (1977).
- [69] N. Isgur and G. Karl, *Phys. Lett.*, **B74**:353, (1978).

- [70] N. Isgur and G. Karl, *Phys.Rev.*, **D18**:4187, (1978).
- [71] N. Isgur and G. Karl, *Phys.Rev.*, **D19**:2653, (1979).
- [72] G. Karl, N. Isgur and R. Koniuk, *Phys.Rev.Lett.*, **41**:1269, (1978).
- [73] N. Isgur and G. Karl, *Phys.Rev.*, **D20**:1191, (1979).
- [74] F. F. Schoberl W. Luchat and D. Gromes, *Phys.Rept.*, **200**:127–240, (1999).
- [75] H. Georgi, A. De Rujula and S. L. Glashow, *Phys.Rev.*, **D12**:147, (1975).
- [76] P. Mathews, K. Sridhar and R. Basu, *Phys. Rev.* **D60**:014009, (1999).
- [77] Chin-Wen Hwang and Zheng-Tao Wei, *J.Phys.* **G34**:687, (2007).
- [78] B. A. Thacker and G. P. Lepage, *Phys. Rev.* **D43**:196, (1991).
- [79] W. E. Caswell and G. P. Lepage, *Phys. Lett.* **B167**:437, (1986).
- [80] G. T. Bodwin, E. Braaten and G. P. Lepage, *Phys. Rev.* **D51**:1125, (1995)
- [81] A. V. Manohar. *Phys. Rev.* **D56**:230, (1997)
- [82] H. Y. Cheng, C.Y.Cheung and C.W.Hwang, *Phys.Rev.* **D55**:1159, (1997)
- [83] Nora Brambilla, arXiv:hep-ph/0702105, (2007)
- [84] S. Nussinov and W. Wetzel, *Phys.Rev.*, **D36**:130, (1987).
- [85] N. Isgur and M. B. Wise, *Phys. Lett.*, **B232**:113, (1989).
- [86] N. Isgur and M. B. Wise, *Phys. Lett.*, **B237**:527, (1990).
- [87] M. B. Voloshin and M. A. Shifman, *Sov.J.Nucl.Phys.*, **45**:292, (1987).
- [88] M. B. Voloshin and M. A. Shifman, *Sov.J.Nucl.Phys.*, **47**:511, (1988).

- [89] H. D. Politzer and M. B. Wise, *Phys.Lett.*, **B206**:681, (1988).
- [90] H. D. Politzer and M. B. Wise, *Phys.Lett.*, **B208**:504, (1988).
- [91] E. V. Shuryak, *Phys.Lett.*, **B93**:134, (1980).
- [92] B. Grinstein, *Nucl.Phys.*, **B339**:253, (1990).
- [93] J. G. Korner *et al.*, *Prog.Part.Nucl.Phys.*, **33**:787, (1994).
- [94] Olga Lakhina in the Thesis "Study Of Meson Properties In Quark Models", University of Pittsburgh, 2008. .
- [95] Antonio Vairo. arXiv:hep-ph/0709.3341, (2007)
- [96] Y. Nambu, *Phys.Rev.*, **D10**:4262, (1974).
- [97] G. S. Bali *et al.*, *Phys.Rev.*, **D71**:114513, (2005).
- [98] D. Becirevic *et al.*, arXiv:hep-ph/1103.4024, (2011).
- [99] E. Eichten *et al.*, *Phys. Rev. Lett.*, **34**:369, (1975).
- [100] K. D. Born *et al.*, *Phys. Rev.* **D40**:1653, (1989).
- [101] J. M. Cornwall and J. Papavassiliou, *Phys. Rev.* **D40**:3474, (1989).
- [102] J. L. Richardson, *Phys. Lett.* **B82**:272, (1979).
- [103] X. T. Song, *J.Phys.* **G17**:49, (1991).
- [104] L. Motyka and K. Zalewski, *Eur.Phys.J.* **C4**:107, (1998).
- [105] Sameer M. Ikhdair and Ramazan Sever, *Int.J.Mod.Phys.* **A19**:1771, (2004).
- [106] A. Martin, *Phy. Lett.* **B93**:338, (1980).

- [107] K. Heikkila, N.A. Tornquist and S. Ono, *Phys. Rev.* **D29**:110, (1984).
- [108] A. K. rai, B. Patel and P. C. Vinodkumar, *Phys.Rev.* **C78**:055202, (2008).
- [109] I. M. Narodetskii, M. A. Trusov, *Phys. Atom. Nucl.* **65**:917, (2002).
- [110] G. Plante and A. F. Antippa, *J. Math. Phys.* **46**:062108, (2005).
- [111] M. Chaichian and R. Kokerler, *Ann. Phys. (N.Y.)* **61**:124, (1980).
- [112] A. M. Badalian and D.S. Kuzmenko, *arxiv:hep-ph/0104097*, (2001).
- [113] D. Ebert, R.N.Faustov and V.O.Galkin, *Phys.Rev.* **D79**:114029, (2009).
- [114] Mao ZHI Yang, *arXiv:hep-ph/11043819*, (2011).
- [115] D. Scora and N. Isgur, *Phys. Rev.* **D52**:2783, (1995).
- [116] H. M. Choi,C. R. J and Ziyue Li, *arXiv:hep-ph/1206.3351*, (2012).
- [117] A. K. Grant and J. L. Rosner, *arXiv:hep-ph/9211313*, (1992).
- [118] D. K. Choudhury and P. Das *et al* . *Pramana-J. Phys.*, **44**:519, (1995).
- [119] D. K. Choudhury and P. Das *et al* . *Pramana-J. Phys.*, **46**:349, (1996).
- [120] D. K. Choudhury and N. S. Bordoloi, *Mod. Phys. Lett.* **A17**:29;1909, (2002).
- [121] D. K. Choudhury and N. S. Bordoloi, *Mod. Phys. Lett.* **A26**:443, (2009).
- [122] M. Peter, *Phys. Rev. Lett.* **78**:602, (1997).
- [123] Y. Schröder, *Phys. Lett.* **B447**:321, (1999).
- [124] S. Godfrey and N. Isgur, *Phys.Rev.* **D32**:189, (1985).
- [125] A. M. Badalian, A.I.Veselov and B.L.G Bakker, *Phys. Rev.* **D70**:016007, (2004).

[126] A. Abulencia *et al.*, (*CDF Collaboration*) *Phys. Rev. Lett.* **96**:082002, (2006).

[127] S. Deoghuria and S. Chakrabarty, *Z. Phys. C-Particles and Fields*, **53**:293, (1992).

[128] A. N. Mitra *Quarks, few body systems and relativity in few methods- principles and applications*, ed. T.K.lim *et al* , p 777, *World Scientific, Singapore*, (1986).

[129] A. N. Mitra and I. Santhanam, *Few body systems*, **12**, p.41, (1992).

[130] N. Isgur, *Proceedings of XVI International school of sub-nuclear Phys. Erica, 1978*", Page107.

[131] S.Godfrey and N.Isgur. *Phys.Rev.*, **D32**:189, (1985).

[132] A.Dalgarno. *Stationary Perturbation Theory in Quantum theory-I.* , Academic, NewYork, (1961).

[133] J.J.Sakurai, *Advanced Quantum Mechanics*, p 128, Addison-Wesley, Massachusetts, (1967).

[134] C.Itzykson and J.Zuber, *Quantum Field Theory*, p 79. International Student Edition, McGraw-Hill, Singapore, (1986).

[135] K. K. Pathak and D. K. Choudhury, *Chinese Physics Lett.* **28**:101201, (2011).

[136] D Ebert, R N Faustov and V O Galkin, *Phys. Lett.* **B635**:93-99, (2006).

[137] D Ebert, R N Faustov and V O Galkin, *Phys. Rev.* **D79**:114029, (2009).

[138] Hadizadeh M R and Tomio Lauro, arXiv:hep-ph/1104.3891, (2011).

[139] K. K. Pathak and D. K. Choudhury, *Pramana J.Phys.* DOI 10.1007/s12043-012-0342-1(2012).

[140] D.E.Groom *et al.*, (Particle Data Group). *Eur.Phys.J.C.*, **15**:1, (2000).

- [141] A. K. Rai, B. Patel and P. C. Vinodkumar, *Phys. Rev.* **C78**:055202, (2008).
- [142] D. Asner *et al.*, (*Heavy Flavor Averaging Group*), arXiv:hep-ph-1010.1589, (2010).
- [143] Wolfgang Lucha, Dmitri Melikhov, Silvano Simula, arXiv:hep-ph/1101.5986, arXiv:hep-ph/1108.0844(2011).
- [144] Mao-Zhi Yang, arXiv:hep-ph/1104.3819, (2011).
- [145] C. Aubin *et al.*, *Phys. Rev. Lett.* **95**:122002, (2005).
- [146] T. W. Chiu *et al.*, *Phys. Lett.* **B624**:31, (2005).
- [147] Bhavin Patel and P C Vinodkumar, *Chinese Physics* **C34**:9, (2010).
- [148] A. Adb El-Hady, M. A. K. Lodhi and J. P. Vary, *Phys. Rev.* **D59**:094001, (1999).
- [149] S. Godfrey, *Phys. Rev.* **D70**:054017, (2004).
- [150] A. J. Buras, arXiv:hep-ph/1009.1303v1, (2010).
- [151] C. T. H. Davies *et al.*, *J. Phys. Rev.* **D82**:114504, (2010).
- [152] A. Bazavov *et al.*, (*Fermilab Lattice and MILC Collaborations*), PoS LAT2009, 249 (2009).
- [153] G. Cvetic *et al.*, *Phys. Lett.* **B596**:84, (2004).
- [154] M. Gell-Mann and A. Pais, *Phys. Rev.* **97**:1387, (1955).
- [155] C. Albajar *et al.*, (UA1 Collaboration), *Phys. Lett.* **B186**:247, (1987).
- [156] H. Albrecht *et al.*, (*ARGUS Collaboration*) *Phys. Lett.* **B192**:245, (1987).
- [157] Chih-Hsiang Cheng, in the Thesis *A Measurement of the Lifetime and Mixing Frequency of Neutral B Mesons with Semileptonic Decays in the BABAR Detector*, Stanford University Stanford, CA 94309. SLAC-Report-645.

[158] C. Gay, *Annu. Rev. Nucl. Part. Sci.* **50**:577, (2000).

[159] N. Cabibbo, *Phys. Rev. Lett.* **10**, 531 (1963); M. Kobayashi and T. Maskawa, *Prog. Theor. Phys.* **49**, 652 (1973).

[160] E. Lunghi and A. Soni, *Phys. Rev. Lett.* **104**:251802, (2010).

[161] J. Laiho, E. Lunghi and R.S. Van de Water, *PoS FPCP2010* **40**, (2010) [arXiv:hep-ph/1102.3917].

[162] A. Lenz *et al.*, *Phys. Rev.* **D83**:036004, (2011).

[163] U. Nierste, *B mixing in the Standard Model and Beyond*, 7th International Workshop on the CKM Unitarity Triangle, Cincinnati, Ohio, USA.

[164] S. Hansmann-Menzemer, U. Nierste, F. Wilson, *WG IV Summary: Mixing and mixing-related CP violation in B system*, 7th International Workshop on the CKM Unitarity Triangle, Cincinnati, Ohio, USA.

[165] E. Eichten *et al.*, *Phys. Rev. Lett.* **34**:369, (1975).

[166] B. J. Hazarika and D. K. Choudhury, *Pramana J. phys.* **75**:423, (2010).

[167] W. A. Bardeen *et al.*, *Phys. Rev.* **D18**:3998, (1978).

[168] K. Hagiwara *et al.*, *Phys. Rev.* **D66**:1, (2002).

[169] M. Jamin and A. Pich, *Nucl. Phys.* **B507**:334, (1997).

[170] Yu. A. Simonov, *Yad. Fiz.* **58**:113, (1995).

[171] G. Parisi and R. Petronzio, *Phys. Lett.* **B94**:51, (1980).

[172] A. M. Badalian and B. L. G. Bakker, *Phys. Rev.* **D62**:094031, (2000).

[173] D. Griffiths in *Introduction to Elementary Particles*, p 131, J. Wiley and Sons, (1987).

[174] F. Halzen and A. D. Martin in *Quarks and Leptons*, John Willey and Sons, New Work,(1984).

[175] B. Pan, arXiv:hep-ph-1106.3028, (2011).

[176] D. Ebert, R. N. Faustov and V. O. Galkin, *Phys. Rev* **D67**:014027, (2003).

[177] M. D. Pierro *et al.*, *Phys. Rev.* **D64**:114004, (2001).

[178] A. Buras, *Phys. Lett* **B566**:115, (2003).

[179] Quang Ho-KIM and Pham Xuan Yem in *Elementary particles and their interactions*. Springer publication, Germany,(1998).

[180] T. Inami and C. S. Lim, *Prog. Theo. Phys.* **65**:1772, (1981).

[181] F. Abe *et al.*, (*CDF Collaboration*) *Phys. Rev.* **D60**:051101, (1999).

[182] V. M. Abazov *et al.*, (*Fermilab-Pub-06/055-E*),arXiv:hep/ex-0603029,(2006).

[183] C Bernard *et al.*, *Phys. Rev.* **D66**:094501, (2002).

[184] M Jamin *et al.*, *Phys. Rev.* **D65**:056005, (2002).

[185] A. Abulencia *et al.*, (*CDF Collaboration*), *Phys. Rev. Lett.* **97**:242003, (2006).

[186] S Godfrey, *Phys. Rev.* **D33**:5, (1986).

[187] Seung-il Nam, *Phys. Rev.* **D85**:034019, (2012).

[188] C. W. Hwang, *Phys. Rev.* **D81**:114024, (2010).

[189] Z. Ghalenovi, A.A. Rajabi and M. Hamzavi, *ACTA PHYSICA POLONICA* **B42**:8, (2011).

[190] A. M. Badalian, B. L. G. Bakker and Yu. A. Simonov, *Phys. Rev.* **D75**:116001, (2007).

- [191] G. L. Wang, *Phys. Lett.* **B633**:492, (2006).
- [192] J. L. Rosner, S. Stone in (*PDG-2012*), arXiv:hep/ex-1201.2401, (2012).
- [193] E. T. Neil et al. (*Fermilab Lattice and MILC Collaborations*) arXiv:hep-lat-1112.3978, (2011).
- [194] C.T.H Davies *et al.*, *Phys. Rev.* **D82**:114504, (2010).
- [195] Bhavin Patel and P C Vinodkumar, arXiv:hep-ph/0908.2212, (2009).
- [196] Wolfgang Altmannshofer *et al.*, arXiv:hep-ph/0909.1333, (2009).
- [197] A. Khodjamirian, *Phys. Rev.* **D79**:031503, (2009).
- [198] A. Bazavov *et al.*, (*Fermilab/MILC Collaboration*) arXiv:hep-ph-1112.3051, (2011).
- [199] M Neubert, *Phys.Rep.* **245**:259, (1994).
- [200] D. K. Choudhury and N. S. Bordoloi, *Int. J. Mod. Phys.* **A15**:23, (2000).
- [201] A. M. Badalian and D S Kuzmenko, *Phys. Rev.* **D65**:016004, (2009).
- [202] F. JUGEAU *et al.*, arXiv:hep-ph/0412144,(2004).
- [203] A. Le Yaouanc, L. Oliver and J.C. Raynal, *Phys.Rev.* **D69**:094022, (2004).
- [204] D. Ebert, R. N. Faustov and V. O. Galkin, *Phys. Rev.* **D75**:074008, (2007).
- [205] K.C. Bowler *et al.*, *UKQCD Collaboration*, *Phys. Lett.* **B637**:293, (2002).
- [206] D. Buskulic *et al.*, (*ALEPH collaboration*), *Phys. Lett.* **B395**: 373387, (1997).
- [207] K. Abe *et al.*, (*Belle collaboration*), *Phys. Lett.* **B526**: 258268, (2002).
- [208] A. Le Yaouanc, L. Oliver and J. C. Raynal, *Phy.Rev.* **D69**:094022, (2004).

- [209] Y. B. Dai, C. S. Huang, M. K. Huang and C. Liu; *Phys.Lett.* **B387**:379, (1996).
- [210] M. A. Ivanov *et al.*, *Phy.Rev.* **D56**:348, (1997).
- [211] M Neubert, *Int.J.Mod.Phys.* **A11**:4173, (1996).
- [212] G. M. de Divitiis *et al.*, *Phys. Lett.* **B655**:4549, (2007).
- [213] F. Abe *et al.*, (*CDF Collaboration*) *Phys. Rev.* **D58**:112004, (1998).
- [214] J. D. Bjorken, *draft report 07/22/86 (1986)[unpublished]*.
- [215] I. P. Gouz *et al.*, *Phys. Atom. Nucl.* **67**:1559, (2004).
- [216] V. V. Kiselev, A. E. Kovalsky, and A. K. Likhoded, *Nucl.Phys.* **B585**:353, (2000).
- [217] T. Huang and F. Zuo, *Eur.Phys.J.* **C51**:833, (2007).
- [218] M. A. Ivanov, J. G Körner and P. Santorelli, *Phys. Rev.* **D63**:074010, (2001).
- [219] M. A. Ivanov, J. G Körner and P. Santorelli, *Phys. Rev.* **D71**:094006, (2005).
- [220] M. A. Ivanov, J. G Körner and P. Santorelli, *Phys. Rev.* **D73**:054024, (2006).
- [221] D. Ebert, R. N. Faustov and V. O. Galkin, *Phys. Rev.* **D68**:094020, (2003).
- [222] D. Ebert, R. N. Faustov and V. O. Galkin, *Eur. Phys. J.* **C32**:29, (2003).
- [223] C.H. Chang and Y.Q. Chen, *Phys. Rev.* **D49**:3399, (1994).
- [224] J.F. Liu and K.T. Chao, *Phys. Rev.* **D56**:4133, (1997).
- [225] A. Abd El-Hady, J. H. Munoz, and J. P. Vary, *Phys. Rev.* **D62**:014019, (2000).
- [226] P. Colangelo and F. De Fazio, *Phys. Rev.* **D61**:034012, (2000).
- [227] M. A. Nobes and R. M. Woloshyn, *J. Phys.* **G26**:1079, (2000).

[228] E. Hernndez, J. Nieves and J. M. Verde-Velasco, *Phys.Rev.* **D74**:074008, (2006).

[229] W. Wang, Y. L. Shen and C. D. Lü, *Phys. Rev.* **D79**:054012, (2009).

[230] M. Lusignoli and M. Masetti, *Z. Phys.* **C51**:549, (1991).

[231] D. Du and Z. Wang, *Phys. Rev.* **D39**:1342, (1989).

[232] R. Dhir, N. Sharma and R.C. Verma, *J. Phys.* **G35**:085002, (2008).

[233] M. Wirbel, B. Stech and M. Bauer, *Z. Phys.* **C29**:637, (1985).

[234] N. Isgur *et al.*, *Phys. Rev.* **D39**:799, (1989).

[235] P. Colangeloa and F. De Fazio, *Phys.Rev.* **D61**:034012, (2000).

[236] E. Jenkins *et al.*, *Nucl. Phys.* **B390**:463, (1993).

[237] M. A. Sanchiz-Lozano *Nucl. Phys.* **B440**:251, (1995).

[238] A. M. Badalian and D. S. Kuzmenko, *Phys. Rev.* **D65**:016004, (2009).

[239] I. J. R. Aitchison and J. J. Dudek, *Eur. J. Phys.* **23**:605, (2002).

[240] D. K. Choudhury and Krishna Kingkar Pathak, arXiv:hep-ph/1304.7074, (2013)

[241] B. J. Hajarika, K. K. Pathak and D. K. Choudhury, *Mod. Phys. Lett.* **A26**:1547-1554, (2011).

[242] K. K. pathak and D. K. choudhury, *J. Mod. Physics* **3**:821-826, (2012).

[243] Abramowitz and Stegun in *Handbook of Mathematical Functions*, Dover publications, (1964).

[244] F. E. Close and A. Wambach, *Nucl. Phys.* **B412**:169, (1994).

[245] D. K. Choudhury and N. S. Bordoloi, *Int.J.Mod.Phys.* **A15**:3667, (2000).

- [246] Myoung-Taek Choi and Jae Kwan Kim, *Phys. Lett.* **B419**:377-380, (1998).
- [247] D. Ebert, R. N. Faustov and V. O. Galkin, arXiv:hep-ph/0401237, (2004).
- [248] Ho-Meyong Choi and Chueng-Ryong Ji, *Phys. Rev.* **D80**:054016, (2009).
- [249] V. V. Kiselev, A. K. Likhoded and A. I. Onishchenko, *Nucl. Phys.* **B569**:473, (2000).
- [250] P. Cea, P. Colangelo, L. Cosmai and G. Nardulli, *Phys. Lett.* **B206**:691, (1988).
- [251] P. Colangelo, G. Nardulli and M. Pietroni, *Phys. Rev.* **D43**:3002, (1991).
- [252] V. O. Galkin, D. Ebert and R. N. Faustov. *Phys. Rev.*, **D57**, 9:5663, (1998).
- [253] B. J. Hazarika and D. K. Choudhury, *Pramana J. Phys.* **75**:3, (2010).
- [254] ZHAO Gong-Bo *et al.*, *Commun. Theor. Phys.* **38**:41-46,(2002).
- [255] R.Jaffe and F.Wilczek. *Phys.Rev.Lett.*, **91**, (2003).
- [256] R.Ramachandran. *Pramana - J.Phys.*, **65**:381, (2005).
- [257] Shi lun Zhu. hep-ph/0406204, 2004.

List of Publication

In Journal

1. *Open Flavour Charmed Mesons in a Quantum Chromodynamics Potential Model.*
Pramana - J.Phys., **79** Issue 6 (2012), Page 1385-1393.
K K Pathak and D K Choudhury.
2. *Oscillation Frequency of B mesons in a QCD Potential Model.*
Chinese Physics Letters **28**, No. 10,(2011) page 101201 .
K K Pathak and D K Choudhury.
3. *Leptonic Decay of Heavy Light Mesons in a QCD Potential Model.*
*Int. J. Mod. Phys. A***28** No.2 (2013) 1350010.
Krishna Kingkar Pathak, D K Choudhury and N S Bordoloi.
4. *Semileptonic Decay of B_c Meson Into $c\bar{c}$ States in a QCD Potential Model.*
*Int. J. Mod. Phys. A***28** No. 19 (2013) 1350097
Krishna Kingkar Pathak and D K Choudhury .
5. *Semileptonic Decay of B_c Meson Into S Wave Charmonium in a QCD Potential Model with Coulombic Part as Perturbation.*
Journal of Modern Physics **3** (2012) 821-826
Krishna Kingkar Pathak and Dilip Kumar Choudhury .

6. *Isgur Wise Function in a QCD Potential Model with Coulombic Potential as Perturbation.*

Mod. Phys. Lett. **A26**, No. 21 (2011) 1547-1554.

B J Hazarika, K K Pathak and D K Choudhury.

7. *On the bounds of CKM matrix element V_{cb} in a potential model.*

International Journal of Modern Physics A **29**, (2014)1450066

Krishna Kingkar Pathak and Dilip Kumar Choudhury .

In Conference Proceedings

1. *Masses and Decay Constants of Mesons in a QCD Inspired Quark Model With Relativistic Effect.*

North-East reaserch in physics,ISBN-81-87500-53-0, (6thPANE Conference-2009).
Krishna Kingkar Pathak, D K Choudhury and N S Bordoloi.

2. *Comments on the Perturbation of Cornell Potential in a QCD Potential Model.*

Journal of Physics: Conference Series 481 (2014) 012022,
(NCHEPC conference-2013)
D K Choudhury and K K Pathak.

ADDENDA

Open flavour charmed mesons in a quantum chromodynamics potential model

KRISHNA KINGKAR PATHAK^{1,*} and D K CHOUDHURY²

¹Department of Physics, Arya Vidyapeeth College, Guwahati 781 016, India

²Department of Physics, Gauhati University, Guwahati 781 014, India

and Physics Academy of Northeast, Guwahati 781 014, India

*Corresponding author. E-mail: kkingkar@gmail.com

MS received 25 January 2012; revised 29 March 2012; accepted 10 May 2012

Abstract. We modify the mesonic wave function by using a short distance scale r_0 in analogy with hydrogen atom and estimate the values of masses and decay constants of the open flavour charm mesons D , D_s and B_c within the framework of a QCD potential model. We also calculate leptonic decay widths of these mesons to study branching ratios and lifetime. The results are in good agreement with experimental and other theoretical values.

Keywords. Heavy-light mesons; masses; decay constants; branching ratio.

PACS Nos 12.39.—x; 12.39.Jh; 12.39.Pn

1. Introduction

Recently, we have reported a regularization procedure to avoid the singularity by introducing a flavour-dependent short distance scale at the origin to study the oscillation frequency of B and \bar{B} mesons in a QCD potential model [1]. The purpose of this paper is to use the potential model to calculate the masses and decay constants of open flavour charmed mesons D , D_s and B_c and then to find the decay width and branching ratio of the same.

If the CKM element is well known from other measurements, then f_P can be measured well. If, on the other hand, the CKM element is not known or poorly measured, having theoretical input on f_P can allow a determination of the CKM element. These decay constants can be accessed both experimentally and through lattice quantum chromodynamics (lQCD) simulations. While for f_π , f_K , f_D , experimental measurements agree well with lattice QCD calculations, a discrepancy is seen for the value of f_{D_s} : The 2008 PDG average for f_{D_s} is 273 ± 10 MeV [2], about 3σ larger than the most precise $N_f = 2 + 1$ lQCD result from the HPQCD/UKQCD Collaboration [3], 241 ± 3 MeV. On the other hand, experiments and lQCD calculations agree very well with each other on the value

The Oscillation Frequency of B and \bar{B} Mesons in a QCD Potential Model with Relativistic Effects

Krishna Kingkar Pathak^{1**}, D. K. Choudhury²

¹Department of Physics, Arya Vidyapeeth College, Guwahati-781016, India

²Department of Physics, Gauhati University, Guwahati-781014, India

(Received 11 May 2011)

Wavefunction at the origin, with the incorporation of a relativistic effect, leads to singularity in a specific potential model. To regularize the wavefunction, we introduced a short distance scale and used it to estimate the mass and decay constants of B_d and B_s mesons within the QCD potential model. These values were then used to compute the oscillation frequency, Δm_B , of B_d and B_s mesons. The values were found to be in good agreement with experimental and other theoretical values.

PACS: 12.39.-x, 12.39.Jh, 12.39.Pn

DOI:10.1088/0256-307X/28/10/101201

Investigations of weak decays of mesons composed of a heavy quark and an antiquark give us an important insight into heavy-quark dynamics. Research into the mixing and decay constants of B meson also provides us with useful information about the dynamics of quarks and gluons at the hadronic scale. The weak eigenstates of neutral mesons are different from their mass eigenstates. This leads to the phenomenon of mixing, whereby neutral mesons oscillate between their matter and antimatter states. This was first observed in the Kaon sector, and subsequently in B_d and B_s mesons. The mass difference Δm_B is a measure of the frequency of the change from a B into a \bar{B} , and is called the oscillation frequency. The decay constants of heavy mesons, one of the input parameters for oscillation frequency, are crucial for interpreting data on particle-antiparticle mixing in the neutral B meson system, and for anticipating and interpreting new signatures for CP violation.

If the CKM element is well known from other measurements, then the pseudoscalar decay constant f_p can be well measured. If, on the other hand, the CKM element is less well or poorly measured, having theoretical input on f_p can allow a determination of the CKM element.^[1] A measurement of the decay constant f_B is difficult, since $B^+ \rightarrow l^+ \bar{\nu}_l$ is cabiboh suppressed in the standard model. Hence f_{B_q} has to be provided from theory.

In this Letter, we calculate the pseudoscalar masses M_{B_q} and pseudoscalar decay constants f_{B_q} to compute the oscillation frequency Δm_{B_q} , $q = d, s$ within the framework of a potential model.^[2-4] To incorporate the relativistic effect, the necessity of a short distance scale, in analogy to QED, is also pointed out.

For the light heavy flavor bound system of $q\bar{Q}$ or $\bar{q}Q$, the hamiltonian can be written as

$$H = -\frac{\nabla^2}{2\mu} + V(r), \quad (1)$$

where $V(r)$ is the spin-independent quark-antiquark potential.

$$V(r) = V_{\text{coul}}(r) + V_{\text{conf}}(r), \quad (2)$$

where V_{coul} represents the coulombic part of the potential and V_{conf} represents the confining potential. The vector and scalar confining potentials in the non-relativistic limit reduce to^[5,6]

$$V_{\text{conf}}^v(r) = (1 - \epsilon_1)(br + C), \quad (3)$$

$$V_{\text{conf}}^s(r) = \epsilon_1(br + C), \quad (4)$$

reproducing

$$V_{\text{conf}}(r) = V_{\text{conf}}^s(r) + V_{\text{conf}}^v(r) = br + C, \quad (5)$$

$$V_{\text{coul}}(r) = -\alpha_c/r, \quad (6)$$

where $\alpha_c = \frac{4}{3}\alpha_s$ with α_s being the strong running coupling constant, ϵ_1 the mixing coefficient, and b and C the potential parameters as used in our previous work.^[3,4]

Considering the linear part of the potential as perturbation, the coulombic part as the parent, and then using the dalgarno method, the wavefunction in the ground state is obtained,^[2-4] i.e.

$$\psi_{\text{rel+conf}}(r) = \frac{N'}{\sqrt{\pi a_0^3}} e^{-r/a_0} \left(C' - \frac{\mu b a_0 r^2}{2} \right) \left(\frac{r}{a_0} \right)^{-\epsilon}, \quad (7)$$

$$N' = 2^{1/2} \cdot \left\{ (2^{2\epsilon} \Gamma(3 - 2\epsilon) C'^2 - \frac{1}{4} \mu b a_0^3 \Gamma(5 - 2\epsilon) C' + \frac{1}{64} \mu^2 b^2 a_0^6 \Gamma(7 - 2\epsilon)) \right\}^{-1/2}, \quad (8)$$

$$C' = 1 + c A_0 \sqrt{\pi a_0^3}, \quad (9)$$

$$\mu = \frac{m_i m_j}{m_i + m_j}, \quad (10)$$

$$a_0 = \left(\frac{4}{3} \mu \alpha_s \right)^{-1}, \quad (11)$$

$$\epsilon = 1 - \sqrt{1 - \left(\frac{4}{3} \alpha_s \right)^2}. \quad (12)$$

**Email: kkingkar@gmail.com

© 2011 Chinese Physical Society and IOP Publishing Ltd

LEPTONIC DECAY OF HEAVY-LIGHT MESONS IN A QCD POTENTIAL MODEL

KRISHNA KINGKAR PATHAK

Department of Physics, Arya Vidyapeeth College, Guwahati 781016, India
kkingkar@gmail.com

D. K. CHOUDHURY

Department of Physics, Gauhati University, Guwahati 781014, India

N. S. BORDOLOI

Department of Physics, Cotton College, Guwahati 781001, India

Received 15 November 2012

Revised 19 December 2012

Accepted 8 January 2013

Published 22 January 2013

We study the masses and decay constants of heavy-light flavor mesons D , D_s , B and B_s in a QCD potential model. The mesonic wave function is used to compute the masses of D and B mesons in the ground state and the wave function is transformed to momentum space to estimate the pseudoscalar decay constants of these mesons. The leptonic decay widths and branching ratio of these mesons for different leptonic channels are also computed to compare with the experimental values. The results are found to be compatible with available data.

Keywords: Heavy-light mesons; masses; decay constants; branching ratio.

PACS numbers: 12.39.-x, 12.39.Jh, 12.39.Pn, 12.38.Lg

1. Introduction

Heavy hadron spectroscopy has played a major role in the foundation of QCD. In the last few years, however, it has sparked a renewal of interest due to the numerous data available from the B factories, CLEO, LHCb, the Tevatron and by the progress made in the theoretical methods. The remarkable progress at the experimental side for the study of hadrons has opened up new challenges in the theoretical understanding of light-heavy flavor hadrons.

The study of the wave functions of heavy-flavored mesons like B and D are important both analytically and numerically for studying the properties of strong interaction between heavy and light quarks as well as for investigating the

1 International Journal of Modern Physics A
 2 Vol. 29 (2014) 1450066 (11 pages)
 3 © World Scientific Publishing Company
 4 DOI: 10.1142/S0217751X14500663



5 **On the bounds of CKM matrix element V_{cb} in a potential model**

6 D. K. Choudhury

7 *Department of Physics, Gauhati University, Guwahati-781014, India*
 8 *Physics Academy of North-East, Guwahati-781014, India*

9 Krishna Kingkar Pathak*

10 *Department of Physics, Arya Vidyapeeth College, Guwahati-781016, India*
 11 *kkkingkar@gmail.com*

12 Received 23 February 2014

13 Revised 27 March 2014

14 Accepted 28 March 2014

15 Considering the allowed range of slope ρ^2 and curvature C of Isgur–Wise function for B
 16 meson, we obtain an allowed range of strong coupling constant α_s as well as the QCD
 17 scale parameter Λ in a specific prescription. The allowed range of Λ is then used to
 18 obtain the theoretical bounds on V_{cb} in a potential model. The recent available data of
 19 V_{cb} are found to lie within this computed range $0.0375 \leq |V_{cb}| \leq 0.0410$.

20 **Keywords:** Mesons; I – W function; CKM elements; branching ratio.

21 **PACS numbers:** 12.39.–x, 12.39.Jh, 12.39.Pn

22 **1. Introduction**

23 In a recent communication,¹ we have reported the results of pseudoscalar decay
 24 constants of heavy-light mesons in a potential model with linear part of the potential
 25 as perturbation. The technique used was the quantum mechanical perturbation
 26 theory with plausible relativistic correction.

27 Exclusive semileptonic decays of hadrons containing a bottom quark provide a
 28 path to measure the Cabibbo–Kobayashi–Maskawa (CKM) matrix elements V_{cb} , an
 29 important parameter to test the Standard Model. It is well known in the literature
 30 that in case of heavy to heavy transitions like $b \rightarrow c$ decays, all heavy quark bilinear
 31 current matrix elements are described in terms of only one form factor, which is
 32 called the Isgur–Wise (IW) function in leading order. The IW function, particu-
 33 larly its slope ($\xi'(1)$) at the zero recoil point is important since it allows a model

*Corresponding author.

Comments on the perturbation of Cornell potential in a QCD potential model

D K Choudhury¹ and Krishna Kingkar Pathak²

¹Physics Department, Gauhati University, Guwahati 781014, India.

²Physics Department, Arya Vidyapeeth College, Guwahati 781016, India.

E-mail: kkingkar@gmail.com

Abstract. We find in the analysis that the linear part of the Cornell potential can be treated as perturbation for a set of larger values of α_s in the range $0.4 \leq \alpha_s \leq 0.75$ with a constant shift within the range of $-0.4 \text{ GeV} \leq c \leq -1 \text{ GeV}$. Moreover with the same range of constant shift in the Potential, we expect better results with Coulombic part as perturbation for $\alpha_s \leq 0.4$.

1. Introduction

In the potential models, the effective potential between a quark and antiquark can be taken as the Coulomb-plus-linear potential,

$$V(r) = -\frac{4\alpha_s}{r} + br + c. \quad (1)$$

This potential has received a great deal of attention in particle physics, more precisely in the context of meson spectroscopy where it is used to describe systems of quark and antiquark bound states. However, it has been found to be questionable about the numbers of free parameters(α_s, b, c) and numbers of findings in any potential model. The success of a phenomenological model depends on reducing the free model parameters to obtain more precise values with proper arguments and analysis.

In this letter, we put forward the comments on linear part of the Potential as perturbation with Coulombic part as Parent [1, 2] as well as Coulombic part as perturbation with linear as parent [3] in a potential model and attempt to put some constraints on the model parameters.

2. The method of perturbation

It is well known that one cannot solve the Schrödinger equation in quantum mechanics with the QCD potential(equation (1)) except for some simple models. Perturbation theory has been helpful since the earliest applications of quantum mechanics in this regard. In fact, perturbation theory is probably one of the approximate methods that most appeals to intuition [4].

The advantage of taking Cornell Potential for study is that it leads naturally to two choices of “parent” Hamiltonian, one based on the Coulomb part and the other on the linear term, which can be usefully compared. It is expected that a critical role is played by r_0 where the Potential $V(r) = 0$. Aitchison and Dudek in Reference [5] put an argument that if the size of a state measured by $\langle r \rangle < r_0$, then the Coulomb part as the “Parent” will perform better



Content from this work may be used under the terms of the Creative Commons Attribution 3.0 licence. Any further distribution of this work must maintain attribution to the author(s) and the title of the work, journal citation and DOI.

ISGUR-WISE FUNCTION IN A QCD POTENTIAL MODEL WITH COULOMBIC POTENTIAL AS PERTURBATION

BHASKAR JYOTI HAZARIKA*, KRISHNA KINGKAR PATHAK† and D. K. CHOUDHURY‡

*Department of Physics, Pandu College, Guwahati-781012, India

†Department of Physics, Arya Vidyapeeth College, Guwahati-781016, India

‡Department of Physics, Gauhati University, Guwahati-781014, India

Received 27 March 2011

Revised 24 April 2011

We study heavy light mesons in a QCD inspired quark model with the Cornell potential $-\frac{4\alpha_S}{3r} + br + c$. Here we consider the linear term br as the parent and $-\frac{4\alpha_S}{3r} + c$, i.e. the Coulombic part as the perturbation. The linear parent leads to Airy function as the unperturbed wave function. We then use the Dalgarno method of perturbation theory to obtain the total wave function corrected up to first order with Coulombic piece as the perturbation. With these wave functions, we study the Isgur-Wise function and calculate its slope and curvature.

Keywords: Dalgarno method; Isgur-Wise function; slope and curvature.

PACS Nos.: 12.39.-x, 12.39.Jh, 12.39.Pn

1. Introduction

Considerable efforts have been made in understanding the physics of hadrons containing at least one heavy quark since long.^{1–9} It is well known that the heavy quark symmetry in the heavy quark limit leads to a single form factor called the Isgur-Wise (I-W) function which can describe the heavy quark bilinear current matrix elements of weak decay. The basic ingredient of the I-W function is the hadronic wave function, the determination of which becomes such a crucial factor. The potential models for this purpose is quite helpful as they contain more input parameters and hence has its firm basis.

Under such circumstances the I-W function has been investigated^{3–9} with considerable success of valid degrees in different models. In the potential models, “Cornell potential” is found to be more useful than the others. It leaves two options of choosing the parent (1) the Coulombic part $-\frac{4\alpha_S}{3r}$ and (2) the linear potential part br .

*Corresponding author

SEMILEPTONIC DECAY OF B_c MESON INTO $c\bar{c}$ STATES IN A QCD POTENTIAL MODEL

KRISHNA KINGKAR PATHAK

*Department of Physics, Arya Vidyapeeth College,
Guwahati-781016, India
kkkingkar@gmail.com*

D K CHOUDHURY

*Department of Physics, Gauhati University,
Guwahati-781014, India*

Received 3 June 2013

Revised 30 June 2013

Accepted 2 July 2013

Published 30 July 2013

The slope and curvature of Isgur-Wise function for B_c meson is computed in a QCD potential model in two different approaches of choosing the perturbative term of the Cornell potential. Based on heavy quark effective theory the exclusive semileptonic decay rates of B_c meson into the $c\bar{c}(\eta_c, J/\psi)$ states are exploited. Spin symmetry breaking effects are ignored up to a particular point and the form factors are connected with Isgur-Wise function for other kinematic point since the recoil momentum of $c\bar{c}$ from B_c is small due to its heavy mass.

Keywords: Dalgarno method; Isgur-Wise function; form factors; decay width.

PACS numbers: 12.39.-x, 12.39.Jh, 12.39.Pn

1. Introduction

The B_c meson is a particularly interesting hadron, since it is the lowest bound state of two heavy (b, c) quarks with different flavors. Because of the fact that the B_c meson carries the flavor explicitly, there is no gluon or photon annihilation via strong interaction or electromagnetic interaction but decay only via weak interaction. Since both b and c quarks forming the B_c meson are heavy, the B_c meson can decay through the $b \rightarrow q$ ($q = c, u$) transition with c quark being a spectator as well as through the $c \rightarrow q$ ($q = s, d$) transition with b quark being a spectator. The former transitions correspond to the semileptonic decays to η_c and D mesons, while the latter transitions correspond to the decays to B_s and B mesons. The CDF Collaboration reported the discovery of the B_c ground state in $p\bar{p}$ collisions

Semileptonic Decay of B_c Meson into S Wave Charmonium in a QCD Potential Model with Coulombic Part as Perturbation

Krishna Kingkar Pathak¹, Dilip Kumar Choudhury²

¹Department of Physics, Arya Vidyapeeth College, Guwahati, India

²Department of Physics, Gauhati University, Guwahati, India

Email: kkingkar@gmail.com

Received May 2, 2012; revised May 31, 2012; accepted June 16, 2012

ABSTRACT

We present the semileptonic decay of B_c meson in a QCD potential model with the coulombic part of the Cornell potential $-\frac{4\alpha_s}{3r} + br + c$ as perturbation. Computing the slope and curvature of Isgur-Wise function in this approach, we study the pseudoscalar and vector form factors for the transition of B_c meson to its S wave charmonium $c\bar{c}$ states. Numerical estimates of widths for the transitions of $B_c \rightarrow J/\psi(\eta_c)l\nu_l$ are presented.

Keywords: Dalgarno Method; Isgur-Wise Function; Form Factors; Decay Width

1. Introduction

The investigation of weak decays of mesons composed of a heavy quark and antiquark gives a very important insight in the heavy quark dynamics. The exclusive semileptonic decay processes of heavy mesons generated a great excitement not only in extracting the most accurate values of Cabibbo-Kobayashi Maskawa (CKM) matrix elements but also in testing diverse theoretical approaches to describe the internal structure of hadrons. The great virtue of semileptonic decay processes is that the effects of the strong interaction can be separated from the effects of the weak interaction into a set of Lorentz-invariant form factors, *i.e.*, the essential informations of the strongly interacting quark/gluon structure inside hadrons. Thus, the theoretical problem associated with analyzing semileptonic decay processes is essentially that of calculating the weak form factors.

The decay properties of the B_c meson are of special interest, since it is the only heavy meson consisting of two heavy quarks with different flavor. This difference of quark flavors forbids annihilation into gluons. As a result, the excited B_c meson states lying below the B_D meson threshold undergo pionic or radiative transitions to the pseudoscalar ground state which is considerably more stable than corresponding charmonium or bottomonium states and decays only weakly. The CDF Collaboration reported the discovery of the B_c ground state in $p\bar{p}$

collisions already more than ten years ago [1]. However, up till recently its mass was known with a very large error. Now it is measured with a good precision in the decay channel $B_c \rightarrow J/\psi\pi$. More experimental data on masses and decays of the B_c mesons are expected to come in near future from the Tevatron at Fermilab and the Large Hadron Collider (LHC) at CERN. The estimates of the B_c decay rates indicate that the c quark transitions give the dominant contribution while the b quark transitions and weak annihilation contribute less. However, from the experimental point of view the B_c decays to charmonium are easier to identify. Indeed, CDF and D0 observed the B_c meson and measured its mass analyzing its semileptonic and nonleptonic decays $B_c \rightarrow J/\psi l\nu_l$.

There are many theoretical approaches to the calculation of exclusive B_c semileptonic decay modes. Some of them are: QCD sum rules [2-4], the relativistic quark model [5-7] based on an effective Lagrangian describing the coupling of hadrons to their constituent quarks, the quasipotential approach to the relativistic quark model [8-10], the instantaneous nonrelativistic approach to the Bethe-Salpeter (BS) equation [11], the relativistic quark model based on the BS equation [12,13], the QCD relativistic potential model [14], the relativistic quark-meson model [15], the nonrelativistic quark model [16], the covariant light-front quark model [17], and the constituent quark model [18-21] using BSW (Bauer, Stech, and Wir-